CANADA

DEPARTMENT OF
ENERGY, MINES AND RESOURCES

MINES BRANCH

OTTAWA

PLAN GEOMETRY AND OTHER FACTORS RELATING TO NATURAL ROCK SLOPE STABILITY APPLIED TO DESIGN OF DE BEERS MINE

D. F. PITEAU

JUNE 1974

Technical Bulletin TB 190

Price: $1.25

Available by mail from Information Canada, Ottawa, K1A 0S9
and at the following Information Canada bookshops:

HALIFAX
1683 Barrington Street

MONTREAL
640 St. Catherine Street West

OTTAWA
171 Slater Street

TORONTO
221 Yonge Street

WINNIPEG
393 Portage Avenue

VANCOUVER
800 Granville Street

or through your bookseller

Price $1.25 Catalogue No. M34-20/190

Price subject to change without notice

Information Canada
Ottawa, 1974

PLAN GEOMETRY AND OTHER FACTORS RELATING TO NATURAL ROCK SLOPE STABILITY APPLIED TO DESIGN OF DE BEERS MINE

(From Ph. D. Thesis, Vol II, University of Witwatersrand, July 1970)

by

D. R. Piteau*

FOREWORD

We in Canada are most grateful to Professor J. Jennings and the University of Witwatersrand for permission to publish Volume 2 of the thesis "Plan Geometry and Other Factors Relating to Natural Rock Slope Stability Applied to Design of De Beers Mine" by D. R. Piteau. Our mining industry continues to produce an increasing proportion of its total output from open pit mines. The economics of these operations can be significantly affected by the slope angles of the walls. Consequently, all practical information, particularly field data, on this subject is of great value.

Dr. Piteau's thesis included several important field studies of the stability of rock slopes. In particular, his work on the effects of the horizontal curvature of a wall on the stable slope angle remains a unique contribution to this day. For this reason, the Mines Branch is glad to make the information gathered on this aspect of the subject easily available to planning engineers in the Canadian industry.

Volume I of the thesis is not included in this report owing to the principal scientific content having been already published in the technical literature. Those who are interested in examining this related work can refer to: Engineering Geology Considerations and Approach in Assessing the Stability of Rock Slopes, Bull. CIM, Vol. 65, No. 721, pp 53-60, May 1972.

D. F. Coates
Director, Mines Branch

Ottawa, Canada

AVANT-PROPOS

Nous sommes très reconnaissants envers le professeur J. Jennings et l'Université de Witwatersrand de nous avoir accordé la permission de publier le Volume 2 de la thèse intitulée "Plan Geometry and Other Factors Relating to Natural Rock Slope Stability Applied to Design of De Beers Mine" du Dr Piteau. Une proportion croissante de la production totale de notre industrie minière provient des mine à ciel ouvert. Or, le degré d'inclinaison du front peut influer beaucoup sur l'économie de leur exploitation. C'est pourquoi toute information d'ordre pratique sur ce sujet, en particulier les données recueillies sur les lieux, possède une grande valeur.

La thèse du Dr Piteau comprend plusieurs études importantes faites sur les lieux mêmes, études qui portaient sur la stabilité des pentes rocheuses. Notons particulièrement le travail de recherche qu'il a effectué sur les effets de la courbure horizontale d'un front sur l'angle d'une pente stable et qui constitue une contribution unique jusqu'à présent. C'est pour cette raison que la Direction des mines est beureuse de rendre l'information recueillie sur cet aspect du sujet facilement disponible aux ingénieurs en planification de l'industrie canadienne.

Le Volume I de la thèse n'est pas compris dans ce rapport, car son principal contenu scientifique a déjà été publié dans des documents techniques. Les personnes qui désirent examiner cette partie peuvent se référee au Bulletin du CIM du mois de mai 1972 qui s'intitule: "Engineering Geology Considerations and Approach in Assessing the Stability of Rock Slopes".

D. F. Coates
Directeur, Direction des mines

Ottawa, Canada

ABSTRACT

As part of a major study relating to the stability of rock slopes of De Beers Mine, a detailed investigation was made of the natural slopes of De Beers Mine and four other mines in Kimberley. Attempt was made to determine the controlling factors which either lead to or detract from the stability of the slopes, the main objective being to assess whether the natural breakback of the slopes would jeopardize the main railway line located in close proximity to the pit.

Current theories of slope stability all deal with a slope as a two-dimensional problem, i. e. a slice of unit length of an infinitely long slope is considered for a condition of plane strain. In this the tacit assumption is made that the plan radii of the crest and toe of the slope are infinite. This is not the condition encountered in practice, particularly in open pit mining where these radii of curvature have important effects on the safe slope angles.

To determine these and other effects a study was made of the slope breakback and other related factors in the four big holes of the diamond mines in the Kimberley area. For each of these holes the same geological sequence is found but the thicknesses of the strata vary and the plan shapes of the big holes are also different. The slopes within the big holes are up to 400 ft high and they formed naturally by breaking back and sloughing into the mined-out kimberlite pipes. A clear relationship is found to have formed between plan radius of curvature of the toe of the slope and the angle of slope which has formed naturally by the breakback. These data have been analyzed statistically and an empirical relationship is produced relating slope angle (or breakback) to the plan radius or curvature.

Other forms of analyses of the basic radius of curvature and breakback data are conducted. It is shown that the major dimensions of the pipes are also important factors for the stability of these slopes. Based on simple experiments the mechanics of failure are determined and also factors such

as comparison of effects of plan radius of curvature on the upper and lower parts of the slopes and possible effects of regional stress are assessed.

RESUME

Dans le cadre d'une importante recherche relative à la stabilité des pentes rocheuses de la mine De Beers, les pentes naturelles de cette dernière et de quatre autres mines de Kimberley ont été étudiées en détail. L'auteur a tenté de découvrir les facteurs déterminants qui influencent la stabilité, l'objectif principal étant d'évaluer le danger que représen tait la rupture naturelle des pentes pour la voie ferrée principale située près de la mine.

Les théories courantes de la stabilité des pentes considèrent toutes la question des pentes comme un problème d'ordre bidimensionnel, c'est-à-dire qu'il est tenu compte d'une pente de longueur infinie en fonction des contraintes parallèles à la surface. Cette façon de penser la question sous-entend que les rayons du plan de la crête et de la base de la pente sont infinis. Or la réalité est toute autre, surtout pour ce qui est des mines à ciel ouvert où ces rayons sont limités en longueur et où les rayons de courbure ont des effets importants sur les angles de pente sûre.

L'auteur a fait une étude de la rupture des pentes et d'autres facteurs connexes des quatre grandes fosses des mines de diamant de la région de Kimberley, en vue de déterminer ces effets et d'autres. Le même schéma géologique se retrouve pour chaque fosse, mais l'épaisseur des strates et les profils varient de l'une à l'autre. Les pentes à l'intérieur des grandes fosses s'élèvent à 400 pieds et se forment naturellement en se fissurant et en glissant dans les colonnes d'où l'on a extrait le minerai kimberlite. Il s'est clairement établi des relations entre le rayon de courbure de la base de la pente et l'angle de pente formé naturellement par la rupture. Ces données ont fait l'objet d'une analyse statistique qui a permis d'établir des relations empiriques entre l'angle de pente ou rupture et le rayon plan ou courbure.

Il se fait actuellement d'autres genres d'analyse des données sur le rayon de courbure de base et sur la rupture. Il est démontré que les principales dimensions des colonnes sont aussi d'importants facteurs quant à la stabilité de ces pentes. Grâce à des expériences simples, les mécanismes entraînant la rupture ont pu être déterminés, ainsi que d'autres facteurs comme la comparaison des effets du rayon plan de courbure en haut et en bas de la pente et les effets possibles de tension dans la région.

TABLE OF CONTENTS

Page

Chapter 1

INTRODUCTION

1.1 SALIENT FEATURES OF THE STUDY

As part of a major study relating to the stability of rock slopes of De Beers Mine, a detailed investigation was made of the slopes which had formed naturally in De Beers Mine and in four other diamond mines in the city of Kimberley, South Africa. The following analyses and results are concerned exclusively with these surface studies. In these studies an attempt was made to ascertain both the natural and unnatural influences on the slopes which either lead to or detract from their stability and to determine any outstanding properties of the naturally formed slopes which could be utilized in analysis of their stability.

The existence of the natural pits, or big holes as they are commonly referred to in this text, in Kimberley represent a unique situation for investigating natural slope phenomena which cannot be found elsewhere in the world. Not only has the whole of the latter part of the development of these big holes been by natural processes, but the geology of each big hole is essentially the same (although the thickness of the lithological units vary) and the plan shapes and dimensions of the stable rim of the kimberlite pipes differ, thus presenting a unique situation for evaluating the effects of plan radius of curvature and general shape of surface excavation on slope stability. Also, breaking-back of the big holes' slopes has been in progress for considerable time (about 75 years) with the result that they approximate the equilibrium condition. These slopes may, therefore, be considered to be in a state of limiting stability, i.e. they have a factor of safety of just less than unity. The location of De Beers Mine and the four other mines considered in this study, i.e. the famous Kimberley Mine and Wesselton, Dutoitspan and Bultfontein Mines, are given in Fig 1.1.

As the study had progressed it became apparent that the plan radius of curvature of the slopes has significant effect on the stability of the big holes in question and also that the major plan dimensions of the pipes are important factors for the stability of a curved slope. Factors such as rate of break-back, comparison of the effects of radius of curvature on the upper and lower parts of the slopes, mechanics of failure and the possible effects of regional stress were assessed.

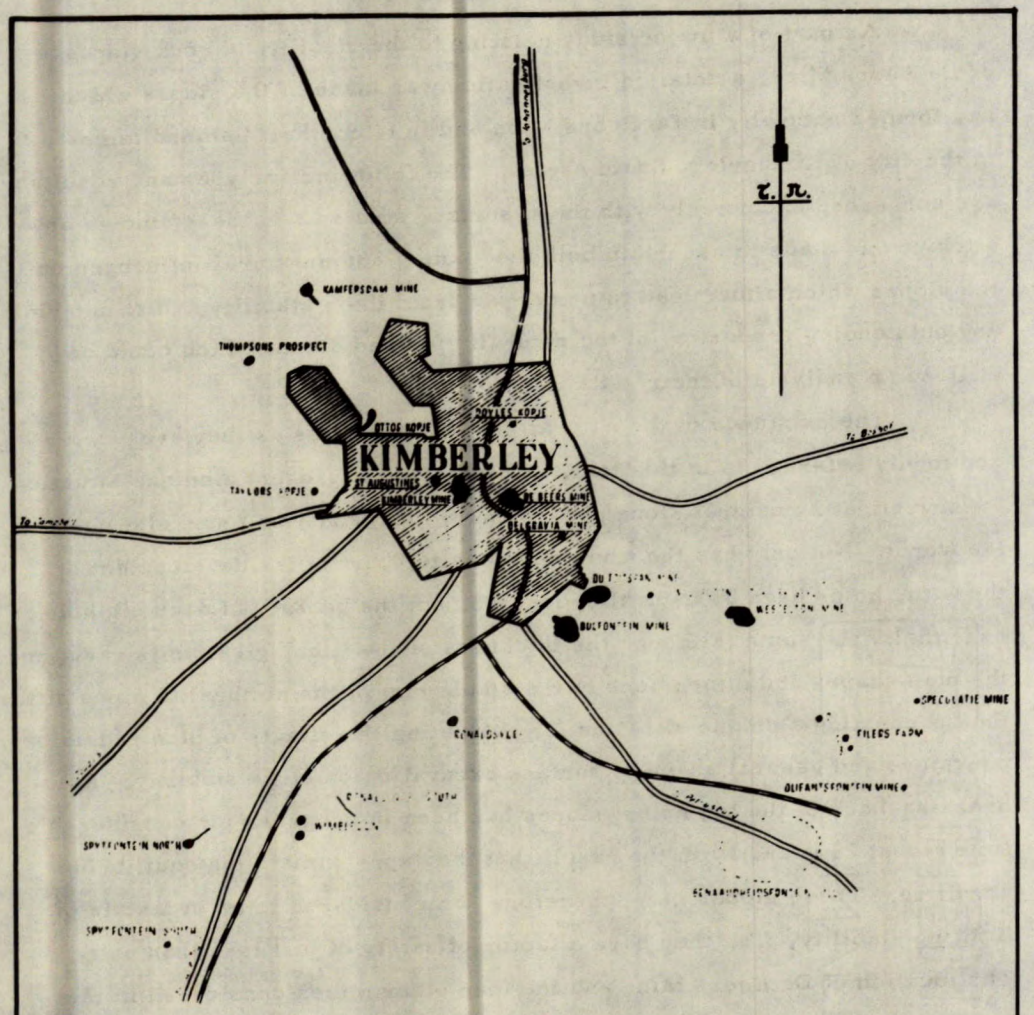

KIMBERLITE PIPES AND FISSURES
IN
THE KIMBERLEY AREA

FIG. 1.1

1.2 STATEMENT OF PROBLEM

De Beers Mine is located within the confines of the densely populated area of the city. The mine closed down in 1908 and since that time the city has developed within close proximity of the edge of the mine's open pit. As shown in Photo 1-(i), on the north and northwest sides of the pit, numerous buildings have been erected and at one point, a city street comes to within 130 ft of the pit edge. Also, the main Johannesburg-Cape Town railway line was built around the south and southwest sides of the pit and is 170 ft away from the open pit at one locality.

Because of the hard nature of the kimberlite in the northwest half of the pipe, except for a limited amount of surface mining in the early days, this section had never been mined from underground as had the other part of the pipe. After a series of preliminary studies, the mine was revaluated and plans were made to mine the remaining kimberlite. The mine was reopened and went into production in 1965.

As shown in Fig 1.2, the slopes of the open pit consist of dolerite overlying shale which have broken back to form an open pit around the pipe. Failed materials from these slopes have collected in that portion of the pipe that was originally occupied by the kimberlite and have filled the pipe to $320 \pm$ ft level at the top of the hard amygdaloidal lava or "melaphyre" which immediately underlies the shale. Since 1908, the dolerite and shale adjacent to the mined-out section on the south-east side have broken back to angles that approximate their natural angles of slope. These same materials that occur on the northwest side of the pit abut against the unmined kimberlite in the lower half of the slope and breakback has been negligible (see Fig 1.2, A-A). As kimberlite in this part of the pipe is mined, it is obvious that breakback of these slopes will continue until they too approximate angles of their natural slope. This would bring the pit edge considerably closer to adjacent civil works.

As mining proceeded, and simultaneously, drawdown of the rubble and kimberlite in the pipe took place, it was discovered that large blocks of the usually stable melaphyre at the south and northwest sides of the pipe were subsiding. The most serious of these subsidences was developing on the south side of the pit adjacent to the railway line, and fears were felt for the safety of this important works. At both of these locations subsidence was

Photo 1. (i) Oblique view of the De Beers Mine big hole showing the railway line and other civil works in close proximity.

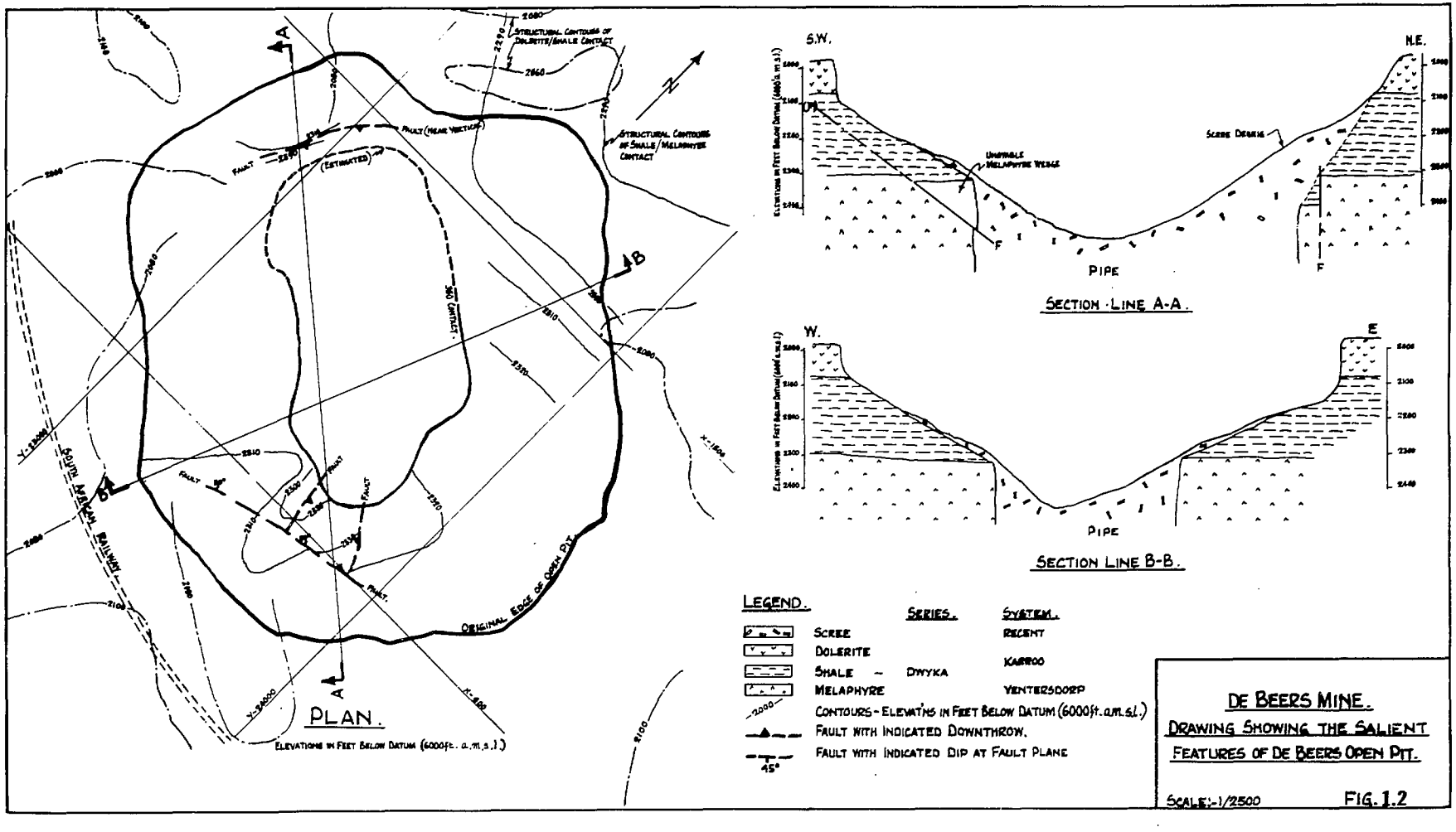

DE BEERS MINE.

DRAWING SHOWING THE SALIENT FEATURES OF DE BEERS OPEN PIT.

SCALE:- 1/2500 FIG. 1.2

associated with ancient faults in the melaphyre. The question arose as to whether the slopes, particularly on the south side of the pit, would breakback sufficiently far to jeopardize the railway line. Hence, the necessity arose to determine the long-term behaviour of the natural slopes in the area, the ultimate objective being to determine whether or not certain stability measures would be required if the slope were allowed to breakback naturally in time.

1.3. DESCRIPTION OF THE SURFACE STUDIES

These surface studies are dealt with in essentially three parts. The first part, Chapter 2, is concerned with a comparative analysis at De Beers Mine of the structural geology and related movements of the subsurface and an airphoto study of the open pit. Chapter 3, which forms the second part, deals with the studies of profiles of the naturally developed slopes of all the big holes in the Kimberley area. These studies involve examination of slope profiles to ascertain both the natural angles of slope of the particular formations in the area and the determination of the rate at which the respective slopes fail. The third and largest part of this study, consisting of Chapters 4 to 10 inclusive, is concerned with an analysis of effects of plan geometry on stability of the natural slopes of the big holes of the mines.

Unlike the analysis described in Chapters 2 and 3, the study of effects of plan geometry is not entirely self explanatory, therefore, further elaboration of this work is worthwhile at this point. As part of the studies of the natural slopes described in Chapters 2 and 3, an important objective was to determine whether there was any discernible effect of a regional stress field of a tectonic nature on slopes in the area. Regardless of the presence or absence of regional stresses as mentioned earlier, it was eventually discovered that the plan radius of curvature, R, of the pipe rim at the top of the melaphyre has an important effect on the angle of naturally developed slope. Smaller radii give rise to steeper slopes.

To determine these effects, the distance of breakback, D, of the big holes was measured and a clear relationship was found to exist between plan radius of curvature (R) of the toe of the slope and breakback

(D) of the slope. These data have been analysed statistically and an empirical relationship was produced relating breakback (D) and slope angle (i) to the plan curvature of the slope.

Theoretical aspects of stress geometry resulting from the effects of plan curvature of the slope on its stability are discussed in Chapter 4. Chapter 5 deals with procedures adopted to measure R & D and also is concerned with the analysis of R and D values. Based on the theory of the ellipse, a mathematical model of the R vs D is established and values R and D are examined seeking a suitable form of plot which would yield a straight line function. These analyses are described in Chapter 6.

In Chapter 7, having established what is considered to be a reasonable plot of the R and D data from the foregoing analysis, based on the general shape and plan geometry of the pipe, the final slope situation of the De Beers open pit is predicted for the case that no provisions be made to improve the situation. Chapter 8 is concerned with a comparative analysis of slope angles of the upper and lower parts of the slope for small and large curvatures of slope. Model tests to determine the effects of plan curvature on cohesionless slope forming materials are described in Chapter 9. From these results the principle mode of failure in the area is hypothesized. In Chapter 10 a series of analyses of the R and D data are conducted to ascertain if regional stress is present in the Kimberley Mines which is of sufficient magnitude to affect the slopes. In these analyses values of D are examined in different ways for cyclic variations which have an amplitude of 180°.

Various aspects relating to underground and surface structural analyses and general stability analyses work concerning De Beers Mine can be found in Jennings (1970), Robertson (1970) and Piteau 1970a and 1970b.

Chapter 2

AIRPHOTO STUDY OF DE BEERS MINE BIG HOLE

2.1 INTRODUCTION

In the early stages of the De Beers Mine investigation a stereoscopic airphoto study of the big hole was carried out. The purpose of this study was to gain a better understanding of the geological environment and to determine the factors which are conducive to instability. With respect to subsurface movement phenomena an attempt was made to reconstruct the sequence of recent events at the site from recognized signs and expressions observed in the photos. With the prospect of studying the natural angle of slope of the materials, a concerted effort was made to determine slopes that were approximately in a state of equilibrium.

2.2 METHOD OF APPROACH

Considerable success has been obtained with airphoto studies as applied to engineering practice - notably by Mollard (1962), Liang and Belcher (1957) and Brink and Williams (1964) and some of their basic principles have been adopted in this study.

An effort was made to analyse the state of fracturing in the slopes to delineate areas affected by movements and to assess the extent of the movements. In this respect attempts were made to correlate slope movements with known deep-seated failure blocks and to determine the extent of their modification by natural slope forming processes.

To facilitate this study all subsurface findings on the 150-, 350- and 412- ft levels were taken into account and were used by super-imposing information of major features through the super-position of a transparent airphoto study sheet which contained all surface information. In this way it was possible to study surface configuration and expression comparatively with subsurface movements and major discontinuities. Through extrapolation, this procedure assisted in pointing out the expected surface trace of discontinuities that had been delineated by subsurface exploration.

The history of mining and change in surface configuration was also considered. The section of kimberlite on the northwest side of the pipe, for example, had only recently been pulled down by underground mining; therefore, the lower half of the slope above the melaphyre rim in this area had been exposed to weathering conditions of the atmosphere

for a relatively short period only and this was considered. A comparison between the 1938 and the present day shape of the edge of the big hole was made to determine which parts have been prone to failure.

Using these methods it was possible to determine why certain slopes have been stable in the past when others have not, and why some slope movements are old and have been stabilized for a long time while others are still active. This was also helpful in assessing the rate and character of slope failure as well as whether failure was relatively shallow or deep. Finally it was possible, after evaluation of all the information at hand, to predict with reasonable certainty which slopes were stable and which of these were representative of long-term stability.

2.3 RESULTS

The results of the airphoto interpretation and subsequent comparative analysis with the subsurface information are shown in Fig. 2.1 included in which is a set of notes describing the salient features and their relationship to slope configuration and other phenomena.

Approximately 75 per cent of the slopes were found to be in a transitory state - either in a phase of ravelling and talus accumulation or in a state of slow translation due to failure in the melaphyre. The talus consists essentially of large blocks of dolerite that have become detached from the upper part of the slope end of cohesionless masses of argillaceous material.

Relative to other parts of the big hole, the south slopes in the vicinity of the major fault where subsidence occurred are topographically depressed giving a "dished out" appearance due to progressive failure. In this area surface stretching and other micro features confirm that these slopes are active. A lineal depression forms a pronounced topographic expression where a section of the hanging-wall of the melaphyre has slid into the pipe leaving an elongate slide chute. This has resulted in a gap occurring in the melaphyre pipe rim which, with the exception of subsidence at the north side, has been otherwise well preserved.

Comparison of past and present plan configuration of the big hole indicates that failure has been confined mainly to the slopes adjacent to the major fault located next to the railway. These slopes

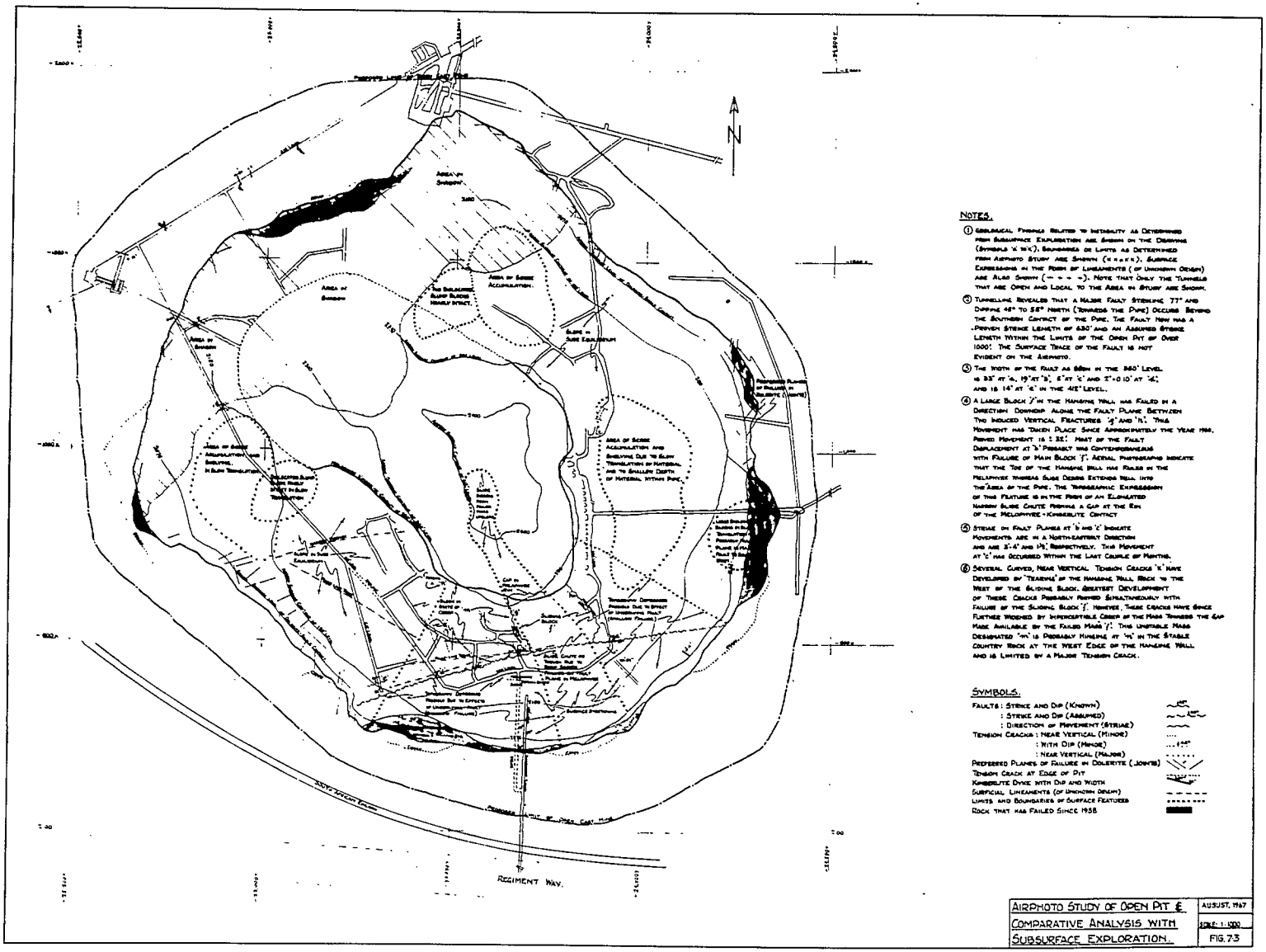

AIRPHOTO STUDY OF OPEN PIT ℄	AUGUST, 1967
COMPARATIVE ANALYSIS WITH	SCALE: 1:1000
SUBSURFACE EXPLORATION.	FIG. 7.3

FIG.2.1

have not only been exposed considerably longer (i.e. approximately 75 years) than adjacent and opposite slopes, but have also been unloaded at the toe due to failure in the melaphyre. The slopes on the north side have been exposed to the atmosphere for a relatively short period only and any toe subsidence in this area has been recent.

Two kimberlite dykes, which had not been known to exist previously at surface, were located using the comparative airphoto - subsurface extrapolation technique. Both of these dykes, since they were highly altered, represent large discontinuities in the mass. One of these dykes, because of differential weathering and erosion as a result of its extreme susceptibility to chemical decomposition in the atmosphere, showed up as a distinct gap in the shale in the slope.

Significant inferences and facts relative to the general geology and to the cause, patterns, mechanics and potentialities of movement were uncovered in this study. As shown in Fig. 2.1, the only slopes that appear to be at their natural angle of slope and to be in a state of equilibrium, are isolated sections on the southwest and northeast sides of the pipe.

Chapter 3

PROFILE STUDIES OF THE NATURALLY FORMED SLOPES OF THE BIG HOLES IN THE KIMBERLEY AREA

3.1 THE BIG HOLES

The occurrence of several mines with big holes in the Kimberley area presented a unique opportunity to investigate both the natural and unnatural factors that influence breakback of these slopes. All of the big holes have been exposed for approximately 75 years and for nearly the whole of this period they have developed through natural slope forming processes.

In each of these big holes the same geological sequence is found (i.e. dolerite overlying shale which is underlain by melaphyre), but the thickness of the lithological units vary and the plan shapes of the holes differ. The location of these mines is shown in Fig. 1.1, Surface dimensions of the big holes and the shape and dimensions of the respective pipes, as seen at the level of the shale-melaphyre contact, are given in Table 3.1.

The slopes break back into the mined out portion of the pipe. The upper part of the big holes, having broken back in the dolerite and shale, look very much like large funnels as shown in Fig. 3.1. The pipe rim provides a stable toe of fixed shape at the base of the shale slope. The pipe itself acts merely as a collector of the failed shale and dolerite materials. In a sense, the stable pipe rims represent a condition which is analogous to draw-off orifices of various shapes in the bottom of a box.

In consideration of pipe dimensions and average slope height it can be seen that the De Beers Mine in both cases falls within the ranges of the other mines (see Table 3.1). The Bultfontein and Kimberley pipes are the largest and smallest, respectively, of the group. The latter is also the smallest with respect to composite slope height, whereas Wesselton is the largest.

3.2 DETERMINATION OF THE NATURAL ANGLES OF SLOPE

3.2.1 Introduction

One practical approach to obtaining

Table 3.1

Dimensional, Shape and Areal Characteristics of the Big Holes

Mine	Pipe Dimensions (ft)		Big Hole Dimensions (ft)		Area (sq ft)		Average Slope Height⊕⊕ (ft)	Pipe Shape
	Length	Width	Length	Width	Pipe	Big Hole		
Kimberley	900	520	1,490	1,480	338,900	1,682,600	273	elongate
Dutoitspan⊕	1,280	730	2,300	1,760	633,000	1,232,600	341	semi-elongate
Bultfontein	1,100	930	2,420	1,880	816,100	2,843,000	339	round
Wesselton	1,260	600	1,900	1,500	670,100	2,383,200	367	kidney
De Beers	1,200*	550	**	**	617,000	**	320	elongate

* Pipe dimensions are taken to include the stable rim of the pipe.

** Values to be predicted.

⊕ Dimensions refer to the west half of the pipe that was used in the study.

⊕⊕ Refers to the composite height of the dolerite and shale.

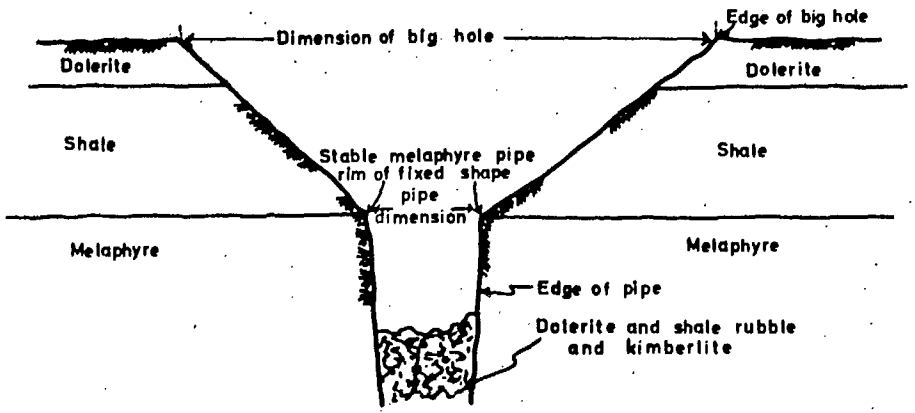

Fig. 3.1. Characteristics of typical big hole in the Kimberley area.

preliminary design of slopes is through examining the slope configuration of stable slopes in the same formation as the proposed slope. It is this aspect which is to be considered here. It is appreciated that, although some guidance in determining the final slope angle can be obtained from a slope that has been surveyed and is known to be stable, such results become completely invalid if any unfavourably orientated major structural zones of weakness exist within the critical zone of the studied formation.

Profiles of the big holes were examined with the view that the natural angles of slope of the respective slope forming materials could be ascertained. Profiles were considered only in areas that were geologically normal and appeared to be in a state of equilibrium. Areas that were affected by conditions such as faulting, abnormal groundwater conditions, burning shales and shelving of slope forming materials were not considered.

3.2.2 Method of Approach

Care was taken to measure profiles that were representative of the intact slope forming materials and not of the loose talus. Slopes covered with deep talus can give misleading results. Metcalf (1966) and others point out that the natural angle of slope of a jointed rock mass can be smaller than the slope angle of the same material if it is blasted and heaped in a pile. In this respect the natural angle of repose of loose talus, being approximately equal to the angle of internal friction of uniformily shattered rock under drained conditions (Lacy, 1964), can be greater than the natural angle of slope of the in situ rock itself due to the unfavourable effects of groundwater in the mass.

The precise combination of environmental characteristics which influence the stability of any given excavation differs from place to place. Hence, comparison of the slope profiles on different sides of the pit was made. Consideration was given to conditions such as jointing, sun radiation and other directional effects which may be overriding factors that influence the ultimate slope angles. In this respect special consideration was given to ascertaining whether the indurated shale was significantly different from its unindurated equivalent.

Contour plans were prepared from aerial photographs taken in 1967 of the various big holes and profiles were produced from the respective surface contour drawings. Twelve, ten and fourteen slope profiles were taken of the De Beers, Kimberley, and Bultfontein big holes, respectively. At De Beers Mine, profiles were taken initially on a random basis, but

following the airphoto study another set was selected that was felt to be representative of natural stable slopes. For the other two mines two profiles were taken where possible at each of eight locations which were equally distributed around the perimeter of the big holes. The majority of the northwest faces of all the big holes were in shadow, hence profiles could not be taken in these areas.

In consideration of the geological environment the following factors were considered:

(i) The slope angle of the top 100 ft of the shale ("top 100' section") in each profile was considered separately from that of the section below ("lower section"). This was done with a view to ascertaining whether induration of the shale had significantly influenced the natural angle of slope in these materials. The thickness of 100 ft was arbitrarily chosen based on the approximate distance that these effects are seen to occur on adjacent sediments in other parts of the Karroo; also the profiles generally showed a change at this point. A profile of a typical slope is shown in Fig. 3.2.

(ii) Approximate duration of exposure (age) of the slopes.

(iii) Approximate amount of sun radiation that a north, south, east and west facing slope is exposed to in the period of a year.

(iv) Mean thickness of the shale and dolerite.

(v) Lithological variation in the shale.

(vi) Jointing in the dolerite and shale.

(vii) Depth of the water table.

With respect to profiles of the dolerite slopes, only those of the Kimberley and De Beers Mine could be used, since most of this material at Bultfontein Mine had either been affected by man or by some anomalous geological condition. The slope angles in the dolerite were considered in two ways. One approach was to include the talus at the base of the sill and the other was to make a reasonable estimate of the mean angle of slope of the in situ dolerite underlying the talus. The former case generally gave flatter profiles but the latter approach was considered the more realistic of the two.

3.2.3 Results

Of the factors listed above none appeared sufficiently different

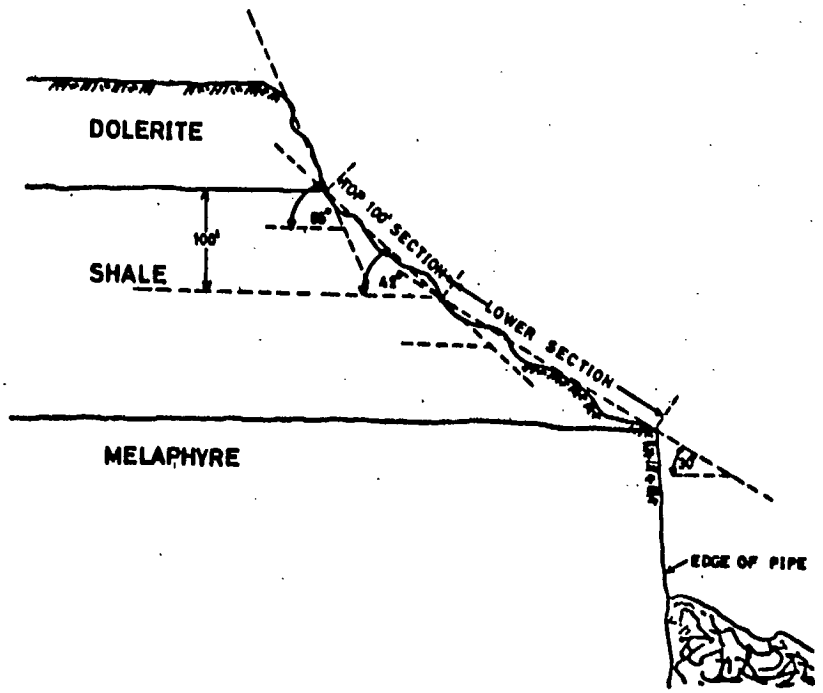

Fig. 3.2. Slope profiles of typical big hole.

at each big hole to significantly affect the pattern of breakback or to introduce a direction bias in the data. The mean slope angles for the shale for the "top 100' section", "lower section" and entire slope ("overall slope") are given in Table 3.II and are summarized in Table 3.III. The results for De Beers Mine include only those profiles of random distribution.

These results show that in each case the natural angle of slope of the "top 100' section" is greater than that of the "lower section", which indicates that induration of the sediments has resulted in substantial toughening of the materials and increased their resistance to natural slope forming processes. The steeper slopes in the "top 100' section" may, however, be partly due to the protective capping provided by the dolerite. Also, the effects of groundwater are more significant in the "lower section" of the shale slope.

It can be seen that the mean angles of slope for De Beers Mine are lower than for the other two mines. This is to be expected since the profiles were randomly selected and thereby included the broad area on the south side of the pipe that had been affected by subsidence failure on the large fault. Also the general level of the material in the pipe is approximately at the shale-melaphyre contact, whereas at the other two mines the material in the pipe is at a much lower level. Unlike the other mines, the talus materials have not been able to run freely off the slopes due to tremendous volumes of these materials collecting at the toe of the slope.

Table 3.III

Summary of Angles of Shale Slope Profiles

Mine	Mean Angle of Slope		
	Top 100' Section	Lower Section	Overall Slope
De Beers *	35.20° (12) **	28.44 (8)	31.81°
Kimberley	38.60° (10)	33.56° (8)	36.08°
Bultfontein	38.78° (14)	30.25° (10)	34.51°
Mean	37.52° (36)	30.75° (26)	34.10°

* Includes profiles of random selection.

** Number in bracket refers to the number of profiles measured.

Table 3.II

Slope Angles of Profiles of Shale Slopes

Slope Location*	Mine	Mean Angle of Slope					
		Overall Slope	Number of Profiles	Top 100' Section	Number of Profiles	Lower Section	Number of Profiles
North	De Beers **	31.93°	4	34.00°	4	29.87°	4
	Kimberley	39.00°	2	41.00°	2	37.00°	2
	Bultfontein	26.87°	2	32.00°	4	21.75°	2
	Mean Angle	32.60°		35.66°		29.54°	
South	De Beers**	30.22°	4	33.45°	6	27.00°	4
	Kimberley	33.21°	4	35.33°	6	31.10°	4
	Bultfontein	35.49°	4	40.91°	6	30.18°	4
	Mean Angle	32.97°		36.56°		29.42°	
East	De Beers **	32.81°	4	35.00°	6	30.62°	4
	Kimberley	36.24°	4	39.62°	4	32.87°	4
	Bultfontein	31.46°	4	39.18°	6	23.75°	4
	Mean Angle	33.50°		37.93°		29.08°	
West	De Beers **	-	-	29.75°	2	-	-
	Kimberley	37.12°	2	42.00°	2	32.25°	2
	Bultfontein	41.31°	4	45.12°	4	37.50°	4
	Mean Angle	39.21°		38.95°		34.87°	

* Profiles used for one slope location could have been used at another, e.g. a profile at the northeast side would be considered in evaluating both the north and east slopes.

** Profiles for De Beers Mine are randomly distributed.

These initial profile results from De Beers Mine were considered unrealistic and, therefore, after the detailed airphoto-subsurface comparative analysis was conducted further profiles were selected. The slopes considered representative of the long-term stable condition consisted of two sections only, confined to small areas on the northeast and southwest sides of the pit as shown in Fig. 2.1. The slopes of the entire northwest half of the pit were not representative of the long-term condition since these had been exposed for only a short time and had not had time to break back to their natural slope. Eleven profiles were selected, six on the northeast side (i.e. profile numbers 1 to 6) and five on the southwest side (i.e. profile numbers 7 to 11). Profiles 1 to 6 are considered the most reliable of the two sets. The results of these profile surveys are given in Table 3.IV.

Table 3.IV

Shale Slope Angles from De Beers Mine
Stable Slopes

Side of Pit	Profile Number	Angle of Slope		
		Top 100' Section	Lower Section	Overall Slope
Northeast	1	43°	27°*	
	2	43°	32°	
	3	41°	32½°	
	4	38½°	27	
	5	48½°	31°	
	6	46°	34°	---------
Southwest	7	29°*	27°⊛	37.31° ***
	8	23°*	⊛⊛	
	9	42½° **	⊛⊛	
	10	24° **	⊛⊛	
	11	38° **	⊛⊛	
Mean Angle		45.40°	31.30°	35.90°

* In close proximity to area affected by fault - omit.

** Reliability of slope angles in doubt.

*** Mean value of profiles 1 to 6.

⊛ Slope affected by surface drainage - omit.

⊛⊛ Talus accumulated at toe of slope.

In comparing the De Beers results of randomly distributed profiles in Table 3. III with those selected in Table 3. IV, it can be seen that the selected slopes are somewhat steeper. The results show that the mean angle of slope from the selected profiles for the "top 100' section" is 40. 50° using profiles 1 to 11 and 43. 33° using profiles 1 to 6, as compared to 35. 20° for the randomly distributed profiles. The mean angle of slope for the "lower section" selected profiles is 31. 30°, as compared with 28. 44° for those taken at random. For the selected profiles the mean "overall slope" is 35. 90° using profiles 1 to 11, and 37. 31° using profiles 1 to 6, compared with 31. 82° for the random profiles.

With regard to the natural angles of slope of the dolerite, as shown in Table 3. V, if the values for Bultfontein are included the angles are 58. 6° and 71. 6° for the two different types of profiles, the estimated profile being the steepest. With the Bultfontein results

Table 3. V

Slope Angles of Profiles of Dolerite Slopes

Mine	Mean Dolerite Thickness (ft)	Mean Angle of Slope	
		Including Talus	Estimating Solid Profile
De Beers (random profiles)	90	63. 5°(14) *	78. 8°(14)
De Beers (selected profiles)	90	74. 8°(11)	77. 2°(11)
Kimberley	81	52. 4°(10)	72. 5°(12)
Bultfontein	57	43. 5°(14)	58. 0°(14)
Mean (including Bultfontein)		58. 6°	71. 6°
Mean (excluding Bultfontein)		63. 5°	76. 2°

* Number in brackets refers to the number of profiles measured.

excluded, these values are upgraded by about 5°, to 63. 5° and 76. 2° respectively.

3. 2. 4 Summary and Conclusions

Incorporating the results for Kimberley and Bultfontein

Mines given in Table 3.III with those for De Beers Mine in Table 3.IV, it would appear that a reasonable estimate of the natural angle of slope of both the indurated and unbaked shale can be obtained. As shown in Table 3.VI, if all eleven profiles are considered the mean angles of slope for the "top 100' section" and the "lowest section" are 39.29° and 31.70°, respectively. If only profiles 1 to 6 are taken, as shown in Table 3.VII, the angle for the "top 100' section" becomes 40.23°, but that of the "lower section" remains at 31.70°. In view of the fact

Table 3.VI

Shale Slope Profiles of Bultfontein and Kimberley Mines Incorporated with Selected Profiles 1 to 11 of De Beers Mine

Mine	Mean Angle of Slope		
	Top 100' Section	Lower Section	Overall Slope
De Beers	40.50°	31.30°	35.90°
Kimberley	38.60°	33.56°	36.08°
Bultfontein	38.78°	30.25°	34.51°
Mean	39.29°	31.70°	35.49°

Table 3.VII

Shale Slope Profiles of Bultfontein and Kimberley Mines Incorporated with Selected Profiles 1 to 6 of De Beers Mine

Mine	Mean Angle of Slope		
	Top 100' Section	Lower Section	Overall Slope
De Beers	43.33°	31.30°	37.31°
Kimberley	38.60°	33.56°	36.08°
Bultfontein	38.78°	30.25°	34.51°
Mean	40.23°	31.70°	35.96°

that the spread of results is relatively small in both cases, it seems reasonable to accept the mean natural angle of slope for the "top 100' section" and the "lower section" to be of the order of 40° and 32°,

respectively.

For the dolerite the procedure in estimating the solid profile is the more realistic of the two methods adopted and, regardless of whether Bultfontein results are included or not, the results give angles greater than 70°. Taking all factors into consideration, the natural angle of slope of the dolerite appears to be conservative yet realistic for an angle of the order of 70°.

It should be appreciated that these angles are taken for only stable slopes and the standard deviation (σ_d) on the slope angle data has not been taken which would result in the acceptable angles being considerably lower.

3.3 DETERMINATION OF THE RATE OF BREAKBACK

Northsouth and eastwest profiles of the slopes of the big holes in the Kimberley area have been taken on a semi-regular basis dating back to 1912 and some are as recent as 1964. By comparing the profiles on their respective section locations, an attempt was made to establish an approximate idea of the rate the slopes fail or break back under natural conditions.

The various profiles for the different years were superimposed on their respective sections and the distance between the top of the oldest and most recent profiles was measured, as shown in Fig. 3.3. In this way it was possible to ascertain, at least for that period under consideration, the extent of breakback in time. Both northsouth and eastwest profiles of Bultfontein and Wesselton Mines, and eastwest profiles of Dutoitspan Mines were available for study. It was decided to use only the oldest and youngest profiles available at each location because profiles taken of intermediate periods were few in number.

Of ten profiles available, five could not be used because of abnormal conditions in the slope, leaving a relatively small amount of available information. The data recorded from the usable profiles is given in Table 3.VIII. It can be seen that the average amount of breakback per year, here designated as "rate of breakback", varies between values as high as 5.58 and 4.53 ft/yr and as low as 0.48 and 1.58 ft/yr, the mean value being 2.87 ft/yr.

The large variation in results would tend to indicate that other factors had had a significant effect during the period considered. Probably the most outstanding of these factors are the general effects

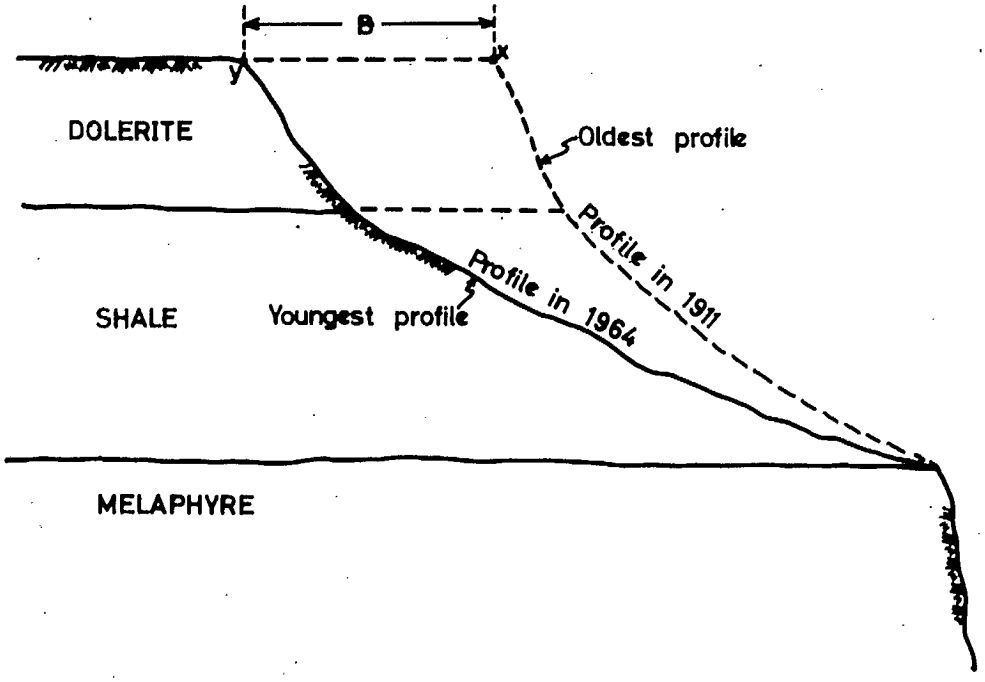

Fig. 3.3. Idealized big hole slope illustrating typical breakback measurement between the oldest and youngest profile.

Table 3.VIII

Breakback Measurements Between the Oldest and Youngest Slope Profiles

Mine	Profile Location	Date of Profile		Difference in Breakback B (ft)	Rate of Breakback $\frac{B}{y-x}$ (ft/yr)
		Oldest (x)	Youngest (y)		
Dutoit-span	East side	1912	1964	290	5.58
Bultfon-tein	West side	1912	1960	100	1.08
	South side	1912	1954	195	4.64
Wessel-ton	West side	1912	1931	30	1.58
	South side	1912	1964	25	0.48
					Mean = 2.87

of environment. That is, some of the slopes in question may have reached a position which approximated their natural angle of slope by, say, the early 1900's for reasons which are mainly man induced, such as for both early open cast and subsequent underground ore selection. Wesselton Mine might fall into this category. Some slopes, on the other hand, may not have approximated their natural slope angles until the mid 1900's. Slopes falling into this category would obviously show a greater difference in breakback (B) during the period studied. Both Dutoitspan and Bultfontein Mines might fall into this category. In either case, as the slope approaches its natural angle, the rate at which the slope breaks back would conceivably decrease.

Insufficient information is available to consider the results to be conclusive: the final position of the pit slopes when the initial open cast mining had ceased, for example, is not known and the general history of the underground mining and the respective disposition of the blue ground in the pipe is obscure. It would have been useful also to have known where the major stockpiles of talus and rubble had been situated in the past, since these accumulations would significantly reduce the breakback of the slope.

Also the thickness of the dolerite and shale varies. It is difficult to predict the effects of change of thickness on the rate of breakback, although it is believed that the rate of failure of a rock slope is related to the ratio of maximum to residual shear strength of the rock forming the slope. In this case the effects of varying thickness of the dolerite may be fairly significant. The dolerite, like any hard rock, would be expected to exhibit a high maximum to residual shear strength ratio and therefore be capable of supporting a much steeper slope than a softer rock. Failure of such rocks probably takes place suddenly. A soft rock such as shale, which can be expected to have a small maximum to residual strength ratio, will support a slope considerably flatter than a harder rock like dolerite. In contrast to the dolerite, the shale will more than likely fail slowly as is usually seen to be the case under normal conditions.

Due to the considerable variation of environmental factors from one mine to another, a value of the rate of breakback can not be determined which would generally apply to any proposed cut in the Kimberley area. The results shown in Table V. III would apply for the particular slope in question for the individual holes only. However, as a preliminary estimate for predicting the rate of breakback, the mean value of 2.87 ft/yr might be used as an approximate figure upon which to proceed. This figure though, should be used with discretion and considerable judgment must be exercised in comparing the history of the studied slope to that which is to be predicted.

3.4 DISCOVERY THAT THE PLAN RADIUS OF CURVATURE OF THE PIPE MARGIN AFFECTS STABILITY OF THE SLOPES OF THE BIG HOLES

During examination of the general configuration of the slope profiles of the big holes for signs of regional stresses or some other directional effects, it was recognized that within the same big hole some sections were obviously much steeper than other sections. The reason for this phenomenon could not be explained through geological reasoning, nor could it be attibuted to coincidence. It was apparent that some other significant factors were affecting the natural slope development, either favourably or unfavourably, that had not be accounted for.

Upon closer inspection it could be seen that the steepest slopes in the big holes invariably occur adjacent to the ends of the pipe. That is, the slopes are steepest where the radii of curvature of the pipe margin

are least. This phenomenon is illustrated in Photo 3. (i) and 3. (ii) of the famous Kimberley Mine "Big Hole".

After it was recognized that the radius of curvature of the pipe margin had a direct bearing on the extent of breakback of the materials overlying the melaphyre, an extensive study was carried out to ascertain these effects quantitatively. From this study it was anticipated that, provided it could be shown that there was a statistical normality in the relationship between radius of curvature of the slope and slope breakback, a reasonable estimate of the final edge of the De Beers Mine could be made when its slopes eventually break back to their natural angle.

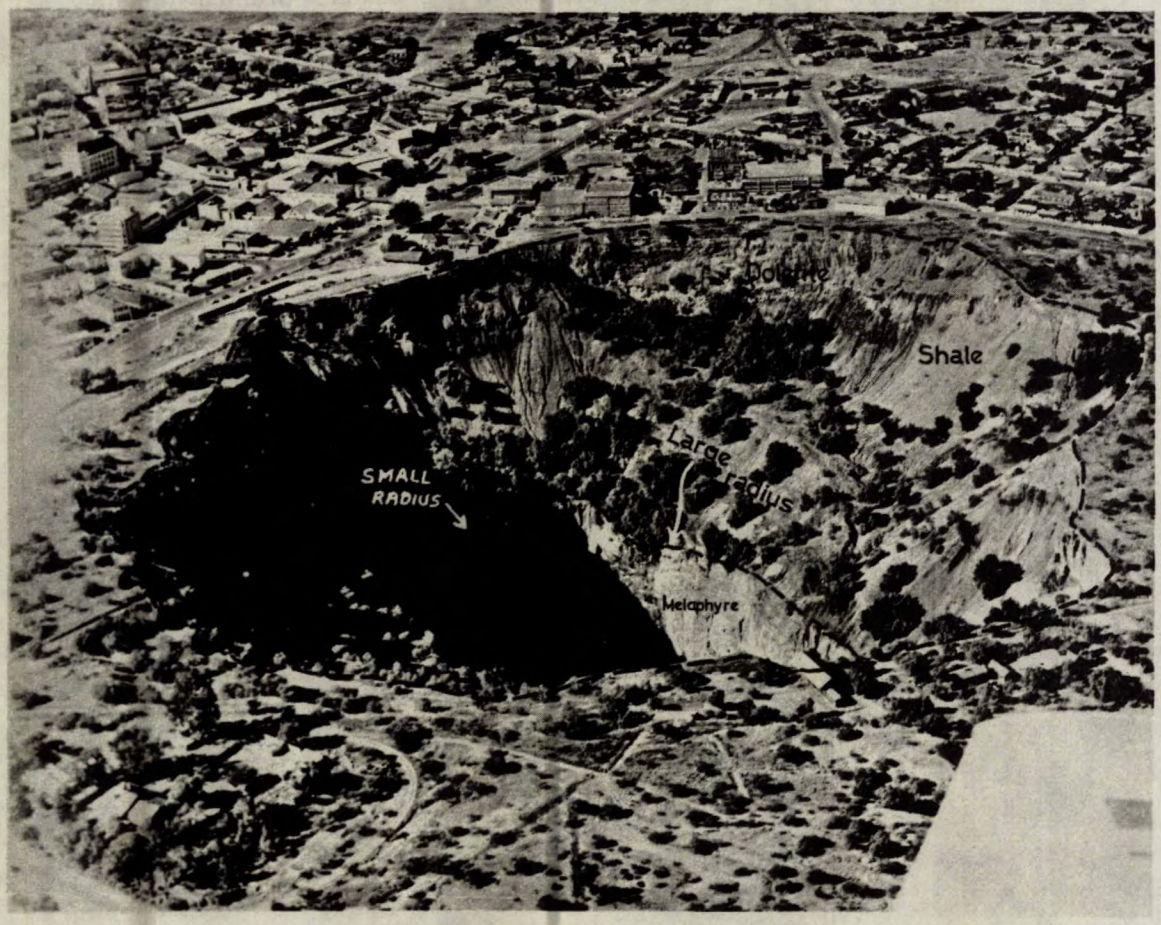

Photo 3. (i). Oblique view of the Kimberley Mine "Big Hole" showing that the slopes are steepest where the radii of curvature of the pipe margin are least.

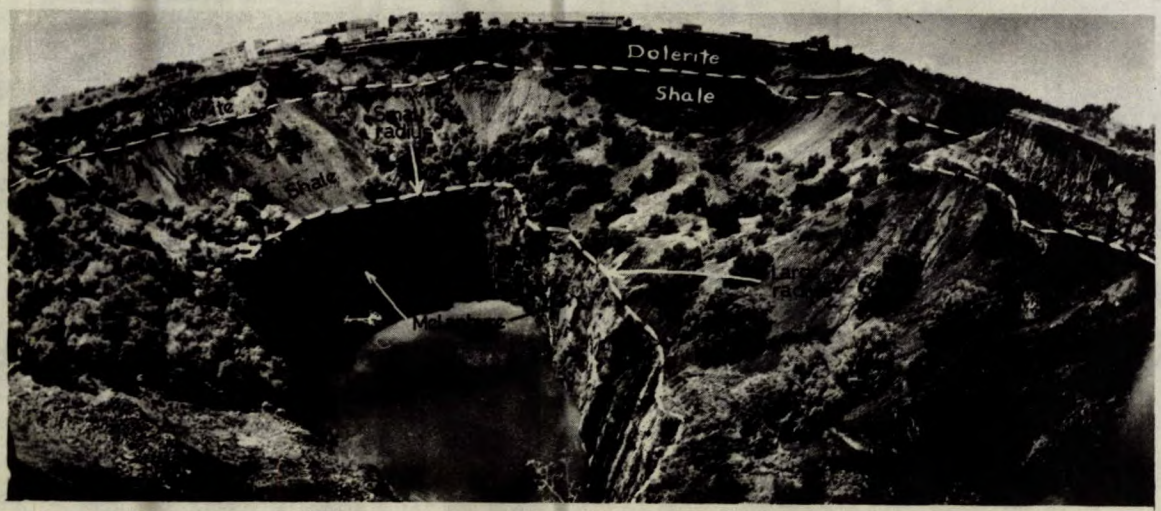

Photo 3. (ii). Oblique view of the Kimberley Mine "Big Hole" showing that the slopes are steepest where the radii of curvature of the pipe margin are least.

Chapter 4

CONCEPTS AND FINDINGS RELATING TO THE EFFECTS OF PLAN CURVATURE ON STABILITY OF ROCK SLOPES

Current theories of slope stability all deal with the slope as a two-dimensional problem, i.e. a slice of unit length of an infinitely long slope is considered for a condition of plane strain. In this the tacit assumption is made that the plan radii of the crest and toe of the slope are infinite and no attention is given to the plan geometry of the slope. This is not the condition encountered in practice, particularly in open pit mining where these radii of curvature can have important affects on the slope stability. That is, the slope angle is not only a function of slope height, strength of the mass and geometry of structural discontinuities, but also is dependent upon the plan geometry of the slope. Technically speaking, adequate analysis of the slope must be three-dimensional, the third dimension being that of plan geometry and the analysis that of its subsequent effects.

Before proceeding with the analysis of the effects of plan geometry on the natural slopes in the Kimberley area, it is worthwhile examining the findings of some workers relating to the concepts of the distribution of stress, etc. due to plan geometry and the manner in which this appears to affect the stability of slopes in rock.

We know that for an infinite slope (i.e. a straight slope in plan) normally specified in rock mechanics, if there is cohesion, c, a slope can be steeper than that indicated by the angle of friction ϕ. However, as such a slope is descended, the effect of cohesion relative to the friction on the strength of the material decreases in which case the slope flattens out to the angle of internal friction (ϕ). As shown in Fig. 4.1, the profile of this slope is concave with an overall angle of slope i_1 from top to bottom and a natural distance of breakback (D_1).

Jenike and Yen (1963) show that this is not the case for a slope which is concave in plan. They claim that the slope will be multiple, as shown in Fig. 4.2 with an angle of slope i_2 and breakback D_2 where $i_1 < i_2$ and $D_1 > D_2$. They examine the effects of curvature on angle of slope for homogeneous solid material obeying a yield function and the analysis assumes plastic, and not elastic, behaviour of the medium. The radius at the top of the hole is assumed to be defined by $R\,\gamma/c$. The safe slope angle, θ_{min}, for the curved slope in axial symmetry, is plotted as a

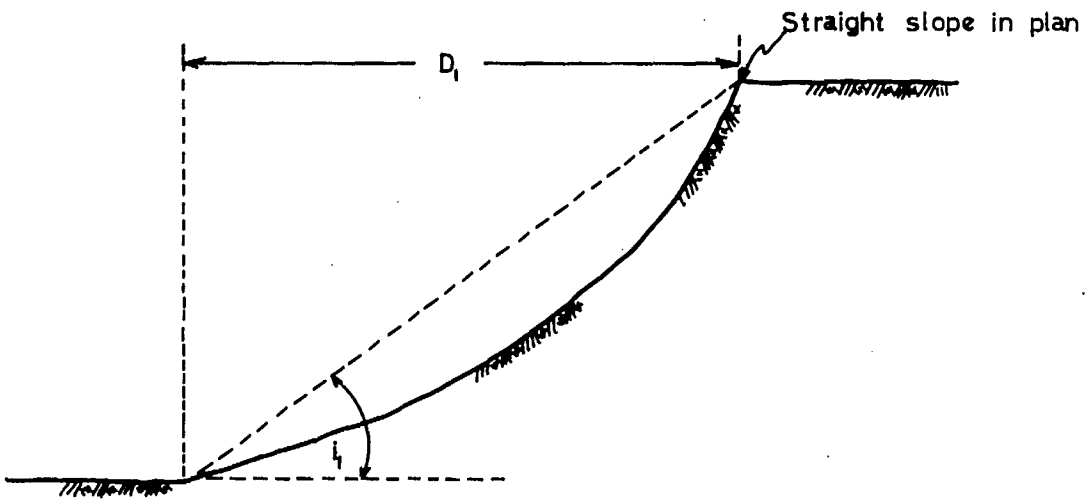

Fig. 4.1. Straight slope in plane strain with concave curved profile.

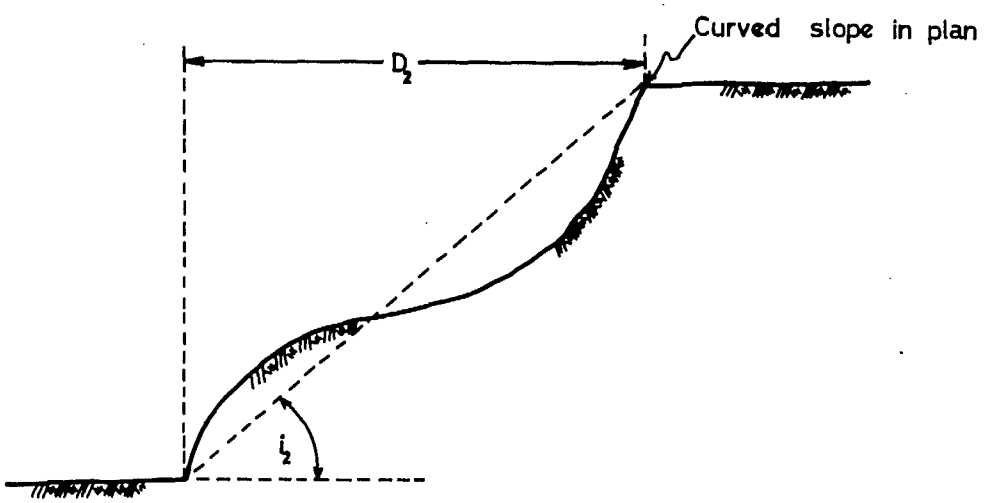

Fig. 4.2. Concave curved slope in plan with multiple profile due to plan radius of curvature effects.

function of $R\gamma/c$ for several values of ϕ, as shown in Fig. 4.3, where

R = radius of curvature at the top of the excavation

γ = unit weight of the material

c = cohesive strength

ϕ = friction angle

The double curvature in the slope in Fig. 4.2 appears to arise from the stabilizing effect of the decreasing radius of the hole which explains why θ_{min} increases as R decreases. They suggest that the safe slope in plane strain is equal to the friction angle ϕ and curvature on the axis of symmetry increases the safe slope in plane strain. As R increases to infinity, the enclosing effect of the decreasing radius of the central portion of the slope is negligible and θ_{min} approximates the value of ϕ. That is, as the radius of horizontal curvature of the slope increases the profile of the stable slope in axial symmetry approaches the profile of the stable slope in plane strain.

Long et al. (1966) put forth the idea that tangential stress concentrations in the boundary of an open pit develop as a function of the horizontal component of the stress field, the horizontal stress being developed "by lateral constraint of rock load by the overlying material, by tectonic forces, or by both". Further, the tangential stress concentrations could be either compressive or tensile depending upon the pit geometry and the horizontal stress field and that the former would be favourable for stability if these stresses do not exceed the strength of the rock, whereas the latter would be unfavourable.

Horizontal stresses tangent to the pit slope would be beneficial in a concave slope since they create an arch-like effect, whereby the blocks forming the partitioned rock mass will tend to be squeezed together and compressive stresses will substantially improve the shearing strength, corresponding to a cohesion (Long et al. 1966). Hoek and Pentz (1968) note that according to Leeman (1964), as shown in Fig. 4.4, in the case of the concave slope all three principal stresses are compressive and the maximum (σ_1) and minimum (σ_3) stresses act in the vertical and radial direction, respectively. Hence, a tangential compressive condition results.

For the convex slope the converse is the case in that the tangential stresses are tensile. In the case of the convex slope in Fig. 4.5, the maximum principal stress (σ_1) is still vertical whereas the minimum principal stress (σ_3) acts in a direction tangent to the slope and the slope material is in tension. The cohesion that would normally have occurred,

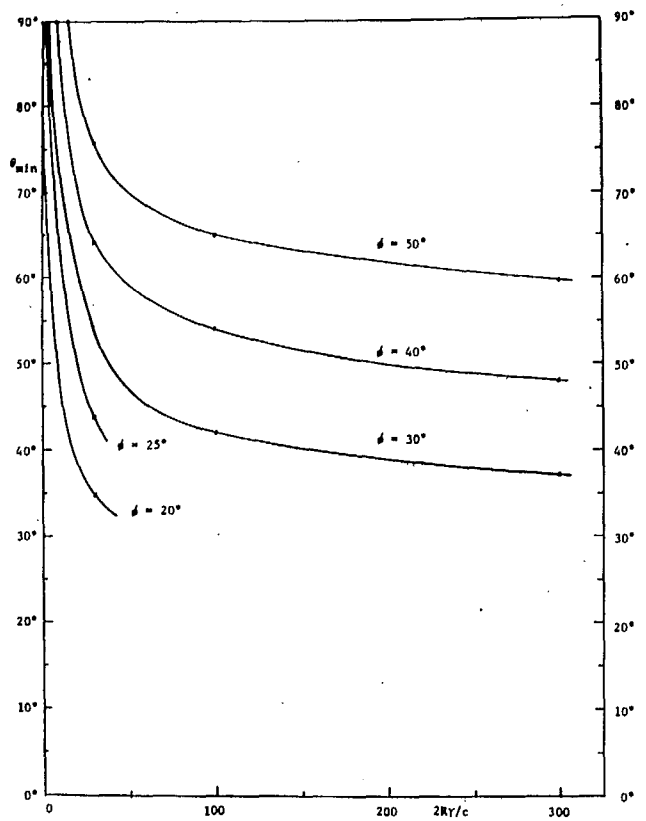

Fig. 4.3. Plot of the safe slope angle θ_{min} as a function of $R\gamma/c$ for different values of ϕ (after Jenike and Yen, 1963).

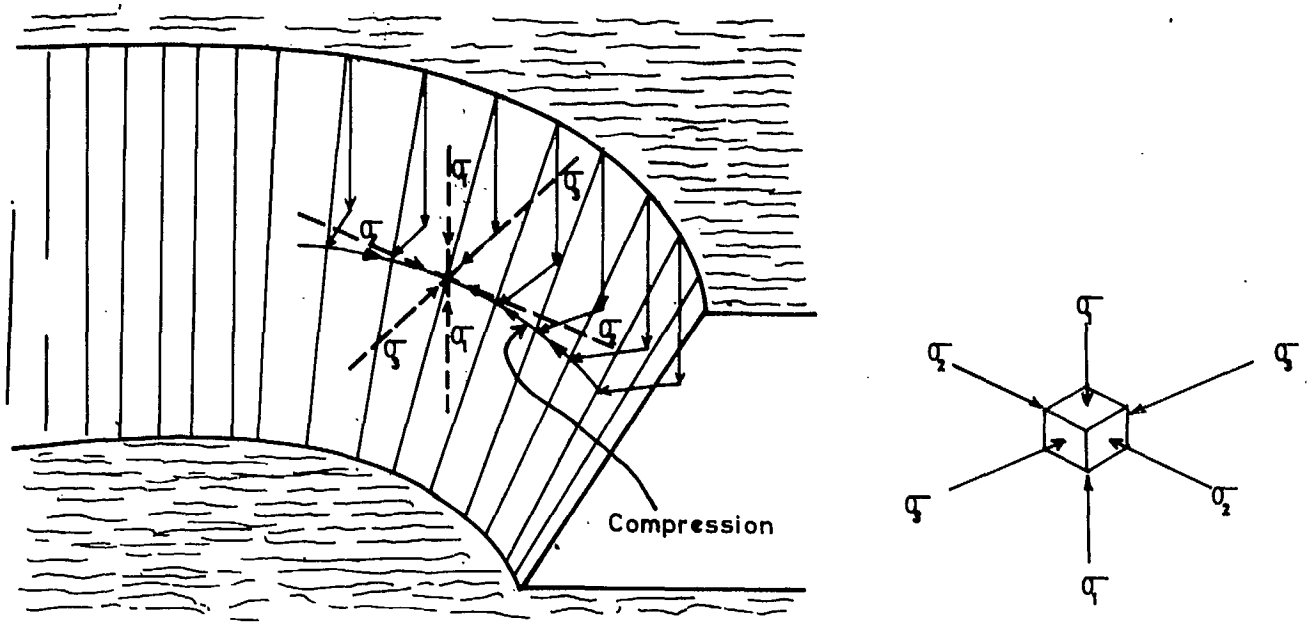

Fig.4.4. Strengthening effect in a concave slope resultant from tangential compressive stresses.

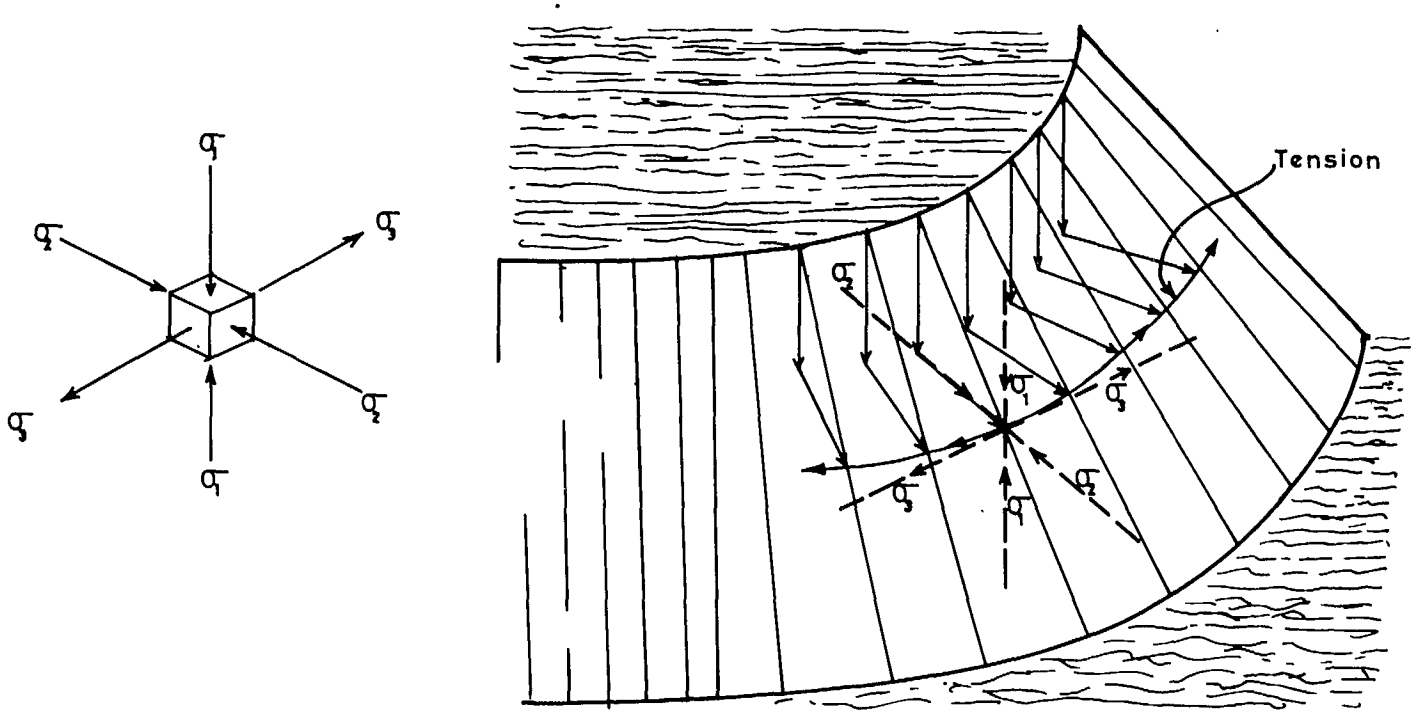

Fig. 4.5. Weakening effect in a convex slope resultant from tangential tensile stresses.

say for the straight slope in plane strain, will be reduced. Since rock is relatively weak in tension, tensile stress concentrations in the slope would induce instability making the sliding out of unrestrained blocks imminent. Förster (1966), having observed that failures in opencut mining invariably occurred in the convex-shaped slope, analysed the stability condition for convex curvatures of the practical range found in open pits and concluded that the conditions for stability are "somewhat smaller" than for those of the plane problem.

It is known that the opening created by a pit excavation affects the stresses in the rock mass at the pit boundary. However, predictions of the magnitude of the stress concentrations and their affects on the stability of the slope are indeed complex (Merrill and Wisecarver, 1967). This appears especially to be the case in an excavation where the plan geometry is irregular and considerable variation in relief occurs from one part of the site to another. Eubanks (1954), in a theoretical solution for the stresses and displacements around a hemispherical pit at a free surface of an elastic body with a Poisson's ratio of 0.25, predicts the stress concentration at the bottom of the pit to be 2.3. The stress concentration determined by Merrill and Wisecarver (1967) at 400 ft depth in the approximately circular Kimbley Pit were not far removed from the value predicted by Eubanks.

To date the results of studies of stress distribution in slopes and the manner in which stresses affect the stability are largely hypothetical and, therefore, have little practical value. Largely due to the complexities of the problem, there are no applicable mathematical or physical models to predict the effects of curvature of slope and the ultimate variation in stress concentration and consequently the safe and efficient slope angle (Merrill and Wisecarver, 1967).

Chapter 5

PROCEDURES IN MEASURING THE EFFECTS OF PIPE GEOMETRY ON SLOPE BREAKBACK OF THE BIG HOLES

In this chapter the methods adopted to determine quantitatively the variation of breakback with changing radius are described as are the procedures which have been utilized to adjust the data such that results for the big holes can be compared.

5.1 DETERMINATION OF PLAN RADIUS OF CURVATURE OF THE PIPE AND SLOPE BREAKBACK

In pursuing the idea put forward that there appeared to be a relationship between breakback distance and geometry of the pipe in plan, it is necessary first to define the various quantities and terms which will be used.

(i) The "radius of curvature" is that curvature in plan, as shown in Fig. 5.1, which is defined by the margin or perimeter of the pipe at the level of the shale-melaphyre contact (i.e. 320 ft $\pm$ below surface). The point at which radius is observed is defined by angular measurements (θ) taken about a good estimate of the centre of the pipe (point O in Fig. 5.1). From the point of intersection of θ at the pit edge (point A) a line is projected back at right angles to the pipe (point B). The radius of curvature is recorded at point B. Angular intervals for θ were taken at 10° using north (000°) as reference.

(ii) "Railway curves" (templates of different radii) were then best fitted to the pipe outline at the point B giving the radius R at the point.

(iii) "Slope breakback" D, is defined as the distance between the edge of the pipe and the edge of the pit taken in a direction normal to the pipe tangent from the point defined by θ. In Fig. 5.1 slope breakback is distance AB.

Plan outlines of the pipe at the shale-melaphyre contact and the edge of the big holes of the four mines, Dutoitspan, Kimberley, Bultfontein and Wesselton are shown in Figs. 5.2 (a to d). These particular outlines for Kimberley Mine are clearly seen in Photo 5. (i). It will be noted that the outlines of the pipe and big hole are fairly irregular, most particularly that of the edge of the big hole. This is to be expected, since slopes seldom weather and break back with a uniform well-defined edge as a

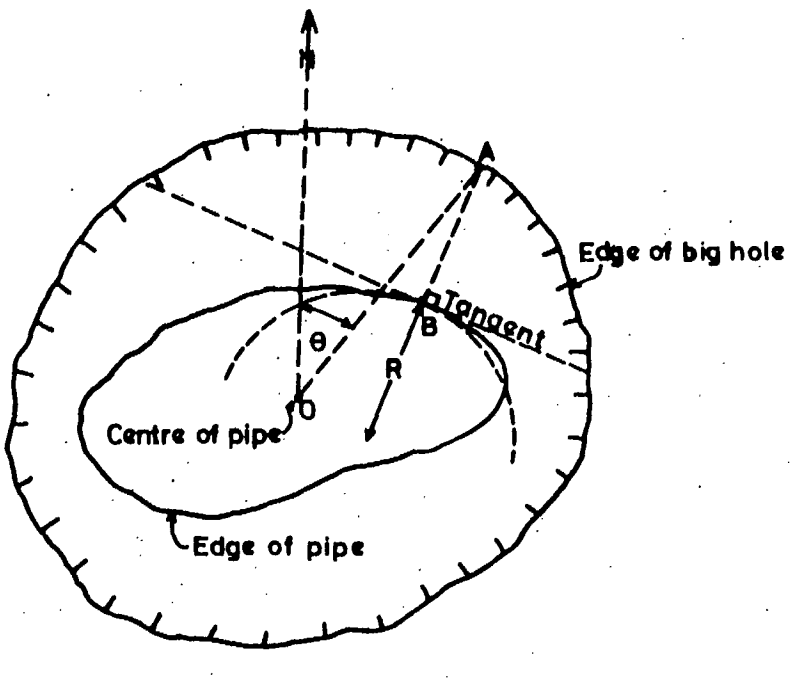

Fig. 5. 1. Method to measure radius of curvature of the pipe and slope breakback.

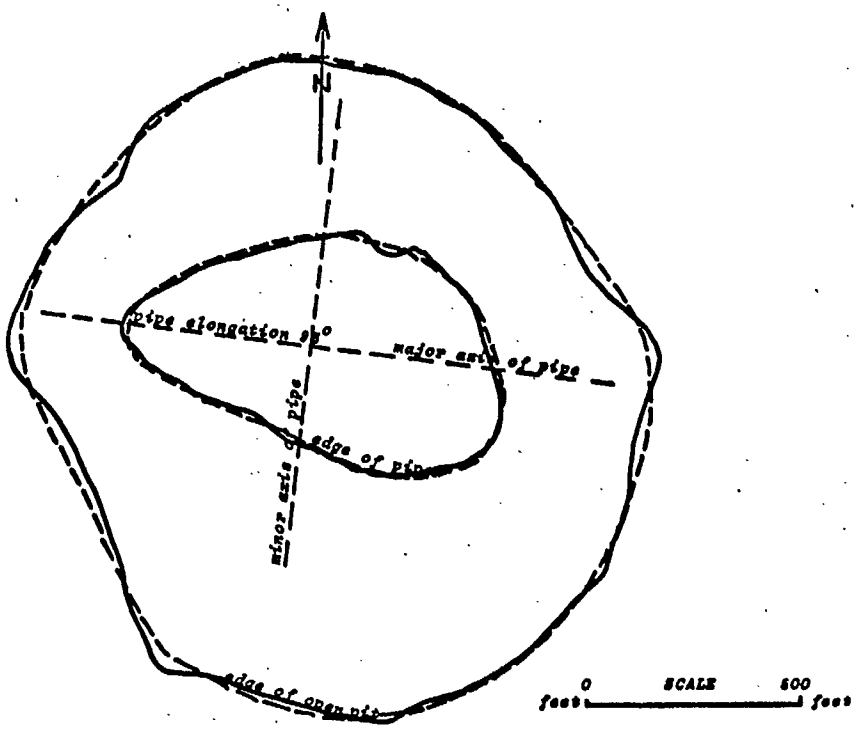

(a) KIMBERLEY MINE

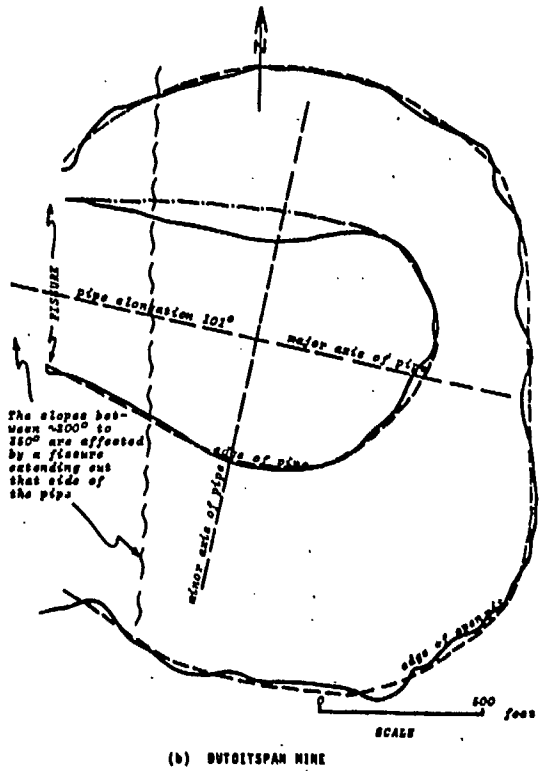

(b) BUTCHITSPAN MINE

Fig. 5.2. Plan outlines of both the actual and smoothed out edges of the pipe and open pit (big hole).

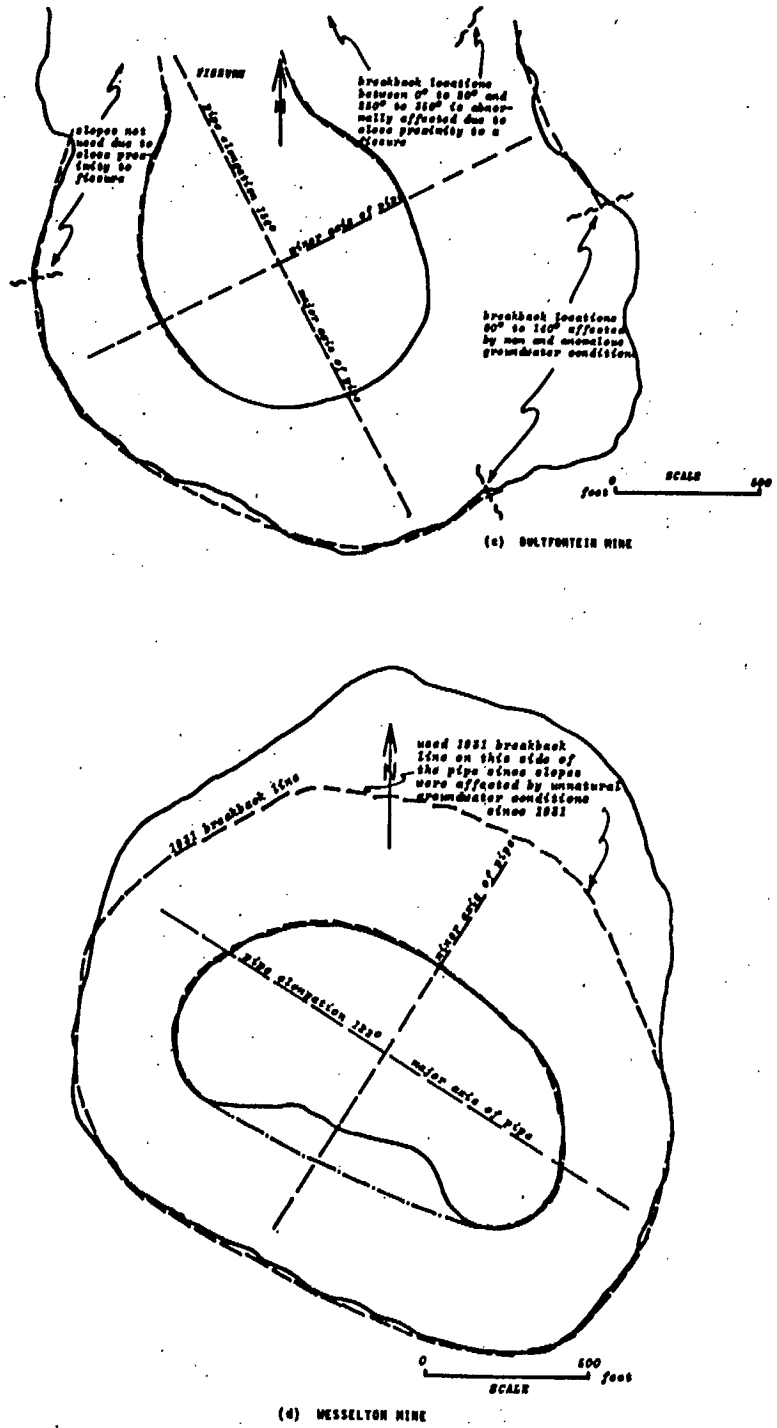

Fig. 5.2. Plan outlines of both the actual and smoothed out edges of the pipe and open pit (big hole).

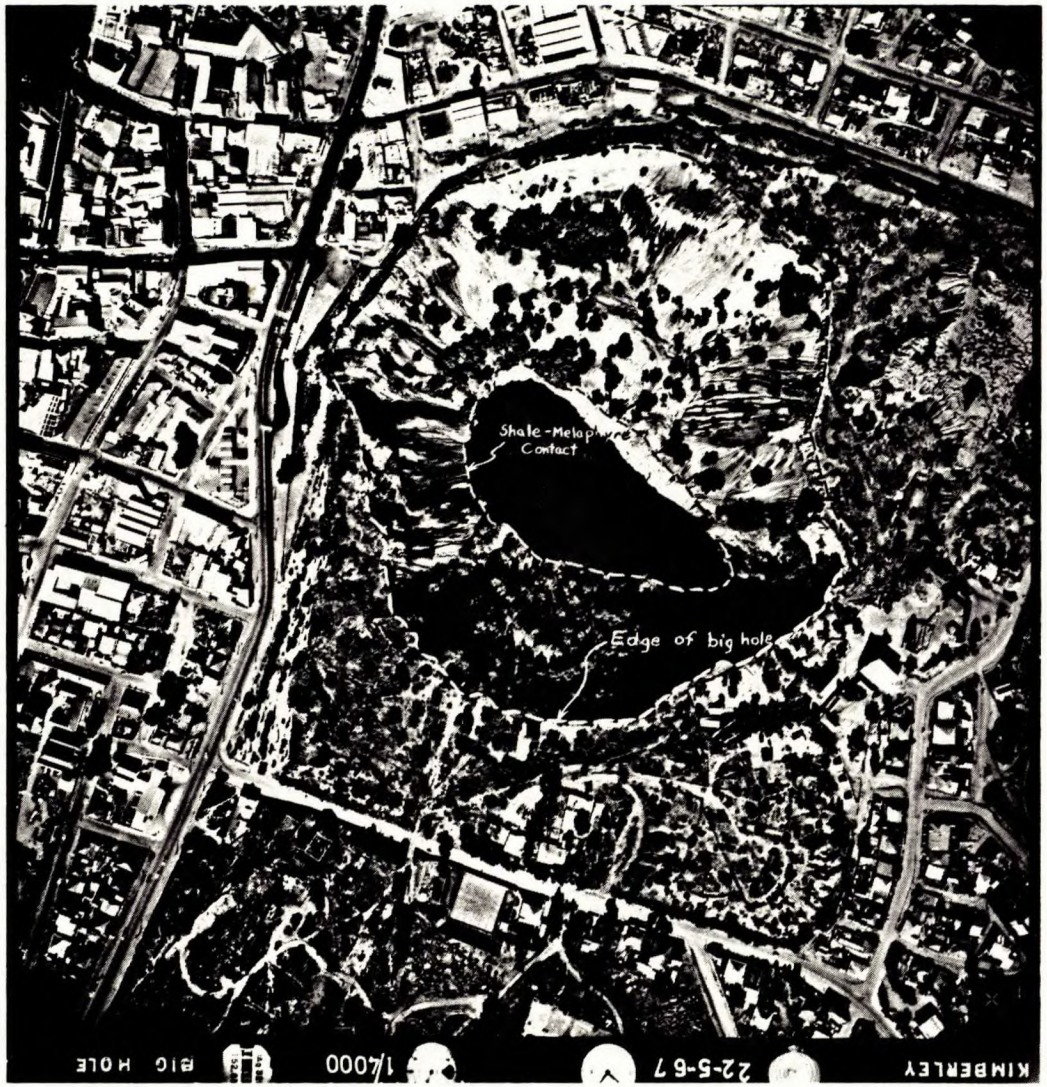

Photo 5. (i). Airphoto of the Kimberley Mine showing the plan outlines of the pipe at the shale-melaphyre contact and the edge of the "Big Hole".

result of minor local anomalous conditions. Hence, it was necessary to smooth these outlines out.

The pipe edge was first idealized, that is, the edge representing the contact was smoothed out such that local, small irregularities in the outline were not considered. Using judgment, this new outline was drawn in such a way that the resulting edge represented the pipe curvature that the adjacent slope would be expected to react to. In Fig. 5.3 the solid line represents the actual pipe shape, the dashed line the idealized pipe shape. All reverse curvatures (convex slope) were changed into positive curvatures (concave slope) shown as the chain-dashed line in Fig. 5.3. The radius is measured at a number of different points in the way already described. All reverse curvatures, and curvatures with radii greater than 1,050 ft were nominally given radii of 1,050 ft. In a similar manner the plan outlines of the big holes were also smoothed out across local irregularities with a line that was felt to approximate the average pit edge. The idealized distance of slope breakback (D) was obtained by measuring between the two average lines in the way already defined. Slopes, as was the case for the slope profile studies discussed earlier, that were considered abnormal due to either anomalous geological conditions or effects by man, were not used in the study. For example, a section of the slopes of both Bultfontein and Wesselton Mines, as shown in Photos. 5.(ii) and 5.(iii), respectively, have broken back excessively due to abnormal ground water and were not included in the analyses.

Initial analysis of the data showed that there might be some differences in the values of R as determined by different observers. Considerable judgment and common sense had to be exercised in choosing the radius of curvature (R) of the pipe margin, particularly in the transition sections between the ends and sides of the pipes. In comparison, measuring the breakback distance D was reasonably straight forward. For this reason the values of R were observed independently by five competent persons. The data on radius of curvature and slope breakback for the respective pipes are given in Tables 5.1 (a to d).

5.2 MANIPULATIVE CORRECTIONS AND COMPARATIVE ANALYSIS OF THE DATA

The values for breakback of the pit slopes given in Tables 5.1 (a to d) refer to the actual measured distances on the plans of the big holes shown in Figs. 5.2 (a to d). It should be appreciated that these values are not directly comparable because the slopes involved are of composite profile and are of differing heights (H_o) as shown in Fig. 5.4.

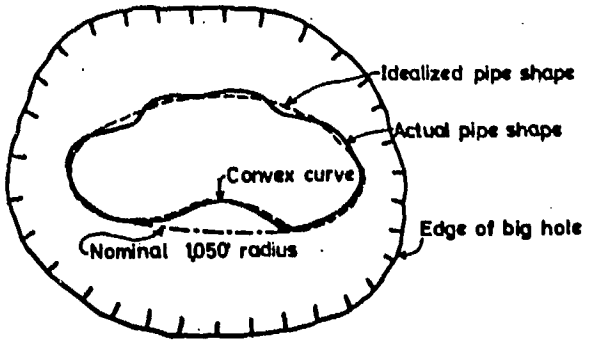

Fig. 5.3. Illustration of smoothing out of the plan outline of a hypothetical pipe.

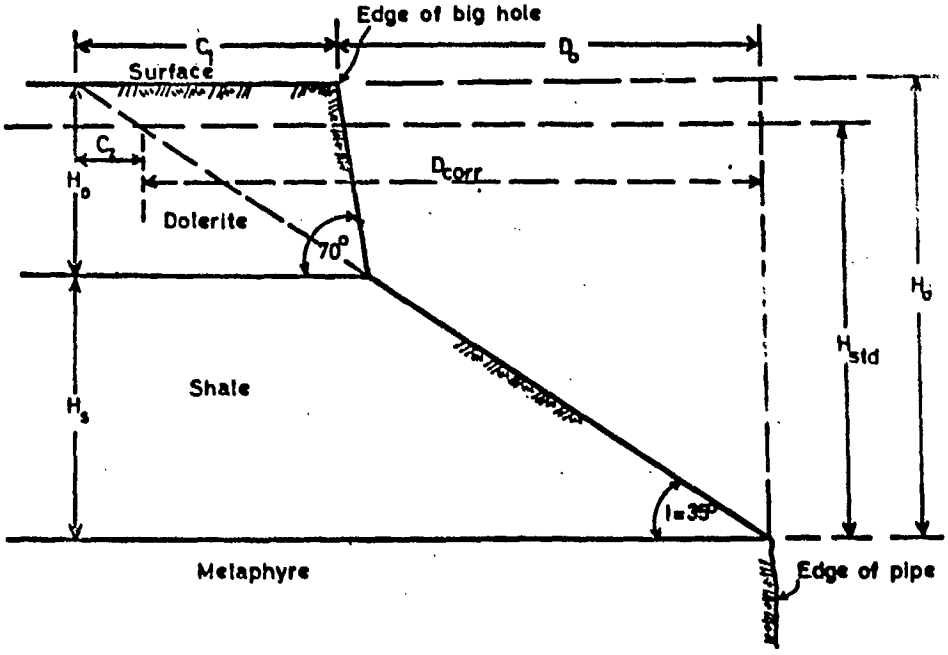

Fig. 5.4. Idealized slope profile of a big hole showing dimensions for mathematical correction of breakback to a standard height.

Photo 5. (ii). Oblique view of Bultfontein Mine big hole showing slopes (on the right side of the photo) which have broken back excessively due to abnormal ground water conditions and accordingly were not included in the analyses.

Photo 5. (iii). Oblique view of Wesselton Mine big hole showing slopes (on the left side of the photo) which have broken back excessively due to abnormal ground water conditions and accordingly were not included in the analyses.

Table 5.I (a)

KIMBERLEY MINE: Measured Values of Radius of Curvature of the Pipe Margin Determined by Different Observers and Breakback Distances of the Big Hole.

Location of Breakback Measurement (Θ degrees)	Average Distance of Breakback (B) (ft)	Radius of Curvature of the Pipe Margin R as Determined by Individuals Below (ft)				
		Piteau	Cohen	Hollings	Neille	Hutchinson
0	400	550	545	375	630	600
10	398	500	335	500	520	470
20	384	450	335	334	420	340
30	360	380	350	292	375	300
40	338	350	380	334	290	200
50	320	340	380	375	335	300
60	310	335	380	500	290	300
70	312	335	400	500	290	330
80	330	335	420	500	570	420
90	342	335	420	500	630	500
100	342	170	210	334	335	330
110	338	150	105	250	210	170
120	355	125	105	167	125	100
130	390	200	105	167	125	170
140	438	225	105	167	165	170
150	484	400	420	417	290	250
160	530	590	670	667	500	370
170	560	630	800	1050	500	500
180	582	670	925	1050	570	620
190	584	750	925	667	630	700
200	576	840	925	1050	1050	1000
210	536	965	925	1050	1050	1000
220	458	840	925	1050	920	1000
230	404	590	925	1050	750	900
240	338	400	750	667	540	600
250	285	250	590	500	335	420
260	236	80	150	150	83	170
270	215	80	85	150	83	130
280	208	80	85	83	125	100
300	290	335	590	417	460	250
310	322	400	880	500	710	650
320	348	500	880	1050	790	830
330	570	520	1050	1050	920	1000
340	414	545	1050	1050	1050	1000
350	402	590	755	500	920	900
290	240	80	320	250	165	170

Table 5.I (b)

PREMIER (TRANSVAAL) MINE: Measured Values of Radius of Curvature of the Pipe Margin Determined by Different Observers and Breakback Distance of the Big Hole.

Location of Breakback Measurement (Θ degrees)	Average Distance of Breakback (B) (ft)	Radius of Curvature of the Pipe Margin R as Determined by Individuals Below (ft)				
		Piteau	Cohen	Hollings	Neille	Hutchinson
0	532	1000	1000	1050	1050	1050
10	486	800	500	790	1000	1050
20	464	630	500	790	790	500
30	432	380	500	790	460	420
40	415	390	500	667	335	400
50	393	400	500	417	375	360
60	366	420	450	250	335	330
70	318	420	350	250	335	330
80	276	400	250	292	460	250
90	280	380	250	334	250	330
100	340	400	250	375	210	360
110	450	460	380	417	500	420
120	570	545	460	500	500	600
130	650	545	460	458	420	600
140	690	520	460	417	420	580
150	702	505	460	250	420	670
160	705	505	460	500	460	500
170	682	505	460	667	460	500
180	670	600	545	500	460	500
190	660	725	545	417	420	500
200	648	755	545	375	460	750
CUT? 340	416	1000	1000	1050	1050	1050
350	485	1000	1000	1050	1050	1050

Table 5.I (c)

FULTONTHEIN MINE: Measured Values of Radius of Curvature of the Pipe Margin Determined by Different Observers and Breakback Distance of the Big Hole.

Location of Breakback Measurement (θ degrees)	Average Distance of Breakback (B) (ft)	Radius of Curvature of the Pipe Margin R as Determined By Individuals Below (ft)				
		Piteau	Cohen	Hollings	Neille	Hutchinson
20	456	630	925	584	1050	850
30	514	630	925	540	1800	700
40	556	650	840	540	570	600
50	574	630	715	710	375	400
60	594	650	715	825	630	500
70	616	670	715	1050	790	670
80	646	630	630	875	790	750
90	686	590	530	667	710	580
100	718	335	420	562	570	500
OMIT 110	725	370	420	458	290	430
120	704	420	420	457	375	370
130	666	420	420	334	500	330
140	598	500	420	417	375	330
150	546	500	420	540	570	500
160	512	500	420	584	540	660
170	474	520	420	500	420	500
180	432	545	420	417	540	350
190	408	545	420	417	540	420
200	392	600	420	584	500	500
210	388	650	420	500	420	550
220	394	650	420	417	420	520
230	402	670	500	417	570	540
240	414	670	545	417	650	600
250	398	670	545	604	460	670
260	384	670	600	790	670	700
OMIT 270	370	690	690	1000	1050	830
280	350	715	755	1050	920	1000
290	324	715	755	1000	710	1080
300	302	715	755	750	420	670

Table 5.I (d)

WESSELTON MINE: Measured Values of Radius of Curvature of the Pipe Margin Determined by Different Observers and Breakback Distance of the Big Hole.

Location of Breakback Measurement (θ degrees)	Average Distance of Breakback (B) (ft)	Radius of Curvature of the Pipe Margin R as Determined by Individuals Below (ft)				
		Piteau	Cohen	Hollings	Neille	Hutchinson
0	420	800	380	834	375	440
10	444	840	700	1050	460	750
20	472	950	1050	1050	670	1050
30	496	1050	1050	1050	790	1050
40	494	1800	1050	1050	1000	1050
50	472	900	1050	1050	1050	900
60	450	880	1050	1050	570	900
70	405	800	800	1050	630	700
80	360	715	545	1050	570	500
90	330	630	545	834	375	500
100	338	545	545	584	630	420
110	330	335	545	417	335	420
120	325	250	545	417	500	370
130	315	170	380	250	335	250
140	330	250	125	167	165	170
150	360	250	125	167	125	100
160	370	400	600	250	165	330
170	382	630	1050	500	375	670
180	445	800	1050	1050	1050	1050
190	508	1000	1050	1050	1050	1050
200	480	1800	1050	1050	1050	1050
210	474	1800	1050	1050	1050	1050
220	412	800	1050	1050	1050	1050
230	362	650	535	1050	790	500
240	345	400	335	417	250	330
250	345	400	335	250	210	250
260	355	250	385	250	165	250
270	330	275	335	250	250	170
280	328	300	335	334	290	250
290	352	335	425	334	355	400
300	365	400	500	334	375	500
310	375	460	670	667	500	500
320	375	500	670	667	570	500
330	305	545	545	584	570	420
340	390	650	460	250	335	330
350	395	700	380	540	335	370

To get the data onto a comparative basis it is necessary to make corrections for the dolerite thickness (H_D) and also to bring the height to a common simple value. These corrections are made in the following way:

(i) i is taken at 35^o - this is the value somewhere near the value obtained taking the statistical mean value for D.

(ii) Correction for dolerite thickness

$$C_1 = H_D (\cot 35^o - \cot 70^o) = H_D (1.4281 - 0.3640)$$
$$= 1.0641\ H_D \quad \ldots\ldots 5.(1)$$

(iii) Correction to a standard height (H_{std}) which is taken as 320 ft, which is approximately the composite depth of the shale and dolerite of De Beers Mine

$$C_2 = (H_o - H_{std}) \cot 35^o = (H_{std} - H_o)\ 1.4281 \quad \ldots\ldots 5.(2)$$

(iv) Then D corrected (D_{corr}) $= D_o + C_1 - C_2$ $\quad \ldots\ldots 5.(3)$

(v) The correction for height difference has been taken as changing linearly with H_o.

Corrected values of the average distance of breakback, D_{corr}, as determined from the theory above, and the data on the mean radius of curvature (R) from the five observers are given in Tables 5.11 (a to d) for the four big holes. Corrected values of D are plotted against the mean R's as shown in Fig. 5.5 (a to d) for the four mines. In the chapters following, although not yet specifically mentioned in all cases, the data used in the various analyses will be that of Table 5.11 (a to d), i.e. the values of mean radius (R) and corrected breakback (D_{corr}).

In using the results from Figs. 5.5 (a to d) for the estimation of the breakback of any big hole in the Kimberley area the following rules apply:

(i) Looking at the plan shape of the pipe under consideration, choose the shape of the four pipes investigated above which corresponds in the nearest way to the pipe where breakback is to be predicted and use this plot for making the estimates of D's which apply in the particular case. The method adopted to determine which curve is appropriate for predicting the breakback configuration of De Beers Mine slopes is discussed in Chapter 7.

(ii) Depending upon the security which is required in the particular case, i.e. depending upon the risk which might be involved in an uncorrected assessment of D, examine the value of the standard

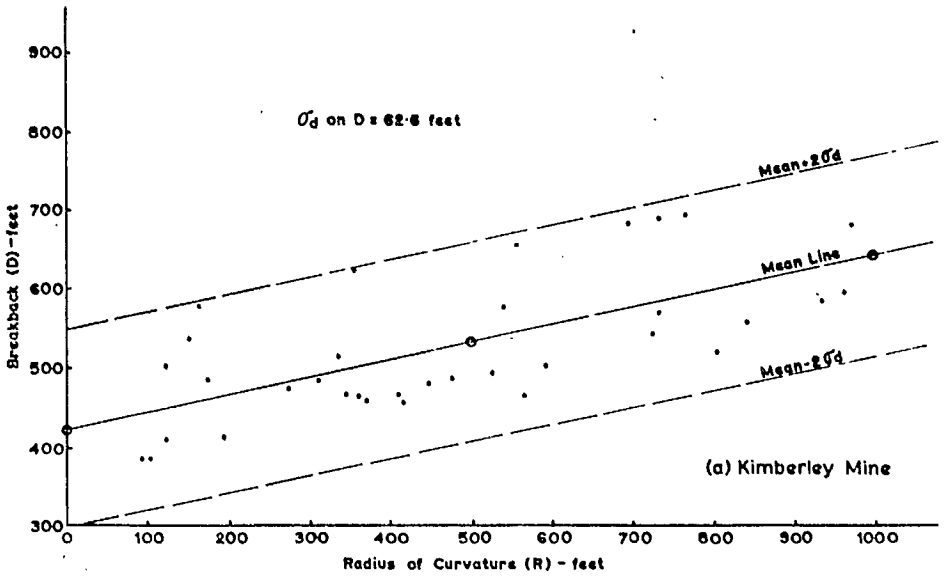

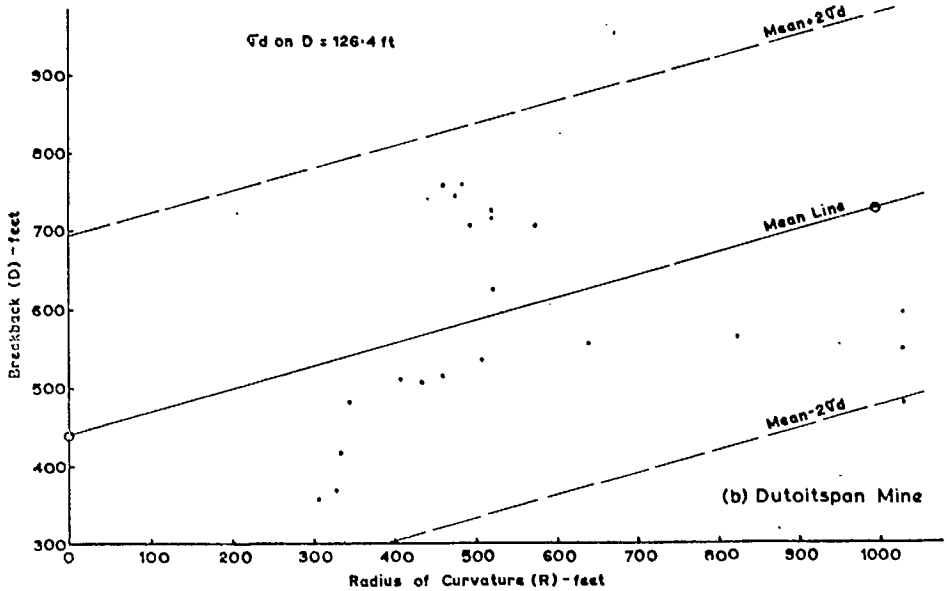

Fig. 5.5. Plot of radius of curvature (R) against breakback (D).

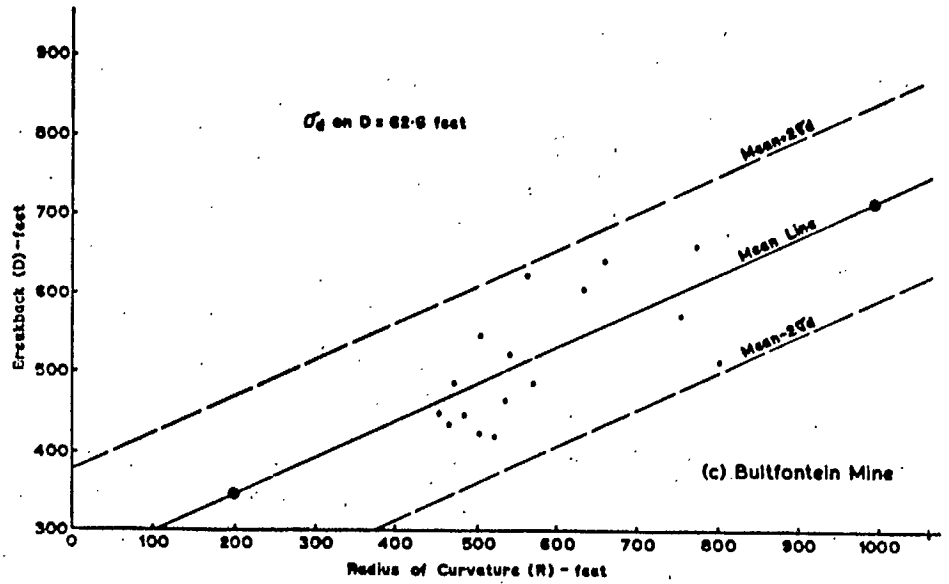

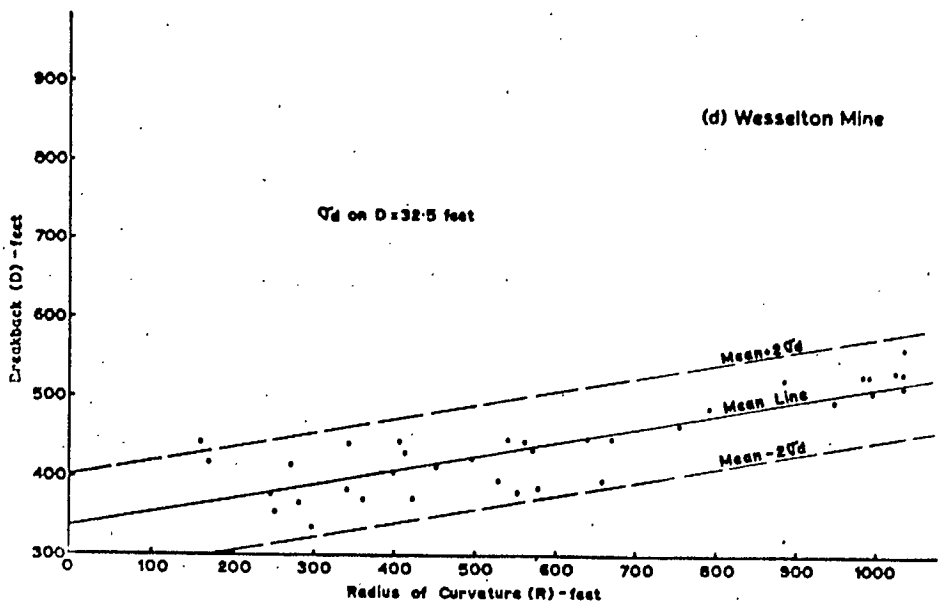

Fig. 5.5. Plot of radius of curvature (R) against breakback (D).

Table 5.II (a)

KIMBERLEY MINE: Corrected Breakback Distance and Mean Radius of Curvature of the Pipe Margin.

Location of Breakback Measurement (θ degrees)	Average Distance* of Breakback (B)	Thickness* of Dolerite (H_D)	Height of Slope (H_O)	C_1* = 1.0641 ($H_{std} - H_O$)	C_2* = 1.4281 ($H_{std} - H_O$)	Average Distance* of Breakback Corrected (B_{corr})	Mean Radius*(R) (From R's in Table 5.I (a to d))
0	480	65	245	69	+ 107	576	540
10	398	65	258	69	+ 100	567	465
20	384	65	255	69	+ 93	546	376
30	360	65	260	69	+ 86	535	559
40	538	70	270	74	+ 71	483	311
50	320	65	265	69	+ 78	467	346
60	510	55	260	58	+ 86	454	361
70	512	45	250	48	+ 100	460	571
80	350	48	245	45	+ 107	480	449
90	542	55	260	58	+ 86	486	477
100	342	70	280	74	+ 57	473	276
110	338	85	280	90	+ 57	485	177
120	355	85	280	90	+ 57	502	124
130	590	85	280	90	+ 57	537	155
140	438	85	285	90	+ 50	578	166
150	484	90	290	96	+ 42	622	356
160	550	90	300	96	+ 29	655	559
170	560	95	305	101	+ 21	682	696
180	582	95	310	101	+ 14	697	767
190	584	100	320	106	0	690	732
200	576	100	320	108	8	682	973
210	536	105	315	112	+ 7	655	998
220	458	105	300	112	+ 29	599	967
230	404	100	285	106	+ 50	560	845
240	350	95	275	101	+ 64	503	591
250	285	90	265	96	+ 78	459	419
260	236	90	265	96	+ 78	410	127
270	215	85	265	90	+ 78	383	106
280	208	85	260	90	+ 86	384	95
290	240	80	268	85	+ 86	411	197
300	290	80	255	85	+ 93	468	410
310	322	75	255	80	+ 93	495	628
320	348	75	255	80	+ 93	521	806
330	570	70	250	74	+ 100	544	728
340	414	70	250	74	+ 100	588	939
350	402	65	250	69	+ 100	571	735

* Data recorded in feet

Table 5.II (b)

PRETORIUSKOP MINE: Corrected Breakback Distance and Mean Radius of Curvature of the Pipe Margin.

Location of Breakback Measurement (θ degrees)	Average Distance* of Breakback (B)	Thickness* of Dolerite (H_D)	Height* of Slope (H_O)	C_1^* = 1.0641 (H_D)	C_2* = 1.4281 ($H_{std} - H_O$)	Average Distance* of Breakback Corrected (B_{corr})	Mean Radius*(R) (From R's in Table 5.I (a to d))
0	532	100	350	106	-43	595	1050
10	486	105	345	112	-36	562	828
20	464	110	340	117	-28	553	642
30	432	115	335	122	-21	535	310
40	415	115	335	"	-21	516	462
50	393	120	330	127	-11	509	410
60	366	115	"	122	-11	477	357
70	318	110	335	117	-21	414	337
80	276	105	"	112	-21	367	550
90	280	100	340	106	-28	358	309
100	340	95	"	101	-28	415	519
110	450	85	345	90	-56	504	435
120	570	"	"	"	"	624	521
130	650	"	"	"	"	704	497
140	690	"	"	"	"	744	479
150	702	"	"	"	"	756	461
160	705	"	"	"	"	759	485
170	682	"	"	"	"	736	1005
180	670	"	"	"	"	724	521
190	660	"	"	"	"	714	521
200	648	"	"	"	"	702	577

* Data recorded in feet

Table 5.II (c)

WHITCHURCH MINE: Corrected Breakback Distance and Mean Radius of Curvature of Pipe Margin

Location of Breakback Measurement (θ degrees)	Average Distance* of Breakback (D)	Thickness* of Dolerite, (H_D)	Height* of Slope (H_0)	C_1 = 1.0641 (H_D)	C_2* = 1.4281 ($H_{std} - H_0$)	Average Distance* of Breakback Corrected (D_{corr})	Mean Radius*(R) (From R's in Tables 5.I (a to d))
20	456	75	535	80	-21	515	504
30	514	"	"	"	-21	575	759
40	556	70	535	74	-21	609	636
50	574	"	"	"	"	627	566
60	594	65	535	69	-21	642	664
70	616	"	"	"	"	664	779
150	546	45	543	48	-36	558	506
160	512	"	"	"	"	524	541
170	474	"	"	"	"	486	472
180	432	40	540	43	-28	447	454
190	408	50	"	53	"	435	468
200	392	60	545	64	-36	420	521
210	388	65	"	69	"	421	504
220	394	70	535	74	-21	447	425
230	408	70	550	"	-11	465	559
240	414	75	525	80	- 6	488	572

* Data recorded in feet

Table 5.II (d)

WHEELTOW MINE: Corrected Breakback Distance and Mean Radius of Curvature of the Pipe Margin.

Location of Breakback Measurement (θ degrees)	Average Distance* of Breakback (D)	Thickness* of Dolerite (H_D)	Height of Slope (H_0)	C_1* = 1.0641 (H_D)	C_2* = 1.4281 ($H_{std} - H_0$)	Average Distance* of Breakback Corrected (D_{corr})	Mean Radius*(R) (From R's in Tables 5.I (a to d))
0	430	115	590	122	-100	422	566
10	444	"	"	"	"	464	760
20	472	120	592	127	-105	496	954
30	496	"	585	"	- 93	550	998
40	484	"	575	"	- 78	533	1050
50	472	115	565	122	- 64	530	990
60	450	"	555	"	- 50	522	890
70	405	"	550	"	- 43	484	796
80	360	110	540	117	- 28	449	676
90	350	"	550	"	- 14	433	577
100	350	"	525	"	- 7	448	545
110	350	105	520	112	0	442	410
120	325	"	525	"	- 7	430	416
130	315	"	550	"	- 14	415	277
140	330	110	540	117	- 28	419	175
150	360	"	545	"	- 36	441	165
160	370	"	550	"	- 43	444	549
170	382	"	535	"	- 50	449	645
180	445	115	560	122	- 57	510	1000
190	508	"	565	"	- 64	566	1048
200	480	"	570	"	- 71	531	1040
210	474	120	580	127	- 86	515	1040
220	412	"	"	"	"	455	1000
230	562	115	"	122	"	590	661
240	345	"	"	"	"	501	346
250	345	110	585	117	- 93	369	289
260	355	"	"	"	"	379	250
270	330	"	"	"	"	354	256
280	320	105	"	112	"	339	302
290	352	"	"	"	"	371	366
300	365	100	590	106	-100	371	426
310	575	-	"	"	"	581	559
320	575	105	"	112	"	587	58'
330	385	"	"	"	"	397	533
340	390	110	"	117	"	407	401
350	395	"	"	"	"	412	465

* Data recorded in feet

deviation, σ_d, on D and decide on a design line misplaced upwards and parallel to the mean line. In the figures, lines displaced at $2\sigma_d$ have been shown. This is a common practice in statistics. However, the choice of the line will depend upon the engineer's judgment of the security he requires in the particular case under investigation.

(iii) The D values obtained by steps (i) and (ii) above are "corrected" values for no dolerite and for a 320 ft deep hole. These corrections must now be reversed to take into account the actual dolerite thickness and depth of hole for the particular case under investigation.

If we examine the influence of radius of curvature of the pipe margin for the various big holes on the actual angle of slope i, the effects are more readily appreciated. From the data in Tables 5.11 (a to d) the angle of slope can be plotted against the radius of curvature as shown in Figs. 5.6 (a to d). In comparing the maximum (i.e. $-2\sigma_d$ curve), mean and minimum (i.e. $+2\sigma_d$ curve) angles of slope for two extreme radii, taken in this case to be 200 ft and 1,000 ft, these effects are immediately apparent as shown in Table 5.III. From Table 5.III it can be seen that for the 200 ft radius the average angle of slope is a maximum of 17.6° and a minimum of 7.9° steeper for the $-2\sigma_d$ and $+2\sigma_d$ curves, respectively, and 12.7° for the mean line.

The results shown plotted in Figs. 5.5 (a to d) and 5.6 (a to d) are for a linear relationship between R and D and R and i, respectively. The line fitting is reasonable, but mathematically the result is open to question, since it means that where R becomes very large, as with a slope which is straight and in plane strain, D will be very large and accordingly i will be very small. This seems unreasonable and an alternative approach was sought.

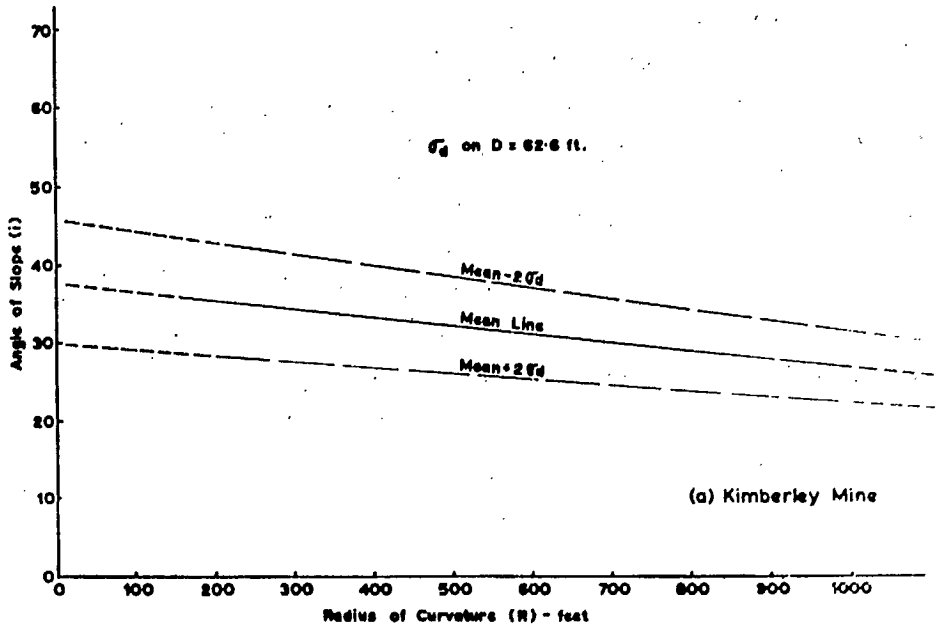

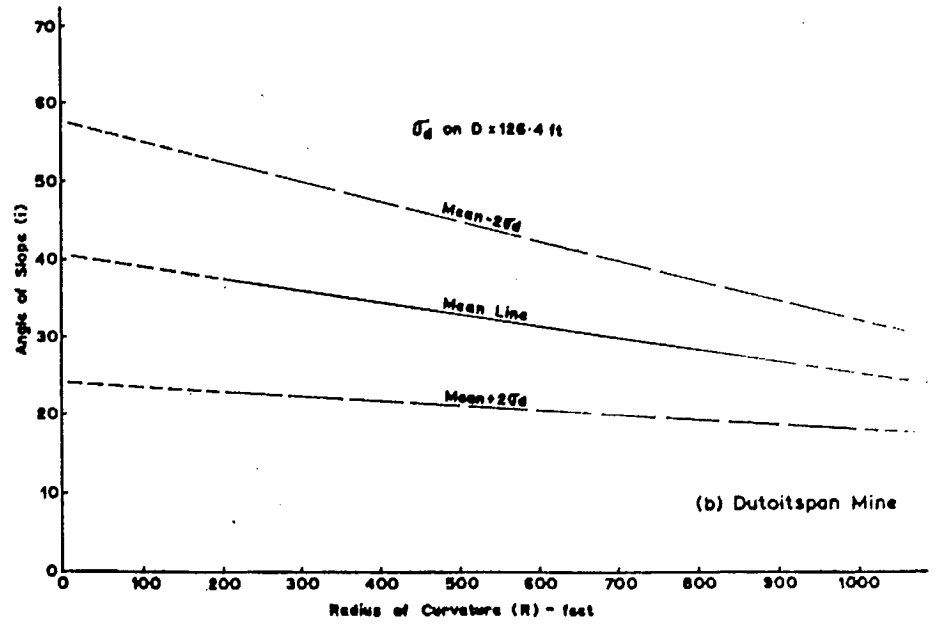

Fig. 5.6. Plot of radius of curvature (R) against angle of slope (i).

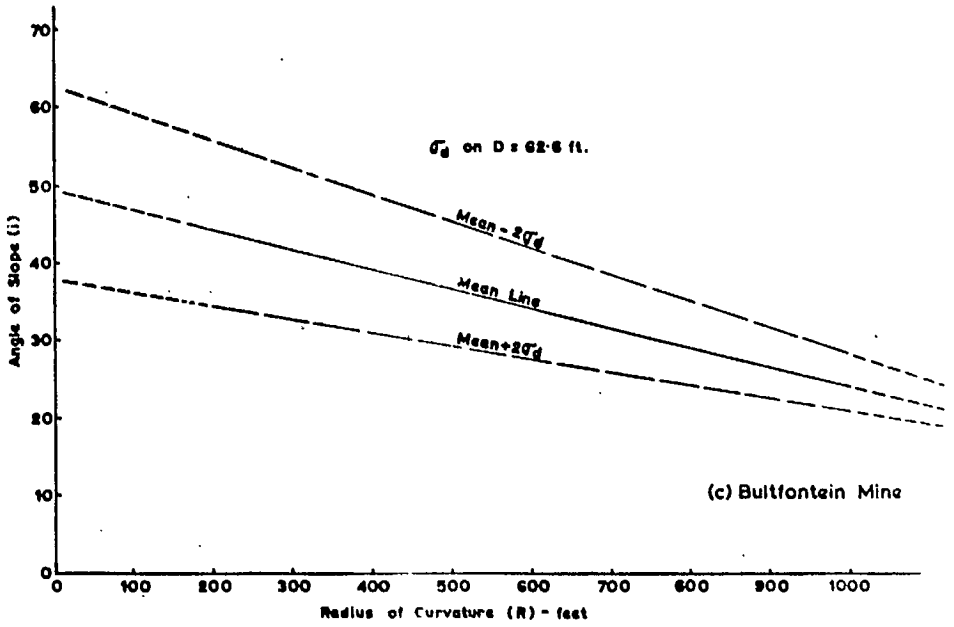

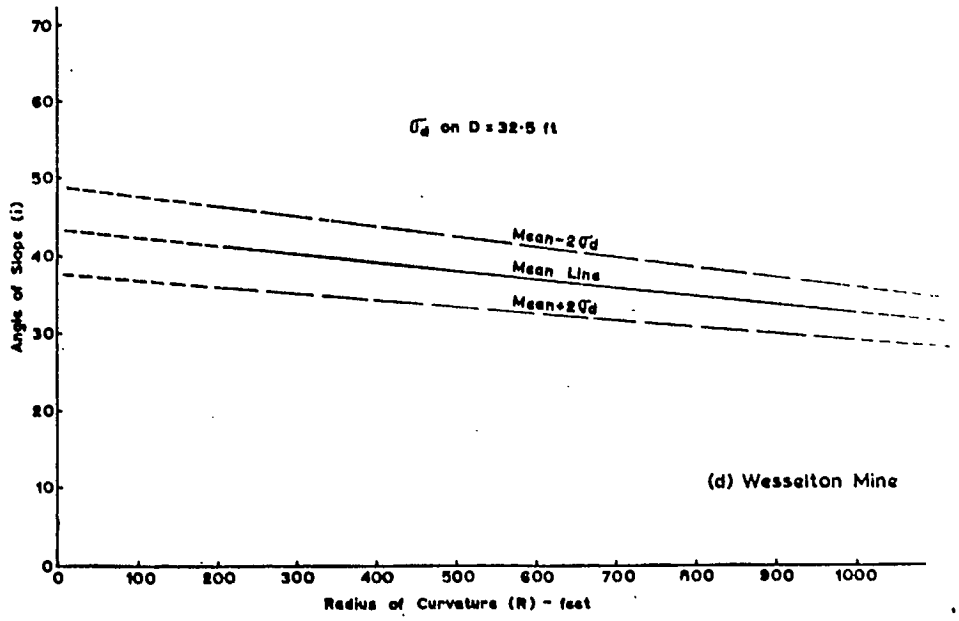

Fig. 5.6. Plot of radius of curvature (R) against angle of slope (i).

Table 5.III

Comparison of Angle of Slope for Small and Large Radius of Curvature

Mine	200 ft Radius of Curvature(R)			1000 ft Radius of Curvature(R)			Angle Difference Between 200 ft and 1000 ft (R)		
	Angle of Slope (i)			Angle of Slope(i)			Angle of Slope (i)		
	Max.	Mean	Min.	Max.	Mean	Min.	Max.	Mean	Min.
Kimberley	43.0°	35.8°	28.5°	31.5°	27.0°	22.5°	12.5°	8.3°	6.0°
Dutoitspan	52.5°	37.8°	23.0°	32.5°	25.3°	18.0°	20.0°	12.5°	5.0°
Bultfontein	56.0°	44.3°	34.5°	28.5°	24.3°	21.0°	27.5°	20.0°	13.5°
Wesselton	46.5°	41.3°	36.0°	36.0°	32.5°	29.0°	10.5°	9.8°	7.0°
AVERAGE	49.5°	39.5°	30.5°	32.1°	27.3°	22.6°	17.6°	12.7°	7.9°

Chapter 6

MATHEMATICAL MODEL OF SLOPE BREAKBACK - RADIUS OF CURVATURE RELATIONSHIP

This chapter is concerned with the application of the theory of the ellipse which has been adopted to illustrate, through analyses of hypothetical cases of big holes of differing geometrical form, the significance of plan shape of the pipe on breakback in the Kimberley big holes. Further, the most satisfactory way of plotting R and D is determined through analyses of various plots for different treatment of R and D.

6.1 INTRODUCTION

It is observed that the outline of the pipes has an approximately elliptical form. On close inspection it can also be seen that the general plan configuration of the pipes approximates an elliptical shape, but with respect to the outlines of the top edge of the big holes this is not as obvious. The Wesselton pipe is the one exception as it is approximately kidney-shaped.

It is no prerequisite that the ellipses be regular and it can be noted that the four quadrants around the major and minor axes may each have an ellipse of different characteristics. Any one mine may be composed of four quadrants, each with different ellipse axes, but nevertheless the elliptical forms still seem to apply. This relationship is clearly seen in the reduced plan outlines of the pipe and pit edge of Kimberley Mine in Fig. 6.1. It is, therefore, worthwhile examining the geometrical properties of the ellipse.

6.2 THE GEOMETRICAL PROPERTIES OF THE ELLIPSE AND ITS APPLICATION TO THE BIG HOLES

The properties of the ellipse are shown in Fig. 6.2. Writing the equations of the ellipse in parametric form, for the inner ellipse form of the diamond pipe we find

$$\left.\begin{aligned} x_o &= a\cos t \\ y_o &= b\sin t \end{aligned}\right\} \qquad \ldots\ldots\ldots 6.(1)$$

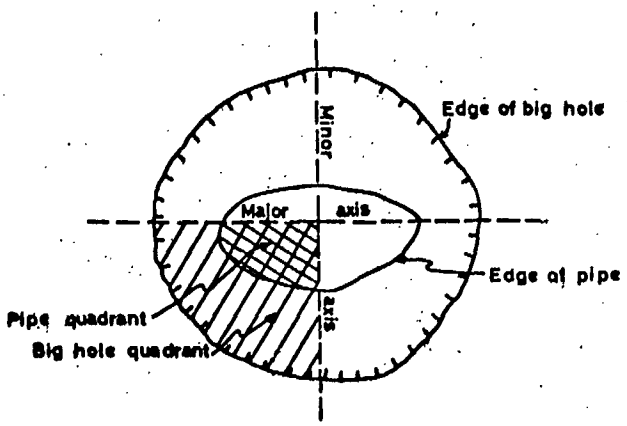

Fig. 6.1. Plan of Kimberley Mine big hole showing elliptical shapes of the pipe and the top edge of the big hole.

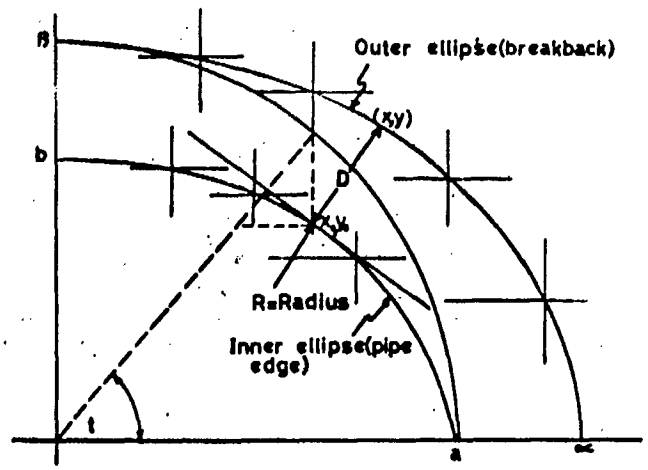

Fig. 6.2. Drawing illustrating the properties of the ellipse.

At $x_o y_o$ R is defined by

$$\frac{1}{R} = \frac{ab}{(a^2\sin^2 t + b^2\cos^2 t)^{3/2}} \qquad \ldots\ldots\ldots 6.(2)$$

where R = radius of curvature.

The breakback D measured at right angles to the tangent of the inner ellipse at $(x_o y_o)$ is given by

$$D^2 = \frac{(x - x_o)^2}{b^2\cos^2 t}\ (b^2\cos^2 t + a^2\sin^2 t) \qquad \ldots\ldots\ldots 6.(3)$$

$$= \frac{(x - x_o)^2}{b^2\cos^2 t}\ (Rab)^{2/3} \qquad \ldots\ldots\ldots 6.(4)$$

Evaluating $(x - x_o)$ we find

$$x - x_o = \frac{\alpha^2 b^2}{a^2\alpha^2\tan^2 t + \beta^2 b^2}\left\{-a\sec t\,(\sin^2 t + \frac{\beta^2}{\alpha^2}\cos^2 t) + \frac{\beta}{\alpha}\cdot\frac{1}{b}\left[a^2\alpha^2\tan^2 t - (b^2 - a^2)\sin^2 t + b^2\beta^2\right]^{\frac{1}{2}}\right\} \qquad \ldots\ldots\ldots 6.(5)$$

From 6.(3) write

$$D = \varphi(t)\,(abR)^{1/3}$$

$$= \varphi(t)\,\sigma^{1/2} \qquad \text{where } \sigma = (abR)^{2/3} \qquad \ldots\ldots\ldots 6.(6)$$

i.e. $\sigma = a^2\sin^2 t + b^2\cos^2 t$

$$\therefore\ \sin^2 t = \frac{\sigma - b^2}{a^2 - b^2} \text{ and } \cos^2 t = \frac{a^2 - \sigma}{a^2 - b^2} \qquad \ldots\ldots\ldots 6.(7)$$

Substituting these values in 6.(5) gives

$$\varphi(t) = \frac{a_1}{a_2\sigma + a_3}\left\{a_4\sigma + a_5 + \frac{\alpha\beta}{b}\left[\sigma^2 + a_6\sigma + a_7\right]^{\frac{1}{2}}\right\} \qquad \ldots\ldots\ldots 6.(8)$$

where

$$\left.\begin{aligned} a_1 &= b(a^2 - b^2) \\ a_2 &= a^2\alpha^2 - b^2\beta^2 \\ a_3 &= b^2a^2(\beta^2 - \alpha^2) \\ a_4 &= \frac{a(\beta^2 - \alpha^2)}{a^2 - b^2} \end{aligned}\right\} \qquad \ldots\ldots\ldots 6.(9)$$

$$a_5 = \frac{a(\alpha^2 b^2 - \beta^2 a^2)}{a^2 - b^2}$$

$$a_6 = \frac{a^2\alpha^2 - b^2\beta^2 - a^4 + b^4}{a^2 - b^2}$$

$$a_7 = \frac{a^2 b^2 (\beta^2 - \alpha^2 + a^2 - b^2)}{a^2 - b^2}$$

..... 6. (9)

From which it follows that D can be written as

$$D = \frac{a_1 \sigma^{1/2}}{a_2\sigma - a_3}\left\{ a_4\sigma + a_5 + \frac{\alpha\beta}{b}\left[\sigma^2 + a_6\sigma + a_7\right]^{1/2}\right\}$$

..... 6. (10)

The relationship in 6. (10) expresses D as a function of σ, which may be taken as an independent variable. We are able to investigate the relationship between D and R and the question which needs to be answered is whether we can effect changes which will give us a linear plot between simple functions of R and D.

For the big holes the following dimensions apply where:

(i) a and α represent dimensions of the pipe and top edge of the big hole, respectively, on the major axis (long axis) of the pipe (Fig. 6.2).

(ii) b and β represent dimensions of the pipe and top edge of the big hole, respectively, on the minor axis (short axis) of the pipe (Fig.6.2).

These particular dimensions of the big holes in Kimberley are given in Table 6.1.

Table 6.1

Dimensions of the Pipe and Top Edge of the Big Holes Along Their Major and Minor Axes

Mine	Dimensions of Pipe		Dimensions of Top Edge of Big Hole	
	Major Axis (2a)	Minor Axis (2b)	Major Axis (2α)	Minor Axis (2β)
Kimberley	900'	520'	1490'	1480'
Dutoitspan	1280'	730'	2300'	1760'
Bultfontein	1100'	930'	2420'	1880'
Totals	3280'	2180'	6210'	5120'
Averages	1100'	730'	2070'	1710'

When $t = 0^{o}$, i.e. on the long axis (major) of the pipe, R is minimum and D is minimum.

When $t = 90^{o}$, i.e. on the short axis (minor) of the pipe, R is maximum and D is maximum.

In Table 6.11 the average breakback of the big holes at the end of the pipes (i.e. on the major axis where $t = 0^{o}$) and on the side of the pipe (i.e. on the minor axis where $t = 90^{o}$) is given.

Table 6.11

Average Breakback of the Big Holes Along the Major and Minor Axes of the Pipes

Mine	Average Breakback of the Big Hole	
	Major Axis $t = 0^{o}$ ($D = (\alpha - a)$)	Minor Axis $t = 90^{o}$ ($D = (\beta - b)$)
Kimberley	395'	480'
Dutoitspan	510'	530'
Bultfontein	660'	475'
Average Values	485'	490'

From the results above, note that for the case of Bultfontein there is a reversal of the expected conditions since $D_{t=90^{o}} < D_{t=0^{o}}$ Referring back to Fig. 5.2(c), it can be seen that Bultfontein Mine has an essentially round pipe, hence the choice of the major and minor axes are subject to doubt. Also parts of the open pit slopes on one side of this mine have been severely affected by failure due to anomalous ground water conditions as shown in Photo 5.(ii). Also, a relatively large kimberlite dyke occurs in the pit slope, which has significantly affected the slope forming materials in close proximity to it. Further, the Bultfontein case so affects the results that the average value for all the pits shows that $D_{t=0^{o}} = D_{t=90^{o}}$. The results for the Kimberley Mine show that $\alpha = 745$ ft $= \beta$ making the final breakback a circle. Hence, none of the results given above are very suitable for testing the validity of the theory.

6.3 APPLICATION OF THE ELLIPSE THEORY FOR A HYPOTHETICAL BIG HOLE

The next approach was to look for a hypothetical case which will straddle the ranges of observations of breakback and radius of curvature given in Tables 5.II(a to d). It can be seen that the radius of curvature R of the various pipe rims varies from about 200 ft to 600 ft, and that D varies from about 300 ft to 600 ft.

The ellipse theory was applied in trying the following hypothetical case where:

$$a = 500 \text{ ft}$$
$$b = 300 \text{ ft}$$
$$\alpha = 800 \text{ ft}$$
$$\beta = 900 \text{ ft}$$

From equation 6.(2) the values for R and D are as follows:

$$\text{R minimum} = \frac{b^2}{a} = \frac{300^2}{500} = 180 \text{ ft}$$

$$\text{R maximum} = \frac{a^2}{b} = \frac{500^2}{300} = 833 \text{ ft}$$

$$\text{D minimum} = \alpha - a = 300 \text{ ft}$$

$$\text{D maximum} = \beta - b = 600 \text{ ft}$$

The ellipses for the hypothetical case are drawn to scale in Fig. 6.3. Working in 100 ft units a = 5, b = 3, α = 8 and β = 9, and putting the values into equations 6.(8) and 6.(10), the calculated values for the hypothetical case were determined and are given in Table 6.III.

Table 6.III

Calculated Results for the Hypothetical Case to Test the Ellipse Theory

R	D	Log R	log D	log(7-D)	log(6-D)	log(5-D)
1.8	3.000	0.2553	0.4771	0.6021	0.4771	0.3010
2.0	3.1342	0.3010	0.4961	0.5872	0.4572	0.2709
3.0	3.7397	0.4771	0.5729	0.5132	0.3541	0.1004
4.0	4.2911	0.6021	0.6326	0.4328	0.2326	- 0.1494
5.0	4.7496	0.6990	0.6767	0.3522	0.0969	- 0.5952
6.0	5.1645	0.7782	0.7129	0.2639	- 0.0780	-
7.0	5.5412	0.8451	0.7436	0.1641	- 0.3383	-
8.0	5.8894	0.9031	0.7701	0.0458	- 0.9563	-
8.33	6.000	0.9208	0.7782	0.0000	- ∞	-

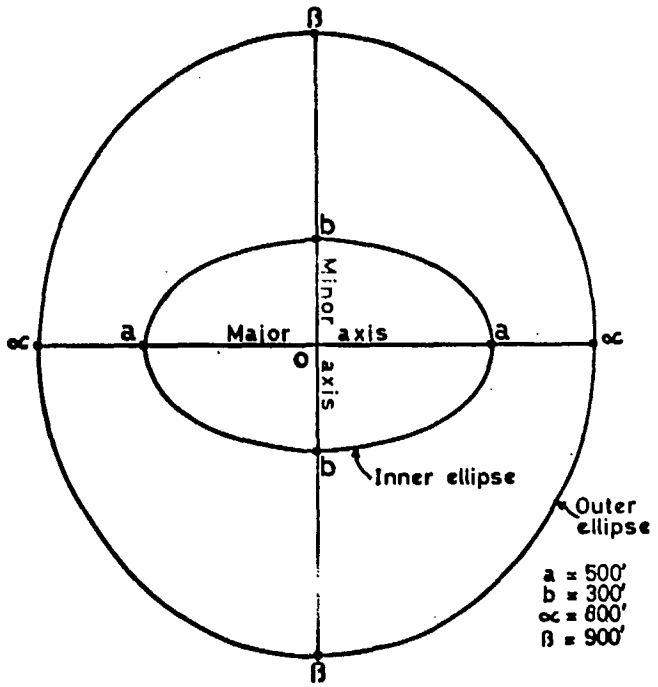

Fig. 6.3. Ellipses for hypothetical case drawn to scale.

The results from Table 6.III are plotted in Figs. 6.4(a to c) for R vs. D, log R vs. log D and R vs. log (C-D), respectively. The most satisfactory straight line is given by the log R vs. log D plot, which points to a hyperbolic relationship between R and D. The plot of log (C-D) vs. R, however, is also fairly good over most of the range, providing C = 7. This points to an exponential relationship. Both the hyperbolic and exponential relationships would be suitable for the practical case, since both lead to an asymtotic value for D at large values of R.

6.4 THE EFFECTS OF PIPE PLAN SHAPE ON BREAKBACK AND ANALYSES OF PLOTS FOR DIFFERENT TREATMENT OF R AND D

6.4.1 Ellipse Theory Applied to Hypothetical Geometric Forms of Big Holes

In an effort to investigate the effects of pipe plan shape on the natural slope breakback, i.e. the ratio of axes a/b and α/β, two other hypothetical shapes were selected for study. One of these shapes is more elongate than the first case, with a/b = 5/2.5 and α/β = 9/10, and the other is more circular with a/b = 5/4 and α/β = 9/10. Essentially similar results for these two cases were found as for the first case. The plots of these results are also given in Fig. 6.4 (a to c) along with those of the first case.

In all the hypothetical cases investigated there are changes in the slope of the mean line fitting the calculated values. For the more elongate pit the mean lines are flatter showing less variation of D with change of R. On the other hand, for the more circular pits the lines are slightly steeper. In this respect it can be concluded that the pipes' general geometric form (i.e. whether it is more circular or more elongate) has clear effect on the relationship between D and R. This aspect is shown in Fig. 6.5 where the slope of the curves are slightly exaggerated for illustrative purposes. These results show that when attempting to make comparisons between big holes, one important factor which must be borne in mind is the general shape of the pipe.

These mathematical relationships based upon the properties of idealised ellipses are not expected to provide methods for estimating the breakback values for big holes in the Kimberley area. They are meant to serve only as a background for the further analysis of the data recorded in Tables 5.II (a to d).

In consideration of the plots in Figs. 6.4 (a to c), the different ways in which the R and D data have been treated can be examined as follows:

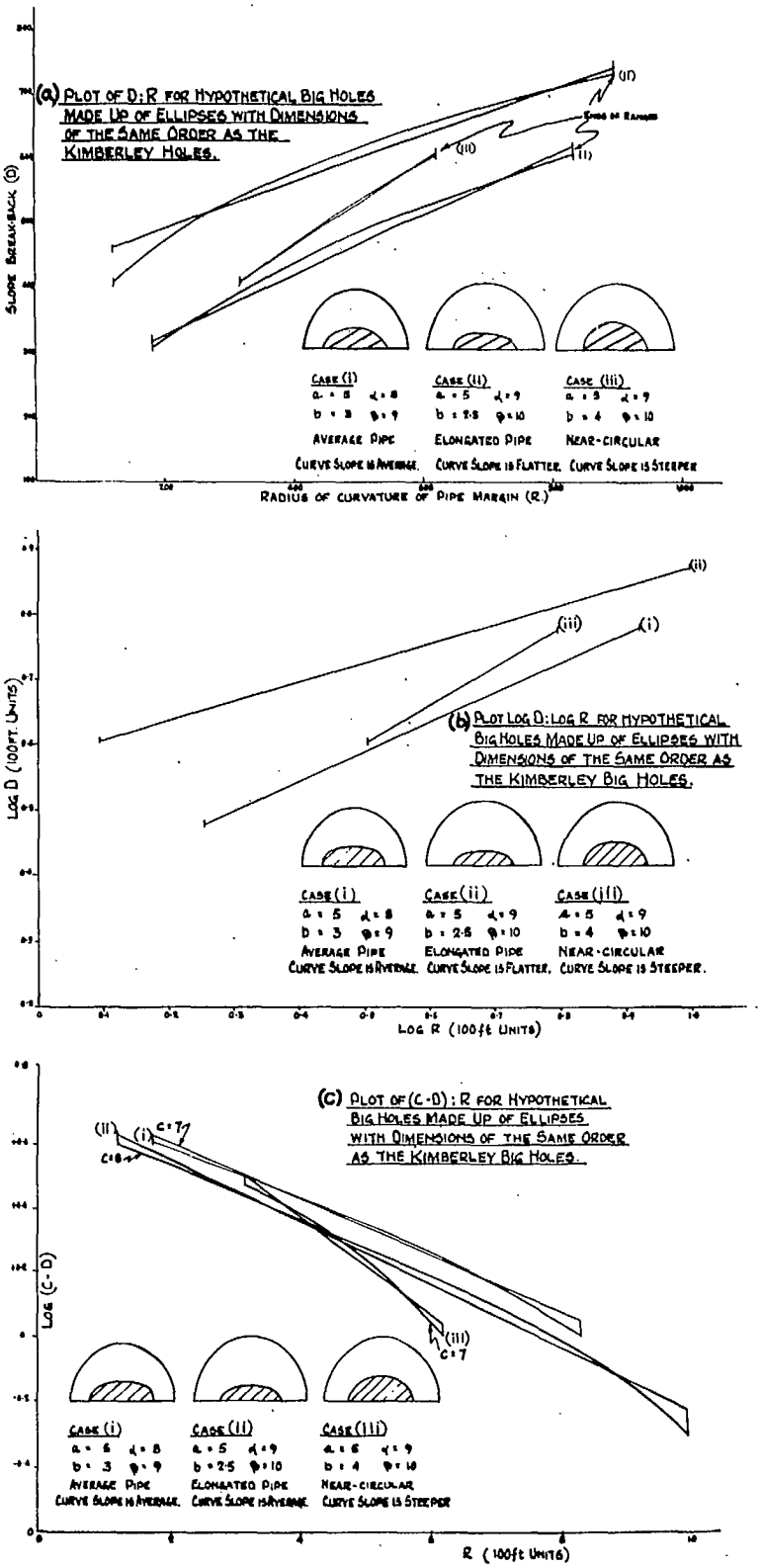

Fig. 6.4. Plots of R and D data for hypothetical big holes based on ellipse theory.

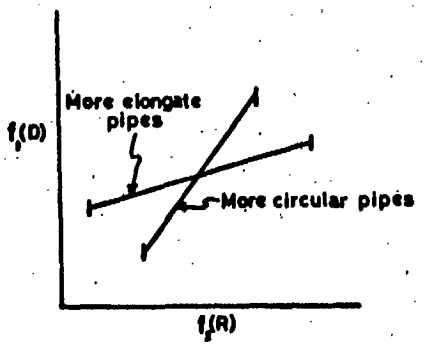

Fig. 6.5. General relationship between D and R for idealized elongate and circular big holes.

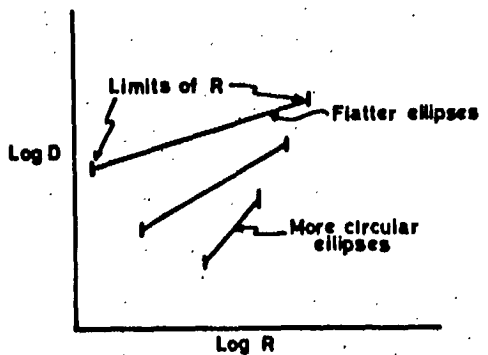

Fig. 6.6: Theoretical relationship between log R and log D from the properties of the ellipses.

(i) Log R vs. Log D Plot

The most satisfactory way of looking at the R and D data is to plot them as log R vs. log D (see Fig. 6.4(b))giving a straight line of the form log D = A + B log R, which results from the relations $D = AR^B$. The limits of R are determined by the axes a and b of the ellipses, therefore, the range of validity for the various equations are fixed, as illustrated in Fig. 6.6, as follows:

(a) For flat ellipses a is consistently greater than b, the slope of the line is gentle and the range of R's is large.

(b) For more circular ellipses a approaches b, the slope is slightly steeper and the range of R's is smaller.

(c) For ellipses which become a true circle, the value for R becomes constant (i.e. a = b), therefore, the line shrinks to a point and $\alpha = \beta$.

(ii) R vs. D Plot

A second approach can be taken whereby the data of R and D can be plotted directly as shown in Fig. 6.4(a). These plots approximate a straight line graph of the form D = A + BR. Once again the limits of R are set depending upon the shape of the ellipse, as shown in Fig. 6.7, as follows:

(a) For flat ellipses the relationship is somewhat curved, and the mean straight line is flatter.

(b) For more circular ellipses where a approaches b, the curve is steeper and is almost a straight line and the range of R's again becomes narrower.

(c) For the case when the ellipses have become circles the line once again shrinks to a point.

(iii) R vs. Log (C-D) Plot

A third approach to evaluating and plotting the data is to think of the relationship of R to D as logarithmic with D approaching a maximum as R increases. This approach is more logical than the straight R:D plot described in (ii) above. The mathematical relationship is as follows:

$$D = C - Ae^{-BR} \qquad \ldots\ldots\ldots 6.(11)$$

that is

$$C - D = Ae^{-BR} \qquad \ldots\ldots\ldots 6.(12)$$

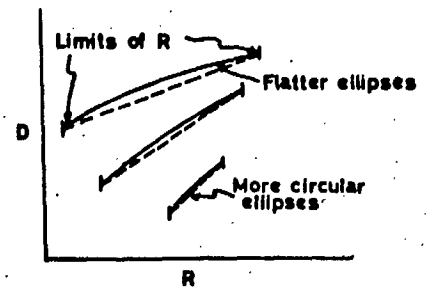

Fig. 6.7. Theoretical relationship between R and D from the properties of the ellipses.

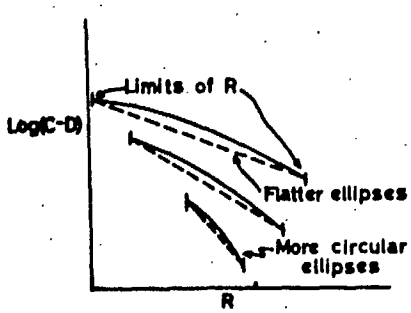

Fig. 6.8. Theoretical relationship between log (C-D) vs. R from the properties of the ellipses.

where C is the breakback at $R = \infty$. In logarithmic form the equation is

$$\log_e (C-D) = \log_e A - BR \qquad \ldots\ldots\ldots 6.(13)$$

The equation 6.(13) has the difficulty that it contains three constants A, B and C and one must search by trial and error to find that value of C which fits the measured data most satisfactorily. The values of D and R are shown plotted in Fig. 6.4(c) for the hypothetical cases. It can be seen that the same general trends have been found, and they only differ in that the curves are inclined in the opposite direction as shown exaggerated in Fig. 6.8. All the curves for log (C-D) vs. R reasonably approximate straight lines as shown in Fig. 6.8. The limits in this case are set as follows:

(a) For the flat ellipses the plot is more curved, the range of R is once again greatest in this case and the mean straight line is flatter.

(b) For more circular ellipses the plot is less curved, the range of R is smaller and the mean straight line is steeper.

(c) For the circular case the line shrinks to a point as was the case for (i) and (ii) given above.

6.4.2 Extension of the Ellipse Theory Relationships for Analyses of the Kimberley Big Holes

Data of R and D for the studied big holes in the Kimberley area have been plotted in the three ways described above (i.e. R vs. D, log R vs. log D and log (C-D) vs. R). In each of these cases the best straight line has been fitted by least squares. The data from these analyses are given in Table 6.IV. From the data it can be seen that the best fits are obtained either from the direct R vs. D plots, already given in Figs. 5.5 (a to d) in the previous chapter, or from the exponential plot with C = 700 ft. The plots for log (C-D) vs. R for C = 700 ft are given in Figs. 6.9 (a to d). In each plot, lines above and below the mean are given for twice the standard deviation (i.e. $2\sigma_d$).

The individual plots, as shown in Figs. 5.5 (a to d), show that each of the four mines gives a different straight line typical of the ellipses for the hypothetical cases described. These relationships, which are slightly exaggerated, are clearly shown in Fig. 6.10. The general rules derived from the study of the ellipses appear to apply, meaning that for the more circular case (Bultfontein pipe) the line is steeper; where the pipes are fairly elongate or analogous to the flat ellipses (i.e. Kimberley and Wesselton

Table 6 IV

Data from Analyses to Fit the Best Straight Line by Least Squares for Different Plots of R and D Data.

MINE	EQUATION OF STRAIGHT LINE	COEFF. OF CORR.	MAXIMUM DEVIATION OF D FROM LINE					
			R = 200'		R = 600'		R =1,000'	
			$\Delta U, D$	$\Delta L, D$	$\Delta U, D$	$\Delta L, D$	$\Delta U, D$	$\Delta L, D$
KIMBERLEY	D = 425.119 + 0.220653 R	0.6955	125.3	125.3	125.3	125.3	125.3	125.3
DUTOITSPAN	D = 438.2305 + 0.290185 R	0.3655	250.4	250.4	250.4	250.4	250.4	250.4
BULTFONTEIN	D = 248.799 + 0.46798 R	0.6525	125.3	125.3	125.3	125.3	125.3	125.3
WESSELTON	D = 336.782 + 0.172952 R	0.8386	65.0	65.0	65.0	65.0	65.0	65.0
KIMBERLEY	LOG(D) = 2.2874 + 0.166506 LOG(R)	0.6949	123.9	97.9	148.6	117.4	161.8	127.8
DUTOITSPAN	LOG(D) = 2.0465 + 0.2586 LOG(R)	0.4233	96.3	133.1	312.6	303.7	355.7	231.8
BULTFONTEIN	LOG(D) = 1.1532 + 0.5653 LOG(R)	0.6786	71.8	93.3	133.8	106.7	178.8	142.7
WESSELTON	LOG(D) = 2.1329 + 0.18637 LOG(R)	0.7430	70.9	59.4	88.1	73.6	97.0	81.1
KIMBERLEY	LOG(800-D) = 2.59677 - .0004051(R)	0.6642	143.6	255.3	98.8	175.9	68.1	121.1
DUTOITSPAN	LOG(800-D) = 2.34518 - .00017748(R)	0.1273	160.3	746.4	136.5	635.3	115.6	538.5
BULTFONTEIN	LOG(800-D) = 2.89641 - .00081126(R)	0.6436	216.9	154.4	102.8	171.5	48.6	81.2
WESSELTON	LOG(800-D) = 2.682788- .00022218(R)	0.8456	73.1	87.9	60.7	71.8	48.7	58.4
KIMBERLEY	LOG(750-D) = 2.5514 - .0005369(R)	0.6484	152.7	338.6	93.0	206.4	56.8	126.1
DUTOITSPAN	LOG(750-D) = 2.3267 - .0004016(R)	0.1966	159.0	1626.8	110.0	1125.1	76.0	776.8
BULTFONTEIN	LOG(750-D) = 2.9306 - .001039(R)	0.6411	254.9	492.6	97.8	188.9	37.6	72.7
WESSELTON	LOG(750-D) = 2.6392 - .0002617(R)	0.8456	341.8	2963.6	168.4	2386.6	211.3	1731.2
KIMBERLEY	LOG(700-D) = 2.5515 - .000939(R)	0.5698	189.5	1050.8	79.8	44.2	33.6	186.5
DUTOITSPAN	LOG(700-D) = 2.4799 - .000351(R)	0.5425	129.7	262.9	92.8	188.3	66.6	135.2
BULTFONTEIN	LOG(700-D) = 3.0527 - .0015036(R)	0.6368	358.3	942.9	89.8	236.2	22.4	59.1
WESSELTON	LOG(700-D) = 2.5932 - .00031928(R)	0.8453	79.9	104.5	59.5	78.1	44.4	58.1
KIMBERLEY	LOG(650-D) = 2.31525 - .0004683(R)	0.5192	97.4	237.2	64.0	157.4	41.7	102.3
DUTOITSPAN	LOG(650-D) = 2.39678 - .00049256(R)	0.4843	147.4	413.8	85.3	262.8	54.2	167.0
BULTFONTEIN	LOG(650-D) = 3.0429 - .0018043(R)	0.4501	396.7	2267.2	75.2	430.0	14.3	81.8
WESSELTON	LOG(650-D) = 2.54767 - .0004111(R)	0.8430	85.6	121.3	58.7	83.1	40.3	57.4
KIMBERLEY	LOG(600-D) = 2.3781 - .001212(R)	0.6505	111.2	594.3	36.4	194.5	12.0	63.6
DUTOITSPAN	LOG(600-D) = 2.5309 - .001072(R)	0.7045	157.1	647.6	58.5	241.1	21.8	89.8
BULTFONTEIN	LOG(600-D) = 7.7716 - .00136717(R)	0.5903	195.4	513.1	155.4	513.1	55.4	145.7
WESSELTON	LOG(600-D) = 2.5175 - .00059025(R)	0.8299	15.8	41.4	59.6	101.1	34.8	58.7
KIMBERLEY	LOG(550-D) = 2.0617 - .00090563(R)	0.4275	63.0	369.7	27.4	160.2	11.9	69.7
DUTOITSPAN	LOG(550-D) = 2.4336 - .0014289(R)	0.6680	120.9	864.4	32.4	231.5	8.7	61.2
BULTFONTEIN	LOG(550-D) = 2.64582 - .0014277(R)	0.6001	134.9	318.1	36.2	88.1	9.7	23.7
WESSELTON	LOG(550-D) = 2.5245 - .00094896(R)	0.8320	121.7	278.0	50.7	115.9	21.2	48.3

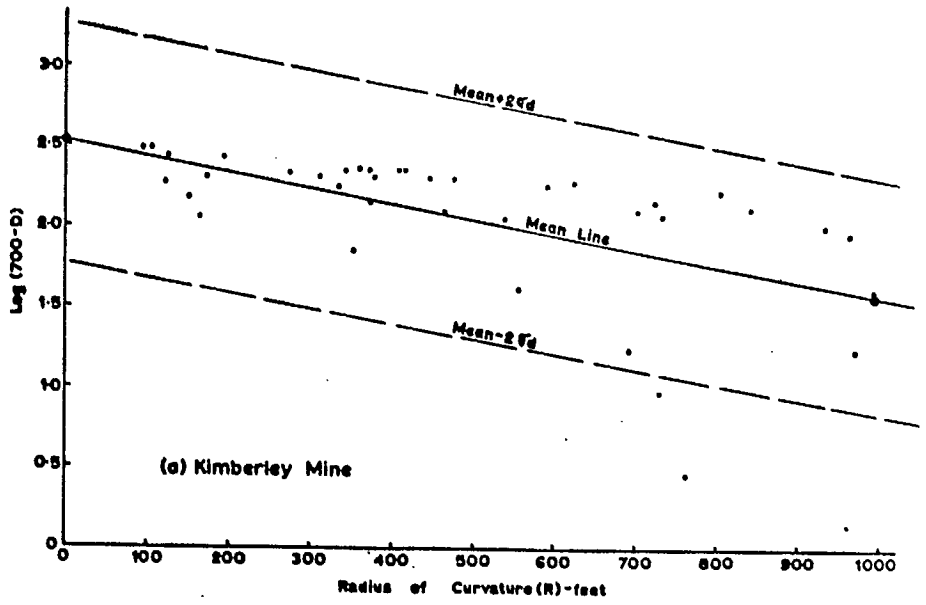

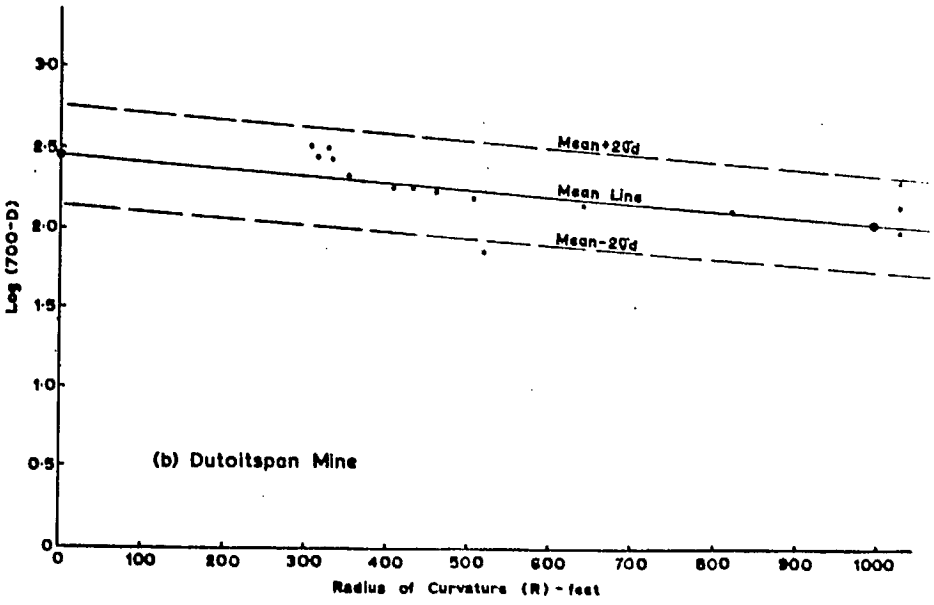

Fig. 6.9. Plot of radius of curvature (R) against log (700-D).

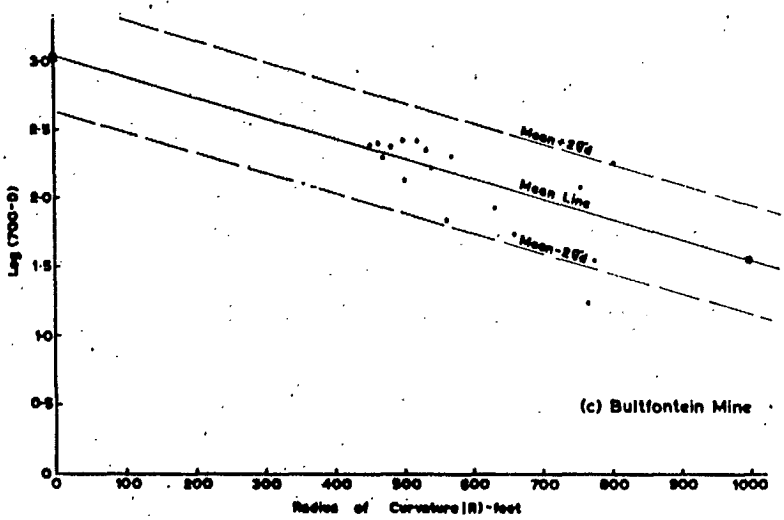

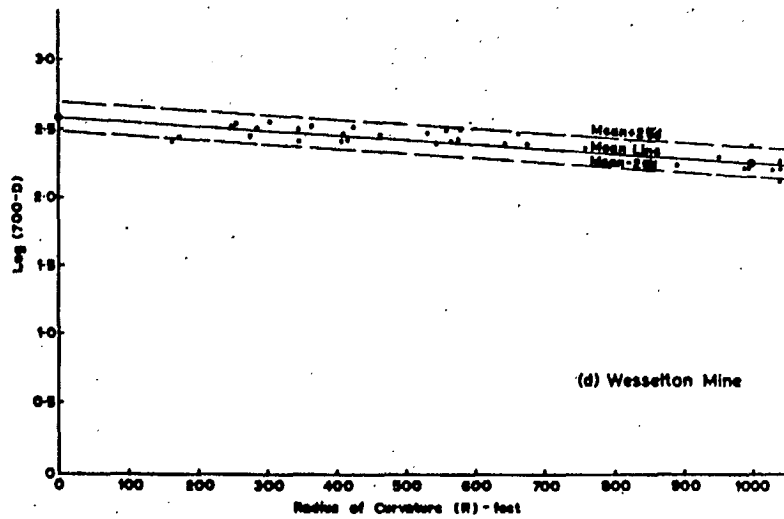

Fig. 6.9. Plot of radius of curvature (R) against log (700-D).

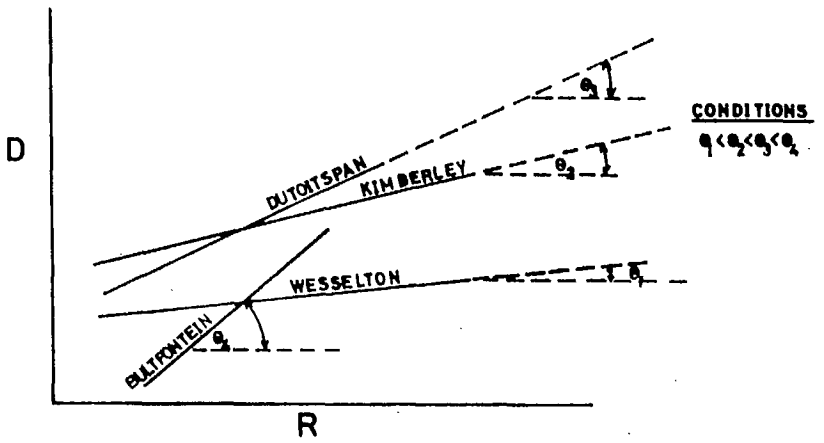

Fig. 6.10. Sketch of exaggerated plots for D against R for the four big holes.

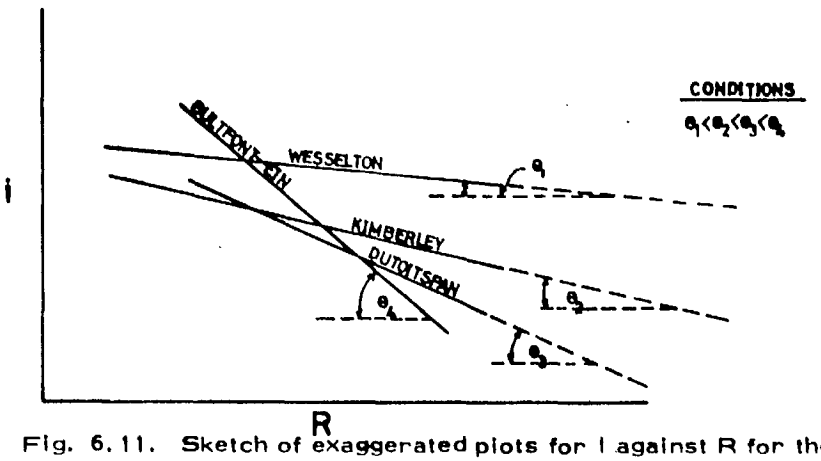

Fig. 6.11. Sketch of exaggerated plots for I against R for the four big holes.

pipes), the curves are flatter. For the pipe intermediate between the elongate and circular shapes, which has been classified as semi-elongate in shape (Dutoitspan pipe), the slope of the line (i.e. Θ_3) falls between the two. The same relationships can be shown in Fig. 6.11 for the I vs. R plots given previously in Fig. 5.6 (a to d). Only in this case the direction of slope is reversed, and the position of the curves are inverted, but the general relationship between Θ_1, Θ_2, Θ_3 and Θ_4 is similar.

In evaluating the treatment of the R and D data and the respective plots thus far, it was considered that this approach may not be entirely satisfactory to represent the breakback of any big hole in the Kimberley area for the following reasons:

(i) Firstly, the graphs with the straight plot of D vs. R, given in Figs. 5.5 (a to d), indicate that when R is very large, as with a straight slope in plane strain, D will also be very large. This in fact is not realistic because it is known that as R approaches infinity, as for a straight slope, D will approximate the natural profile representing the condition for an infinitely long, straight slope.

(ii) Secondly, in the case of the log (C-D) vs. R graphs, given in Figs. 6.9 (a to d), we overcome the difficulty encountered with the R vs. D graphs, as stated in (i) above, in giving the breakback as 700' (i.e. C = 700 ft) for a long straight slope. Another difficulty encountered in using this approach is that both the enclosing lines of twice the standard deviation also approach the asymtotic at D = 700 ft. This is clearly not realistic since the deviations from the average D must be maintained, at least within approximately the same order, for the infinitely long, straight slope.

Since the approach adopted thus far could not be shown to be entirely valid, it was considered necessary to apply the data in some other form to determine which approach more closely approximates the true (i.e. mathematically valid) model.

6.4.3 Application of the R and D Data to an Exponential Curve

For the reasons described above, an attempt was made to find the best fit to an exponential curve of the form $D = C - Ae^{-BR}$ using the rather complex theory which applies to fitting for this form of equation.

The data of the exponential curve of R vs. D for the Kimberley Mine in Table 6.V gave a reasonable result as shown plotted in Fig. 6.12.

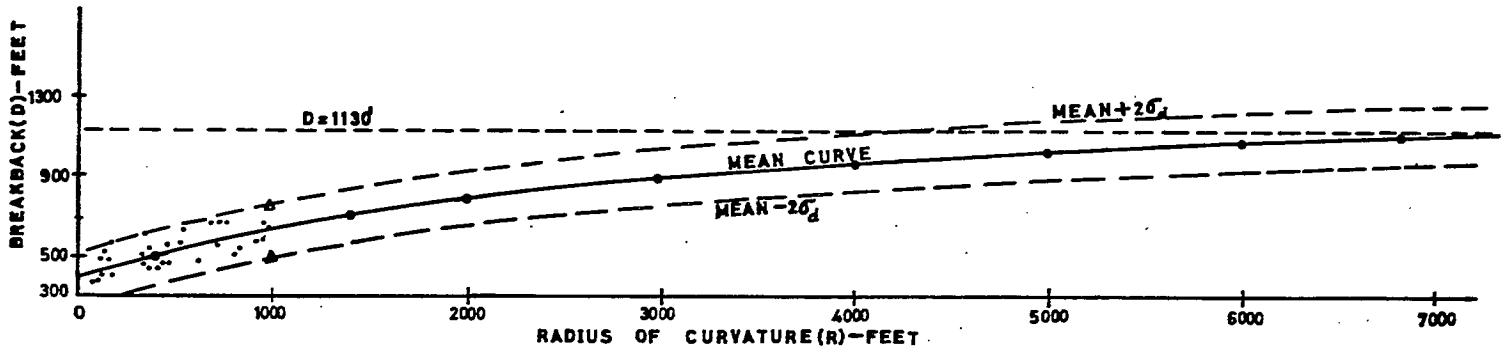

Fig. 6.12. Exponential curve of R against D for Kimberley Mine.

Table 6.V

Data of the Exponential Curve of R vs. D for the Kimberley Big Hole

Radius of Curvature R (ft)	Distance of Breakback D (ft)
0	416
400	516
1,000	640
1,400	708
2,000	794
3,000	899
4,000	972
5,000	1,022
6,000	1,056
6,800	1,075
7,800	1,093

The original measured values of R and D for Kimberley Mine, as given in Table 5.11(a), in comparison to the data in the Table 6.V, covers less than 20 per cent of the range of R's for the exponential plot shown in Fig. 6.12. The measured values are all close to the origin and cover only a small part of the whole exponential curve. Over this limited range of R and D values the curve approximates a straight line and this explains why the straight D vs. R plots gave such satisfactory results. The exponential curve becomes asymtotic at D = 1,130 ft; however, taking this value to be the limiting breakback for the long straight slope (i.e. C = 1,130 ft) is probably high, and is unrealistic due to the limited results scattered over only a narrow portion of the curve near the origin. Considering the results of the values for making the best fit by least squares, which are given in Table 6.IV, it is logical to conclude that the corrected breakback value for the infinitely long straight slope will be approximately 700 ft.

The data from the other three mines were also analysed to find the best fit to an exponential curve of the form $D = C - Ae^{-BR}$. Too few results were available for Bultfontein and Dutoitspan Mines for suitable analysis. The plot for Wesselton Mine was a very flat curve of the wrong shape. However, the initial portion, as was the case for Kimberley Mine, was a straight line similar to that found by the least squares fit for the R and D values, as shown in Fig. 5.5 (d) in the previous chapter.

From this further analysis, it can be concluded that the direct R vs. D plot with a straight line relationship is a good approximation to the exponential function over the ranges of values considered. It also gives satisfactory limiting envelopes, which are taken to be plus or minus two times the standard deviation as upper and lower limits for the values of D. Hence, it can be concluded that the straight R vs D plots given in Figs. 5.5 (a to d) are satisfactory for use in predicting the breakback values for pit slopes in the Kimberley area. It should be kept in mind, that D is a corrected D for a condition of zero dolerite thickness and for a shale slope height, i.e. depth of hole in shale, of 320 ft. Thus, when breakback values are predicted from these curves, corrections must be made to compensate for the dolerite thickness and for the known or potential depth of big hole under consideration.

Chapter 7

PREDICTION OF THE FINAL POSITION OF THE SLOPES OF DE BEERS MINE FOR THE CASE THAT THEY DEVELOP NATURALLY AND NO REMEDIAL PROVISIONS ARE TAKEN

7.1 INTRODUCTION

It has been shown in the previous chapter that the straight R vs. D curves given in Figs. 5.5 (a to d) are the best to use for predicting the breakback of any big hole in the Kimberley area. Further, it has been shown that to make comparisons between big holes in the Kimberley area an important factor which must be borne in mind is the shape of the pipe. Hence, it was further concluded that to predict breakback for any big hole in the local geological environment it is necessary to use the curve from that pipe whose shape approximates the pipe whose breakback is to be predicted.

It is clear that before a R vs. D curve can be selected to predict the final breakback position of the De Beers Mine slopes, the geometrical relationship between the shape of the De Beers pipe and the shape of the other pipes must be established.

7.2 METHOD OF DEFINING PIPE SHAPE

7.2.1 Determination of the Pipe Shape Ratio

In view of the foregoing considerations an effort was made to define the various pipe shapes on a simple mathematical basis. To define the shape of the respective pipes, the ratio of the average width (W_p) to the average length (L_p) was adopted. This parameter is designated the "shape ratio" (S.R.) and is determined as follows:

$$\text{Shape ratio (S.R.)} = \frac{W_p}{L_p} = \frac{\dfrac{W_{p1} + W_{p2} + W_{p3} \cdots\cdots W_{pn}}{n}}{\dfrac{L_{p1} + L_{p2} + L_{p3} \cdots\cdots L_{pn}}{n}} \quad \ldots\ldots 7.(1)$$

where the L_p's and W_p's are dimensions of the pipe taken parallel to the major and minor axes of the pipe, respectively, and n is the number of measurements taken. These measurements are taken at equally spaced intervals across the pipe. The number of measurements (n) was chosen to give satisfactory coverage of the major pipe irregularities. An example of these measurements for a hypothetical case is shown in Fig. 7.1.

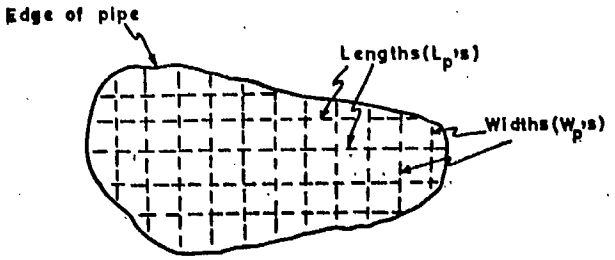

Fig. 7.1. Hypothetical measurements for determining the shape ratio (S.R.) of a pipe.

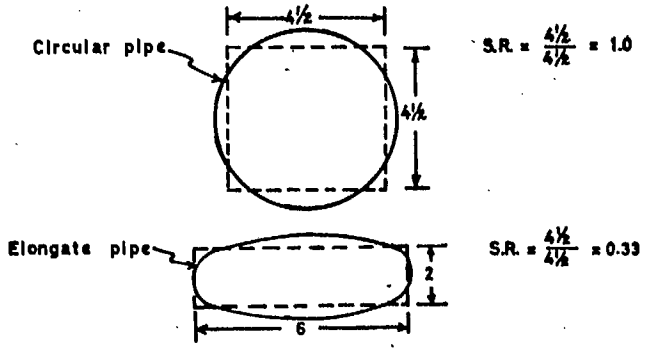

Fig. 7.2. Illustration of the shape ratio of a circular and elongate pipe.

The more circular the pipe the larger the shape ratio is since the difference between W_p and L_p is small. The circular pipe, as shown in Fig. 7.2, is mathematically defined as a square. The converse is the case for the elongate pipe where the difference between W_p and L_p is large, the shape ratio is small and it is numerically represented as a rectangle (see Fig. 7.2). The average length, average width and shape ratio for the various pipes under consideration are given in Table 7.1. With regard to the Wesselton pipe, being that one side of the pipe is convex curved, as shown in Fig. 5.2(d), both L_p and W_p were measured assuming the pipe on the convex side had a radius of 1,050 ft.

Table 7.1

Shape Ratio and Average Width and Length of the Pipes

Mine	Average Length (W_p)	Average Width (L_p)	Shape Ratio (S.R.)
Kimberley	679'	393'	0.579
Dutoitspan	932'	649'	0.696
Bultfontein	859'	768'	0.894
Wesselton	1,093'	528'	0.483
De Beers	997'	497'	0.498

7.2.2 Test for the Validity of the Shape Ratio Concept

To test for the validity of the approach taken to define the shape of the various pipes, the plots of R vs. D (Figs. 5.5 (a to d)) for the four big holes were inspected to ascertain the relationship between their shape ratio and the slope of the respective plots. With regard to the exaggerated curves shown previously in Fig. 6.10, it can be seen in Fig. 7.3 that the slope of the curve (θ) and the shape ratio (S.R.) are systematically related; as θ increases S.R. also increases, i.e. the larger the shape ratio the steeper the curve and vice versa. In view of this relationship existing, defining the pipe shapes in this manner seemed reasonable.

7.3 APPLICATION OF THE BREAKBACK DATA TO DE BEERS MINE FOR PREDICTING BREAKBACK

7.3.1 Selection of the R vs. D Curve Appropriate for De Beers Mine

In Table 7.1 above it can be seen that the shape ratio of the De Beers pipe is 0.498 and falls between that of the Wesselton and Kimberley pipes, which have shape ratios of 0.483 and 0.579, respectively. It is,

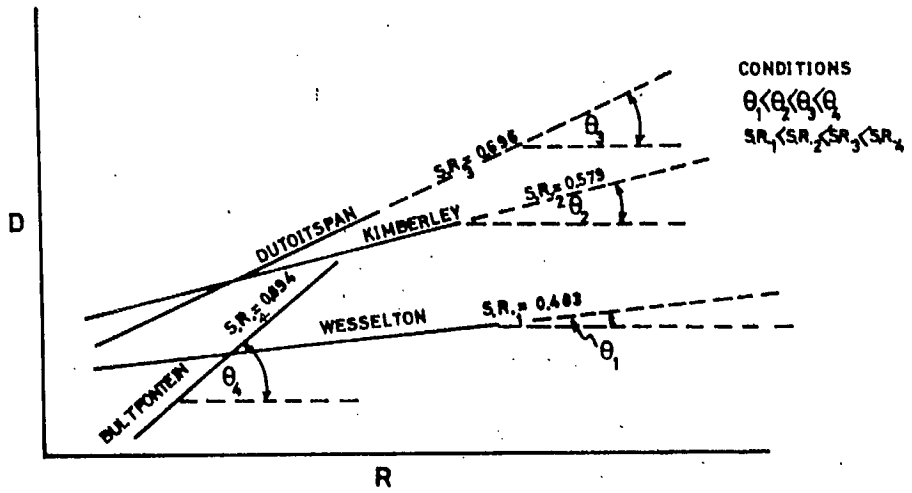

Fig. 7.3. Relationship between R against D plots and the shape ratio for the four big holes.

however, considerably closer to that of the Wesselton pipe which, as shown in Table 3.1, is also approximately the same size as that of the De Beers pipe.

In view of the above, it does not seem unreasonable to accept a curve for the De Beers pipe to lie proportionately, i.e. with respect to its shape ratio and that of the other two mines, between the Wesselton (Fig. 5.5(d)) and Kimberley (Fig. 5.5(a)) curves as shown in Fig. 7.4.

The curves shown in Fig. 7.4, however, are for corrected D (D_{corr}) values for no dolerite and a 320 ft depth of hole. Before the true breakback (D_o), as shown in Fig. 5.4, can be determined for the De Beers big hole, the curve must be corrected for the occurrence of 100 ft of dolerite which has been taken to have a natural angle of slope of 70 degrees. Corrections for depth of hole are not necessary since at the outset all the data for each pit were corrected to a standard height (H_{std}) of 320 ft being the composite depth of shale and dolerite of De Beers Mine.

From Equ. 5.(3) it can be shown for the De Beers case where

$$D_o = D_{corr} - C_1 + C_2 \qquad \ldots\ldots\ldots 7.(2)$$

that from Equ. 5.(2)

$$C_2 = -(H_o - H_{std}) = 0 \text{ since } H_o = H_{std}.$$

For a dolerite thickness (H_D) of 100 ft , from Equ. 5.(1)

$$C1 = (1.0641)H_D = 106.41$$

and the actual breakback (D_o) for De Beers is, therefore,

$$D_o = D_{corr} - 106.41. \qquad \ldots\ldots\ldots 7.(3)$$

To avoid the calculation of Equ. 7.(3) to obtain D_o, by dropping the curve in Fig. 7.4 a distance equivalent to a breakback of C_1 = 106.41 ft, D_o can be determined directly from the plot as shown in Fig. 7.5. As previously stated in Chapter 5, the mean line for R vs. D is not entirely satisfactory for predicting the final breakback position. In statistics it would not be normal to employ either of the $2\sigma_d$ values established for the Kimberley or Wesselton curves (i.e. where σ_d on D = 62.6 ft and 32.5 ft, respectively) for the case of the De Beers curve; however, to obtain some upper and lower limits of the De Beers curve, the mean of the standard deviation (σ_d) on D for these two plots has been taken giving a σ_d = 52.5 ft for De Beers. The $2\sigma_d$ lines displaced upwards and downwards from the mean line are shown in Fig. 7.5.

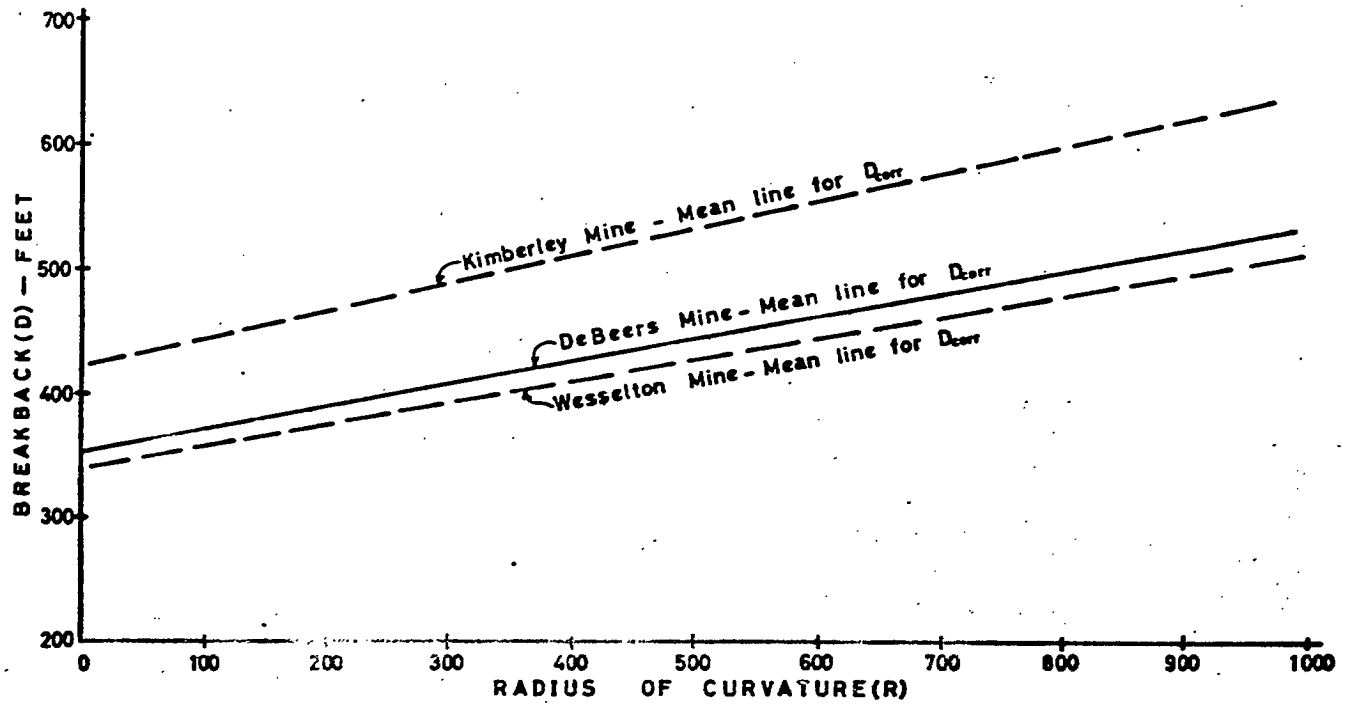

Fig. 7.4. Estimated curve of R against D appropriate for De Beers Mine.

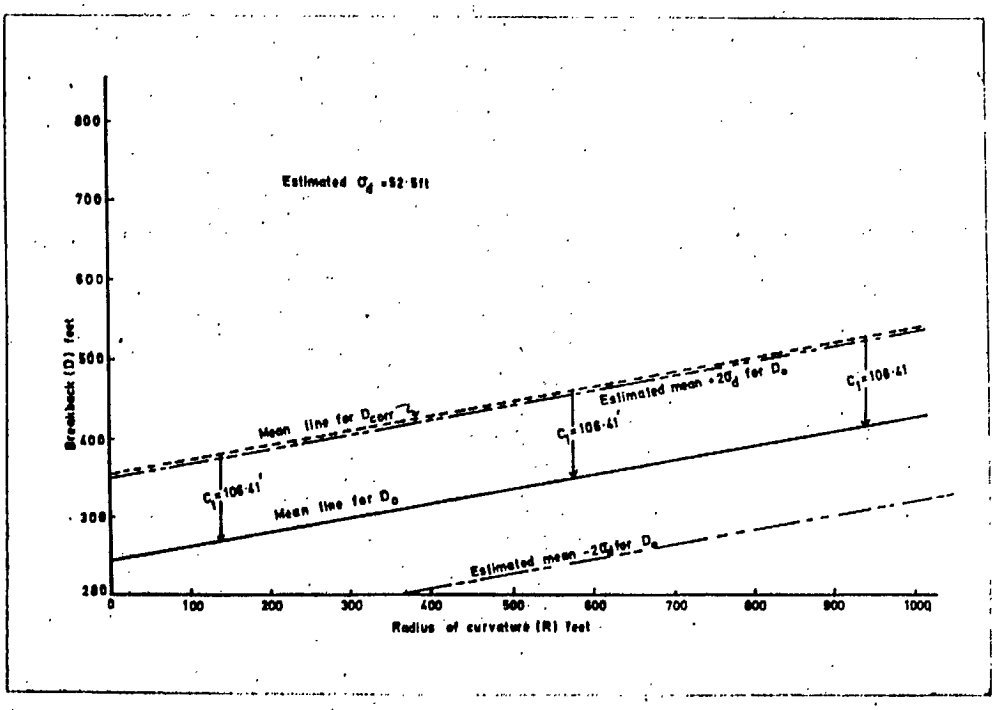

Fig. 7.5. Final estimated curve of R against D appropriate for predicting breakback of the De Beers Mine big hole.

7.3.2 Estimated Final Breakback Position of De Beers Mine

Before the final breakback position of the De Beers pit could be estimated, however, certain other considerations were necessary. Firstly, since the large wedge-shaped block formed by the hanging-wall of the inclined fault on the south side of the pipe cannot be stabilized in any reasonably simple and inexpensive manner, this block must be assumed to slide eventually into the pipe once the level of the materials in the pipe is lowered. Hence, the final rim of the pipe, which the overlying shale and dolerite slopes will develop to, must be accepted as the contact between the stable and unstable material at the top of the melaphyre, as shown hatched in Fig. 7.6. The same can be said for the narrow vertical block on the northwest side of the pipe as shown.

Secondly, the irregularities of the pipe must be smoothed out in the same manner that was carried out for the other pipes when the R and D relationships were initially established. The smoothed out edge of the De Beers pipe is shown as a broken line in Fig. 7.6. Next, the radii of curvature of the pipe at the different locations around its periphery are determined, as explained in Chapter 5, and finally the estimated breakback (D_o) is taken directly from the R vs. D plot in Fig. 7.5.

The curve of the estimated mean $+2\sigma_d$ was taken to estimate the actual predicted breakback (D_o) of De Beers Mine, since this plot gives the greatest, and hence, the most conservative estimate of stability. The estimated breakback of the pit edge for the $+2\sigma_d$ curve is shown in Fig. 7.6. For comparative purposes, the breakback position for the statistical mean value of the uncorrected breakback, D, is also shown, as is the original edge of the big hole before excavation proceeded. The effects of plan radius on the final breakback position are clearly shown in that, at the ends of the pipe (i.e. small R) the predicted breakback is inside the line of the statistical mean value of uncorrected D, and at the sides of the pipe the converse is the case.

It can be seen that the original edge of the big hole falls outside the predicted breakback position on the southeast side of the pit. This abnormally large breakback is attibuted to subsidence along the major fault and to anomalous groundwater conditions in the shale at this location. On both the north and west sides this edge comes reasonably close to the predicted breakback limit and can be explained. The north side in the early days was the site of the roadway out of the pit during the original open cast workings. The close proximity of the west side edge to the predicted breakback line, on the other hand, is due to subsidence, which developed contemporaneously with recent drawdown of the pipe in this area, along an unfavourably orientated set of faults.

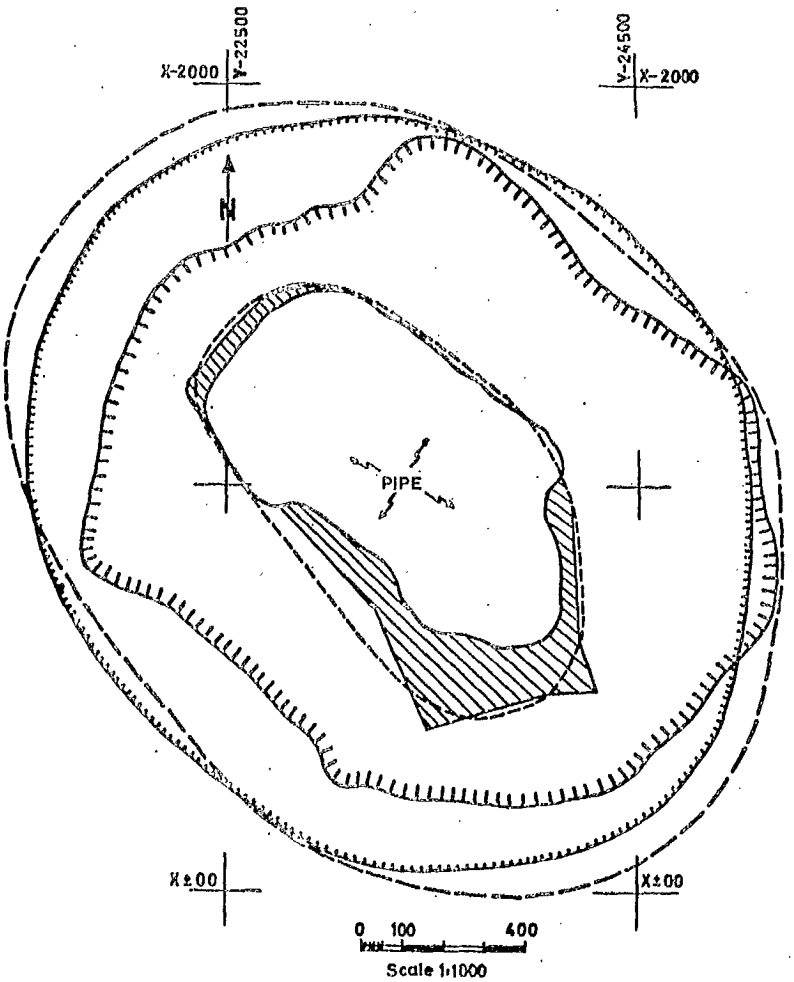

LEGEND

- Breakback for statistical mean value of D
- Predicted final breakback
- Original edge of the big hole
- Smoothed pipe edge
- Material expected to subside into the pipe due to faulting

Fig. 7.6. Predicted breakback for De Beers Mine big hole.

Chapter 8

COMPARISON OF THE EFFECTS OF PLAN RADIUS ON THE UPPER AND LOWER PARTS OF THE SLOPE

8.1 INTRODUCTION

In an effort to assess the different effects of plan radius of curvature for different parts of the slope, a detailed comparative analysis of the slope profiles of the Kimberley Mine big hole was conducted. Kimberley Mine was selected for this particular study, since the slopes, in comparison to the other big holes, had few anomalous conditions and the general plan shape was ideal in that profiles from areas of extreme radii (i.e. located on the major and minor axes) could be compared.

8.2 METHOD OF APPROACH

Six profiles of the shale slope were selected at both ends (i.e. the major axis) and both sides (i.e. the minor axis) of the pipe. These profiles were spaced at 10^{o} intervals (i.e. $\Theta = 10^{o}$) and, therefore, covered an area of slope within a 50 degree interval at both sides of the big hole on the major and minor axes. Similar to the natural angle of slope studies described in Chapter 3, the profile was considered in two parts in that the angle of the "top 100' section" and "lower section" were recorded independently.

8.3 RESULTS

The angles of slope of the shale from the respective profiles are given in Table 8.I and are summarized in Table 8.II.

As expected, the results show that the "overall slope" angle is 6.7^{o} steeper at the ends of the pipe where the radius of curvature is least. Comparison between the respective angles of the "lower section" and "top 100' section" for the sides and ends of the pipe shows that one is significantly less and the other is significantly greater than the mean for the overall slope. The difference in angle between the lower sections (i.e. 8.3^{o}) is greater than the difference between the top sections (i.e. 5.2^{o}) and the overall slope (i.e. 6.7^{o}) by 3.1^{o} and 1.6^{o}, respectively. These results are diagramatically shown in Fig. 8.1 where the angle of slope, i, is plotted against R for the slope angles at the ends ($i_{R_{199}}$) and sides ($i_{R_{791}}$) of the pipe.

The significant difference of slope angle between the "lower sections" as compared to the "top 100' sections" with respect to the major and minor axis of the pipe indicates that lateral constraint provided by

Table 8.1

Profile Angles and Plan Radius of Curvature of Shale Slopes on the Major and Minor Axes of Kimberley Mine

Location of Profile		Radius of Curvature (R)	Angle of Slope	
Slope	Bearing		Top 100' Section	Lower Section
Slopes at Sides of Pipe (Minor Axis)				
North Side	320°	806'	28.5°	27.5°
	330°	728'	30.0°	28.0°
	340°	939'	30.5°	28.0°
	350°	733'	36.5°	24.0°
	0°	540'	47.0°	22.5°
	10°	465'	32.5°	34.0°
	Average	701'	34.2°	27.3°
South Side	180°	767'	A.M.*	A.M.
	190°	732'	A.M.	"
	200°	973'	41.0°	"
	210°	998'	36.5°	"
	220°	967'	38.5°	"
	230°	845'	I.S. **	I.S.
	Average	880'	38.7°	-
Slopes at Ends of Pipe (Major Axis)				
East Side	100°	276'	48.0°	43.5°
	110°	177'	34.5°	38.5°
	120°	124'	46.0°	33.0°
	130°	153'	44.0°	33.0°
	140°	166'	42.5°	32.5°
	150°	356'	50.0°	28.0°
	Average	209'	44.2°	34.8°
West Side	250°	419'	39.0°	32.5°
	260°	127'	40.5°	31.0°
	270°	106'	44.0°	32.5°
	280°	95'	32.0°	43.0°
	290°	197'	29.0°	44.0°
	Average	189'	36.9°	36.6°

* A.M. -- slope affected by man.

** I.S. - slope in shadow, profile not available.

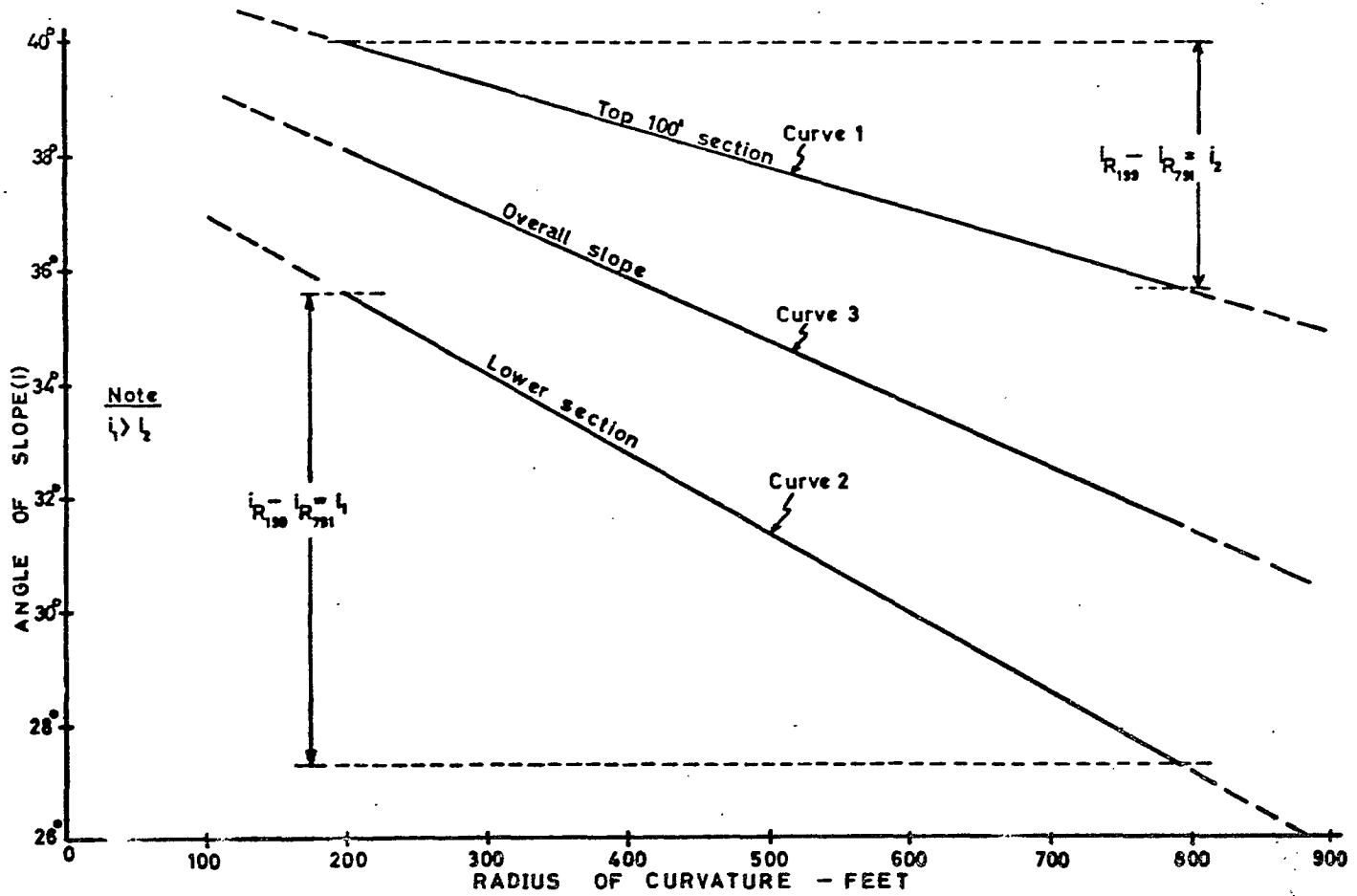

Fig. 8.1. Curves of I against R for upper and lower shale slope at major and minor axes.

curvature of slope is greatest at the toe. Tangential stresses, therefore, appear to diminish in a direction from the toe to the crest of the slope, the rate being mainly a function of R at the toe and height, H, above the toe, since R increases with an increase in H. These results indicate that the radius of curvature of the slope appears to have the greatest relative affect with respect to the upper and lower parts of the slope where the radii are least.

Table 8.11

Summary of Profile Angles and Radius of Curvature Data of Kimberley Mine From Table 8.1

Location of Profiles	Average Angle of Slope			Average Radius of Curvature(R)
	Top 100' Section	Lower Section	Overall Slope	
Sides of Pipe	*35.7°(9)	**27.3°(6)	⊛31.5°(6)	791'
Ends of Pipe	*40.9°(11)	**35.6°(11)	⊛38.2°(11)	199'
Difference	5.2°	8.3°	6.7°	592'

* - Values used in curve (1) of Fig. 8.1

** - " " " " (2) " " "

⊛ - " " " " (3) " " "

(15) - Figure in bracket indicates the number of profiles considered.

Chapter 9

POSTULATION ON THE MECHANICS OF FAILURE OF THE BIG HOLES BASED ON EXPERIMENTS OF MODEL SLOPES IN COHESIONLESS MATERIAL

9.1 INTRODUCTION

The mechanics of failure and the natural processes which form the composite slopes of the big holes were not entirely understood. Evidence of past slide scars and a few on-the-spot observations of actual large-scale failures, however, indicated that at least part of the slope development was due to deep-seated failures. Such failures consist typically of the dolerite moving downwards and outwards "en masse" exhibiting all the signs of deep-seated rotation (Photo 7. (i)).

On the other hand, some slopes of the big holes are reasonably uniform and smooth for considerable distances around the pit faces and are inclined at angles that are reasonably consistent indicating that no such deep-seated failures have taken place. These slopes, unlike those that are characterized by deep-seated failure, suggest that the mechanism of slope formation may be that of imperceptible ravelling of the weathered skin. Such ravelling must involve rocks of low cohesion and entails the free movement of individual fragments whereby the material that ultimately comprises such slopes is non-cohesive. Lacy (1964) notes that such slopes when stable are "independent of the weight of the mass, the height of the slopes, and the size of the fragments", but that the angle of slope is characteristic of each rock material.

Intuition suggested, however, that with a ravelling slope of cohesionless material of any curvature, regardless of the radius, the effect of tangential stresses or "hoop" stresses would be negligible and the R vs. D relationship occurring in the big holes would not exist. Thus, with a view to understanding the nature of the formation of the big holes in the Kimberley area, a series of experiments were conducted in the University laboratory using cohesionless material for tests of model slopes.

9.2 DESCRIPTION AND RESULTS OF THE EXPERIMENTS

For the experiment a 4 ft square 12 in. deep box was used in which various shapes of draw-off ori. ices were made in the bottom of the box. In one test a series of 8 circular openings from 3 in. diameter increasing by 3 in. to 24 in. diameter were used. In another test 7 elliptical openings with dimensions of 12 in. x 1 in. to 24 in. x 24 in. were used (Photo 9. (i)).

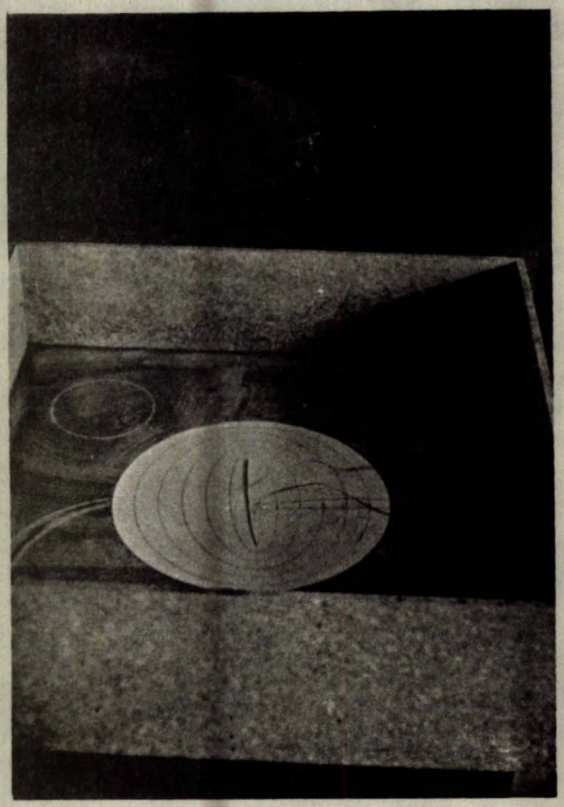

Photo 9. (i). Elliptical draw-off orifices in the bottom of a box.

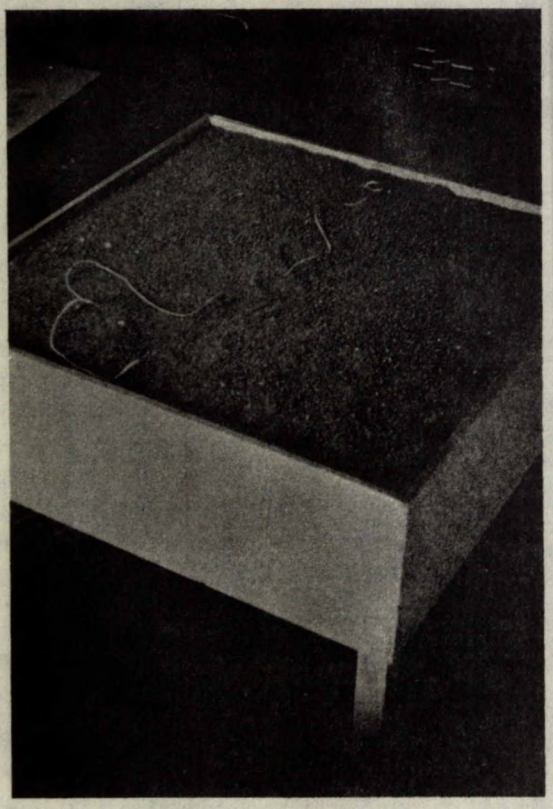

Photo 9. (ii). Box filled with dry artificial sand (agrelite).

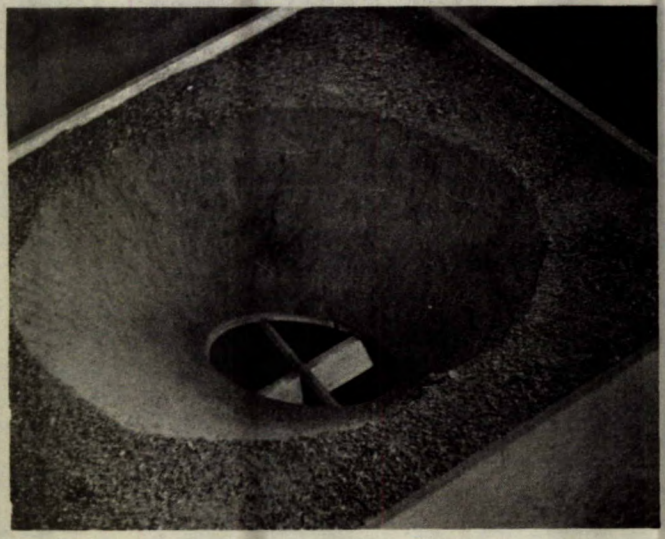

Photo 9. (iii). Ravelled slope in agrelite following removal of the wooden slab forming the orifice.

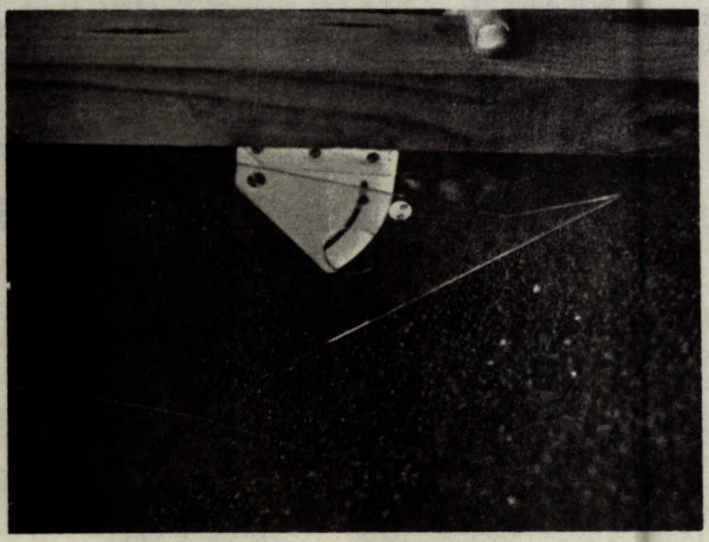

Photo 9. (iv). Measurement of the angle of the slope formed in the agrelite.

The box was filled with dry artificial sand called agrelite (Photo 9. (ii)), which is a light weight aggregate obtained by processing steelmill slag. An attempt was made to secure uniform density of the agrelite by filling the box in $\frac{1}{4}$ in. layers. The agrelite was dried by leaving it spread out over the laboratory floor for several days prior to its use in the tests.

For the first test, circular orifices in the bottom of the box were used. The box was filled to a depth of 11 in. with agrelite of uniform density. The central circle was removed by pulling it upwards through the material and the slopes ravelled back until they reached equilibrium (Photo 9. (iii)). The diameter of the top of the resulting hole and the angle of the slope (Photo 9. (iv) were measured. Each successive circle was removed and the resulting stable slopes were measured. These results are given in Table 9. I and are shown graphically in Fig. 9. I. A line drawn through the points so obtained is shown in Fig. 9. I designated Test No. 1.

Table 9. I

Test No. 1 for Drawdown Condition Using Circular Orifices

Radius of Orifice	Angle of Repose of Agrelite				Diameter of Breakback	
	North	South	West	East	N-S	W-E
$1\frac{1}{2}$"	$60\frac{1}{2}^{o}$	59^{o}	61^{o}	59^{o}	$16\frac{3}{4}$"	$16\frac{1}{4}$"
3"	$65\frac{1}{2}^{o}$	64^{o}	$63\frac{1}{2}^{o}$	$63\frac{1}{2}^{o}$	$17\frac{1}{2}$"	$17\frac{1}{2}$"
$4\frac{1}{2}$"	62^{o}	$65\frac{1}{2}^{o}$	$62\frac{1}{2}^{o}$	62^{o}	$20\frac{1}{4}$"	22"
6"	$60\frac{1}{2}^{o}$	$62\frac{1}{2}^{o}$	63^{o}	55^{o}	$23\frac{1}{2}$"	$24\frac{1}{2}$"
$7\frac{1}{2}$"	64^{o}	62^{o}	71^{o}	56^{o}	$26\frac{1}{4}$"	$25\frac{1}{2}$"
9"	61^{o}	62^{o}	69^{o}	62^{o}	30"	29"
$10\frac{1}{2}$"	62^{o}	$60\frac{1}{2}^{o}$	73^{o}	65^{o}	$32\frac{1}{2}$"	32"
12"	$64\frac{1}{2}^{o}$	$62\frac{1}{2}^{o}$	64^{o}	$62\frac{1}{2}^{o}$	$34\frac{1}{2}$"	35"

After the last slope had been measured, most of the agrelite was removed from the box. Using a spade, agrelite was put back into the box with all the circles removed and this was continued until the addition of material no longer made any change in the slope angles formed. Then the angles of the slopes were measured. The next largest circle was then replaced and more agrelite was added with the spade and angles of slope were again measured. This was repeated for each circle down to 3 in. diameter. The results are tabulated in Table 9. II and are represented graphically as Test No. 2 in Fig. 9. I. In this instance the average

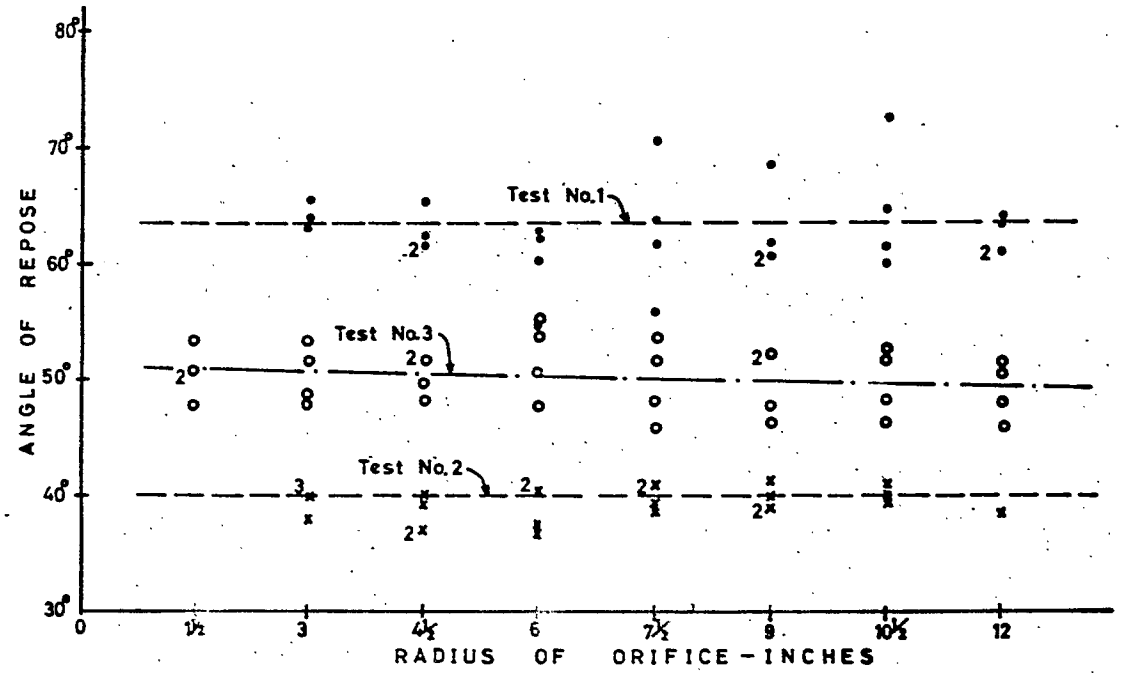

Fig. 9.1. Plot for circular orifices of angle of repose against radius of orifice.

measurement of slope of the pile of agrelite which had fallen from the box onto the floor was also recorded and was found to stand at an angle of repose of $38\frac{3}{4}^{\circ}$.

Table 9. II

Test No. 2 for Filling Condition Using Circular Orifices

Radius of Orifice	Angle of Repose of Agrelite			
	North	South	West	East
12"	$38\frac{3}{4}^{\circ}$	-	-	-
$10\frac{1}{2}$"	$39\frac{1}{2}^{\circ}$	40°	$41\frac{1}{4}^{\circ}$	-
9"	39°	$41\frac{1}{2}^{\circ}$	40°	39°
$7\frac{1}{2}$"	$39\frac{1}{2}^{\circ}$	41°	41°	39°
6"	37°	$37\frac{1}{2}^{\circ}$	$40\frac{1}{2}^{\circ}$	$40\frac{1}{2}^{\circ}$
$4\frac{1}{2}$"	$38\frac{1}{2}^{\circ}$	37°	40°	37°
$1\frac{1}{2}$"	38°	40°	40°	40°

A third test was conducted which was a repeat of the first half of Test No. 1. The results for this test are given in Table 9. III and are designated Test No. 3 in Fig. 9. 1.

Table 9. III

Test No. 3 for Drawdown Condition Using Circular Orifices

Radius of Orifice	Angle of Repose of Agrelite			
	North	South	West	East
$1\frac{1}{2}$"	51°	$53\frac{1}{2}^{\circ}$	51°	48°
3"	$53\frac{1}{2}^{\circ}$	52°	49°	48°
$4\frac{1}{2}$"	52°	52°	50°	$48\frac{1}{2}^{\circ}$
6"	55°	54°	51°	48°
$7\frac{1}{2}$"	52°	54°	$48\frac{1}{2}^{\circ}$	46°
9"	$52\frac{1}{2}^{\circ}$	$52\frac{1}{2}^{\circ}$	48°	$46\frac{1}{2}^{\circ}$
$10\frac{1}{2}$"	53°	52°	$48\frac{1}{2}^{\circ}$	$46\frac{1}{2}^{\circ}$
12"	52°	51°	$48\frac{1}{2}^{\circ}$	46°

A fourth and last test was conducted using the elliptical openings and the procedures were similar to those employed in the first half of Test No. 1. These results are given in Table 9. IV and are shown diagramatically in Fig. 9. 2.

9. 3 DISCUSSION OF RESULTS

Geometrically these model tests are considered to be a fair model of the conditions found at the big holes of Kimberley, where the rim of the pipe in the melaphyre forms a rigid toe similar to the orifices modelled in the bottom of the box. Where the orifice is not of a rigid type, the draw pattern creates an effective orifice which shows the behaviour of a cohesionless sand being drawn from a parallel-sided bin.

The material chosen was not completely cohesionless. Since cohesion varies with moisture content, different cohesion occurred during each test since the moisture content was not constant. With the slopes of small height used in the tests the resulting slope angles were very sensitive to small changes in cohesion. Nevertheless, while such small changes in cohesion do not allow direct comparison between different tests; within any one test the cohesion remained reasonably constant. Therefore, the results within each of the four tests are comparable. It can be seen in Figs. 9. 1 and 9. 2 that within each test the slope angles for different radii are all approximately equal. Comparison between the different tests, however, is not possible because the moisture content, and hence the cohesion, vary.

By placing material in different ways different densities can be obtained(Metcalf, 1966). The angle of slope is increased by increasing density, such as for increasing degrees of interlocking of the grains. This difference is apparent in comparing the angles obtained in Tests Nos. 1 and 2 for the drawdown and filling conditions, respectively. As explained, although these tests are not directly comparable, the drawdown condition gives much higher angles of repose. However, for any given way of placing and for any constant density, the average slope angle remained constant for the different radii of curvature of the orifices. Density determinations gave a value of 81. 3 lb/cu ft for the drawdown condition (Tests Nos. 1 and 3) and 75. 2 lb/cu ft for the filling condition (Test No. 2). Angles of measurement of slopes of the dumped materials of mixed shale and dolerite at De Beers Mine are of the order of 35^{o} to 36^{o}.

From the above results it can be concluded that, if a slope forms by a ravelling process (i. e. the slope is formed by cohesionless material),

Table 9. IV

Test No. 4 for Drawdown Condition Using Elliptical Orifices

Ellipse No.	Measurements on Major Axis					Measurements on Minor Axis				
	Radius of Orifice	Angle of Repose		Diameter of Breakback		Radius of Orifice	Angle of Repose		Diameter of Breakback	
		North	South	North	South		West	East	West	East
1	$\frac{1}{8}$"	$53\frac{1}{2}^{o}$	$53\frac{1}{2}^{o}$	9.1"	8.5"	72"	53^{o}	$53\frac{1}{2}^{o}$	13.5"	14.25"
2	$\frac{3}{4}$"	$54\frac{1}{2}^{o}$	55^{o}	10.75"	10.5"	25"	$56\frac{1}{2}^{o}$	57^{o}	14.9"	14.5"
3	2"	56^{o}	56^{o}	12.9"	12.0"	16"	$56\frac{1}{2}^{o}$	$51\frac{1}{2}^{o}$	15.7"	17.5"
4	4"	54^{o}	56^{o}	15.4"	14.0"	14"	$56\frac{1}{2}^{o}$	56^{o}	16.5"	17.5"
5	$6\frac{1}{2}$"	$53\frac{1}{2}^{o}$	55^{o}	15.5"	16.5"	$12\frac{1}{2}$"	58^{o}	55^{o}	17.8"	19.3"
6	9"	$55\frac{1}{2}^{o}$	$52\frac{1}{2}^{o}$	19.0"	19.0"	12"	$55\frac{1}{2}^{o}$	$52\frac{1}{2}^{o}$	18.6"	19.3"
7	12"	$53\frac{1}{2}^{o}$	53^{o}	21.2"	20.6"	12"	58^{o}	$53\frac{1}{2}^{o}$	20.1"	21.3"

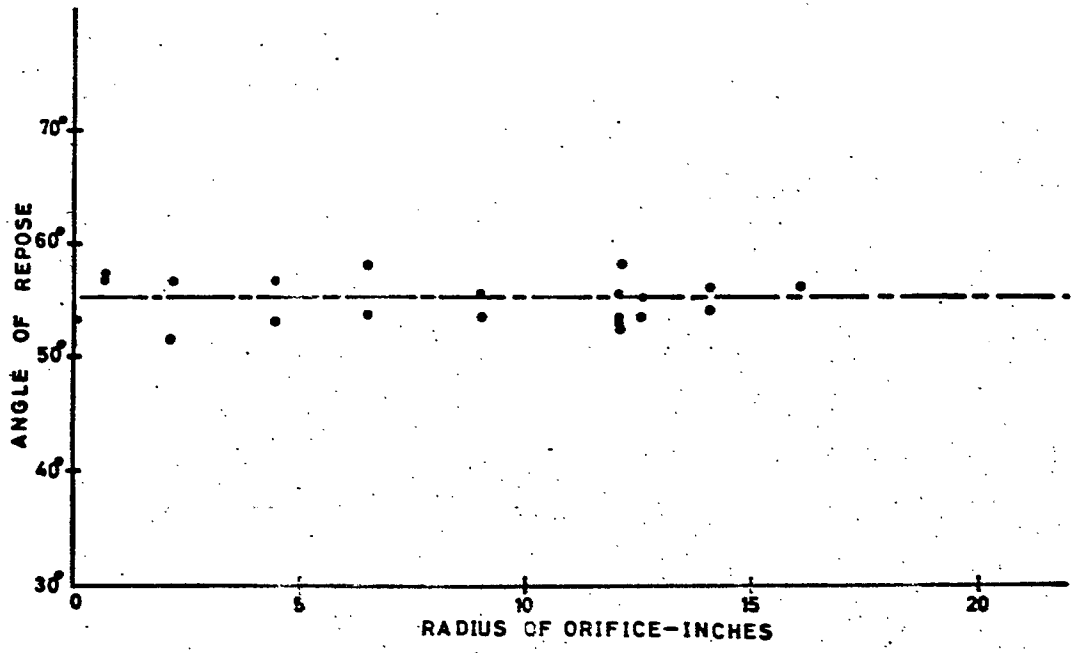

Fig. 9.2. Plot for elliptical orifices of angle of repose against radius of orifice.

the radius of curvature of the slope in plan appears to have no significant affect on the slope angle which is formed. In view of this, it can be further concluded that the most predominant mechanism of failure of the big holes in the Kimberley area, because of the fact that radius of curvature effects are seen to occur, is one of a deep-seated nature and that ravelling, with the possible exception of local sections, does not occur on a large scale.

Chapter 10

INVESTIGATION OF THE PATTERN OF BREAKBACK OF THE BIG HOLES TO DETERMINE THE ABSENCE OR PRESENCE OF SIGNIFICANT REGIONAL STRESS

This chapter deals with an investigation which was conducted to ascertain whether regional stress exists in the Kimberley area which is of sufficiently large magnitude to affect the stability of the slopes. Following the ideas put forward in Chapter 3 (Vol. I), i.e. that a large regional stress field may result in differential slope failure, the pattern of breakback of the various big holes was examined for the occurrence of such effects in the area.

10.1 INTRODUCTION

If a pipe is perfectly circular and if there are no extraneous influences acting on the slopes, such as significant regional stress, of a type and magnitude sufficient to influence the natural slope forming processes, then one would expect the slopes to break in a truly circular fashion as shown in Fig. 10.1. Further, if the orientations of joints, faults and other planes of weakness in the slopes around a circular pipe are favourable with respect to the slope face, circular breakback would be anticipated. Also, if the groundwater conditions were such that they had similar and equal influence at all points around the pipe, once again one would expect the breakback to be reasonably similar.

However, if regional stress of significant magnitude exists, or if there are other influences of a horizontal directional nature we would expect to find that these anomalous conditions will influence the slope breakback. If significant regional stress (S_{hR}) exists we would expect to find that there would be a predominant direction parallel to S_{hR} in which the major principal stress (σ_1) acts. At right angles to S_{hR} another horizontal stress (S_h) will exist in which the minor principal stress (σ_3) acts. Under these conditions we would expect that with a perfectly circular pipe the breakback around it would be different. That is, the pattern of breakback around the pipe would vary and bear relationship to the principal stress directions. Hence, for a circular pipe, breakback would develop as shown in Fig. 10.2.

If the case shown in Fig. 10.2 for a circular pipe existed in the Kimberley area one would expect that observations of R and D would show a single R value with a cyclic variation of D values with an amplitude

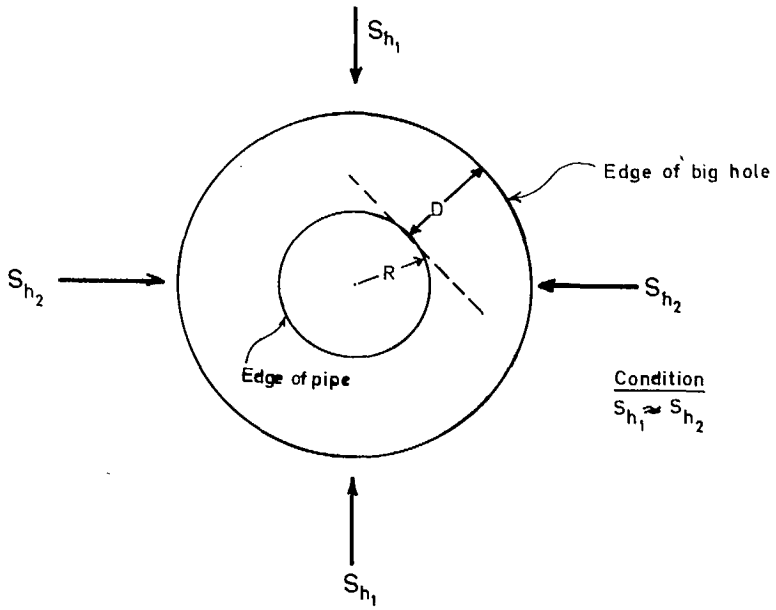

Fig. 10.1. Circular breakback for a circular pipe with no extraneous effects influencing the slope-forming processes.

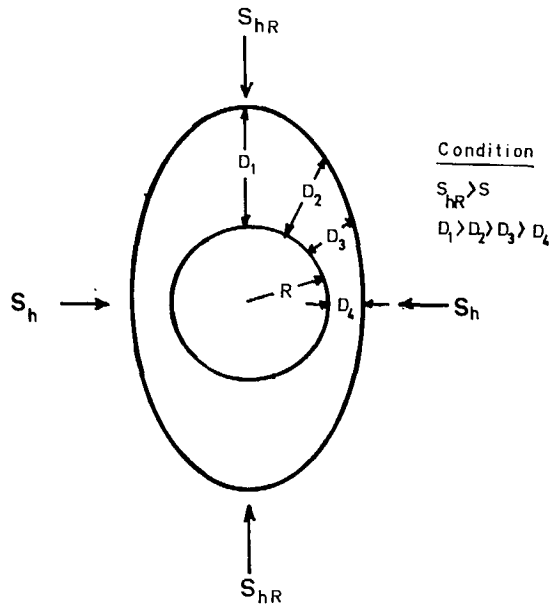

Fig. 10.2. Breakback to be expected for a circular pipe in a significant regional stress field.

of 180° around the compass as shown in Fig. 10.3. If these D values were to be plotted on a rose-diagram, for example, one would expect then that the directions of the principal stresses could theoretically be determined by orientating the major and minor principal stresses to fit the oblong rosette similar to that in Fig. 10.2.

If effects such as regional stress are present in the Kimberley area and if this stress is of sufficient magnitude to affect the natural slope forming processes, it should be possible, in studying the breakback of the big holes, to detect their presence. With this in mind a series of analyses of the R and D data have been carried out for the four big holes in Kimberley. As for the studies discussed earlier, it is assumed that the values of R and D used in this study apply only to slopes in which normal conditions occur. Since no attempt has been made to eliminate regional stresses in the slope, it would follow that if they are present and are sufficiently great in magnitude to effect the slope forming processes, then their effects should be found to be included in the observations.

10.2 ALTERNATIVE APPROACHES ADOPTED TO INVESTIGATE THE BREAKBACK PATTERNS FOR INDICATIONS OF POSSIBLE REGIONAL STRESS.

Of the four big holes studied, only the Bultfontein pipe is approximately circular (i.e. the shape ratio = 0.894). For this pipe the breakback is approximately constant. It is unfortunate, however, that the observations for these slopes are sparse because of the considerable sections of slope that had to be rejected due to the occurrence of anomalous conditions already described. Hence, we must revert to a study of the other big holes, where the pipes are non-circular, to investigate for the possible presence of regional stress.

10.2.1 Examination for Cyclic Effects of D Corrected to a Preselected R Plotted Against Bearing of D

As stated previously, both the plan shape of the pipe and top edge of the big hole of the other three mines have the appearance of crude ellipses. For this reason the fundamental properties of the ellipse have been taken as a guide to the analysis of the R vs D data. In considering the effects of regional stress, as described above, the problem is one of finding a correction which will have the effect of reducing the data to the equivalent values which would apply if the pipe had been a circular one.

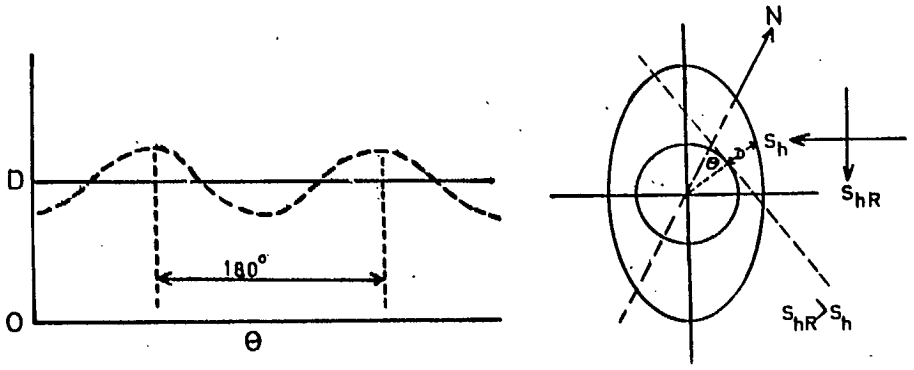

Fig. 10.3. Cyclic variations in breakback for a circular hole in material subject to regional stress (S_{hR}).

At any point on the periphery of a particular pipe the radius is R and the breakback D. To correct for the effect of changing radius the question is what the breakback at the same point would be if the radius were changed to a preselected value R_2. If we have another point on the periphery which has the radius R_2 and breakback D_2, then by rotating the ellipse we can move this second point (i.e. with radius R_2) into the selected position (i.e. where the radius was R and the breakback was D). In writing a general relationship for the particular ellipse.

$$D = A + BR \qquad \ldots\ldots\ldots 10.(1)$$

the change to D, which will be caused by rotating the ellipse will be

$$(D_2 - D) = (A + BR_2) - (A + BR) \qquad \ldots\ldots\ldots 10.(2)$$

giving $$\Delta D = B\,(R_2 - R) \qquad \ldots\ldots\ldots 10.(3)$$

so that the corrected D, D_{cR}, will be given by

$$D_{cR} = D + B\,(R_2 - R). \qquad \ldots\ldots\ldots 10.(4)$$

We have quite a large variation in D values for various R's. Each of these have been handled in this way and the resulting D's, all corrected to a single R_2, have been plotted against compass bearing to ascertain whether there are trends in two directions which might be orientated at 90° to each other.

Two values of R_2 were selected, namely 540 ft and 665 ft which are the two values from Bultfontein and which approximate the mean value of the radius of two sides of the pipe where data are available. These calculated values of D corrected (D_{cR}) to the two single radii were plotted against the bearing of the points from which the values originated. The plots for the four mines are given in Figs. 10.4 (a to d) for the 540 ft radius case and in Figs. 10.5 (a to d) for the 665 ft radius case. These curves were examined for cyclic effects such as any systematic kinks or crests and hollows which would represent extraneous influences at 90° to each other, giving an overall variation with an amplitude of 180°.

If regional stress exists the curve of the plots should idealistically consist of two hollows and two crests spaced 180° apart. Possibly with the exception of Figs. 10.4(a) and 10.5(a) of Kimberley Mine, cyclic effects of this nature are clearly not apparent. The Kimberley Mine plots suggest this cyclic effect only in that two hollows and one crest are evident. Since regional stress is likely to be in the same direction in the general studied area, one would expect, however, that if regional stress

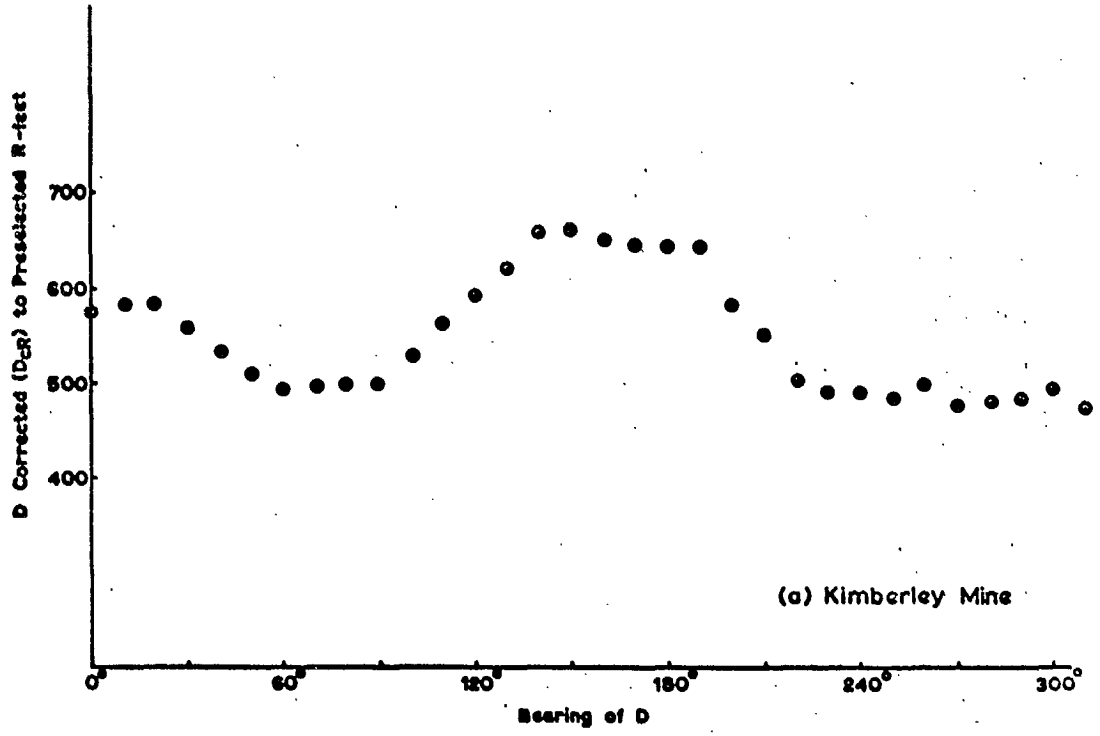

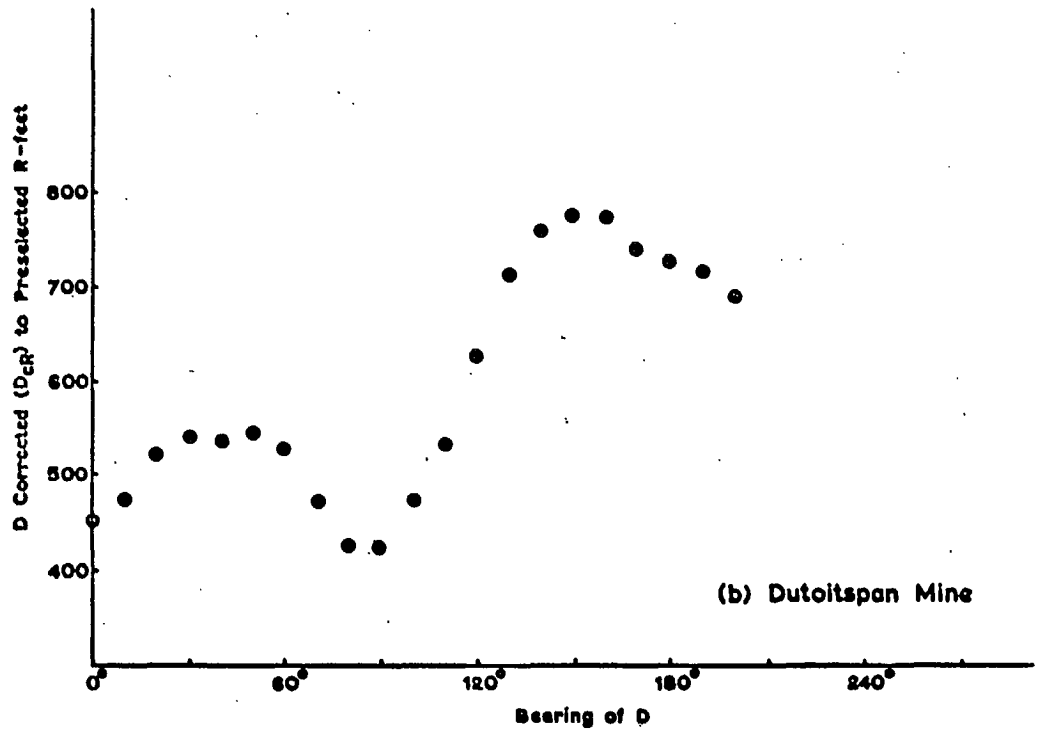

Fig. 10.4. Plot of corrected (D_{cR}) to a preselected R against bearing for 540 ft radius case.

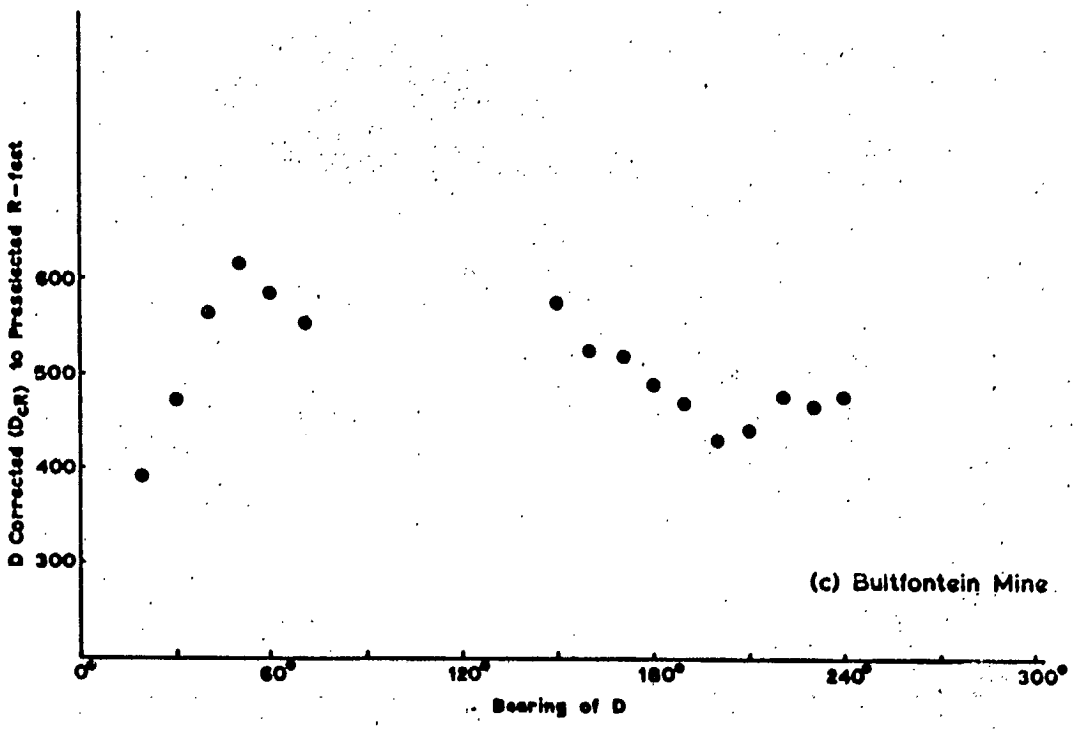

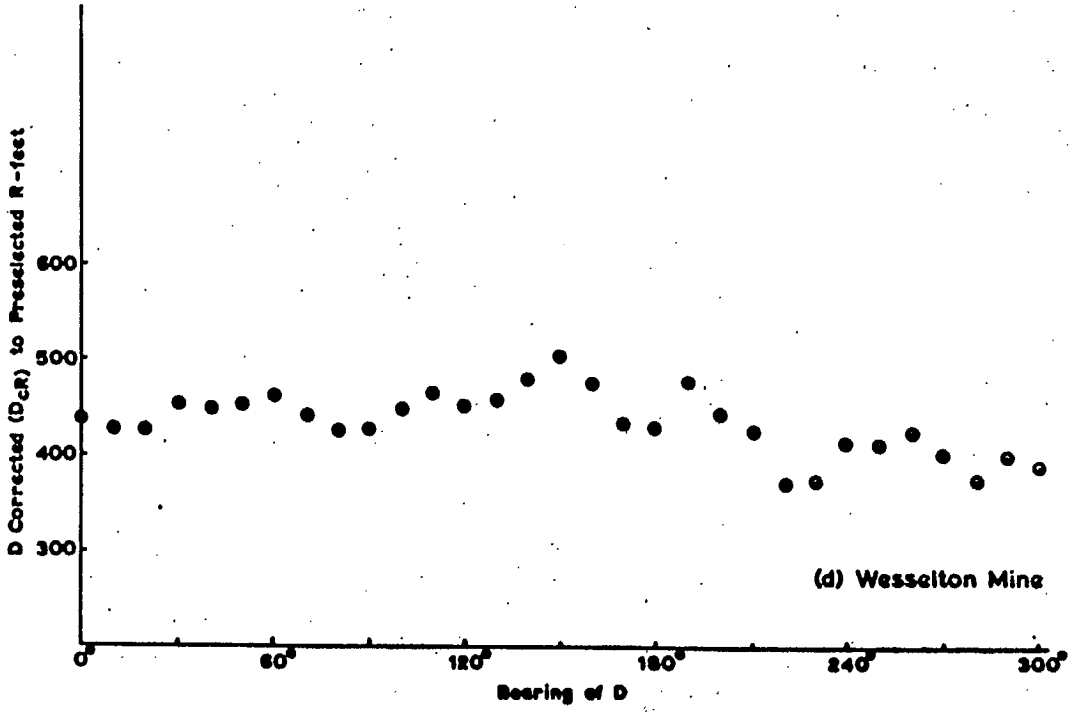

Fig. 10.4. Plot of D corrected (D_{cR}) to a preselected R against bearing for 540 ft radius case.

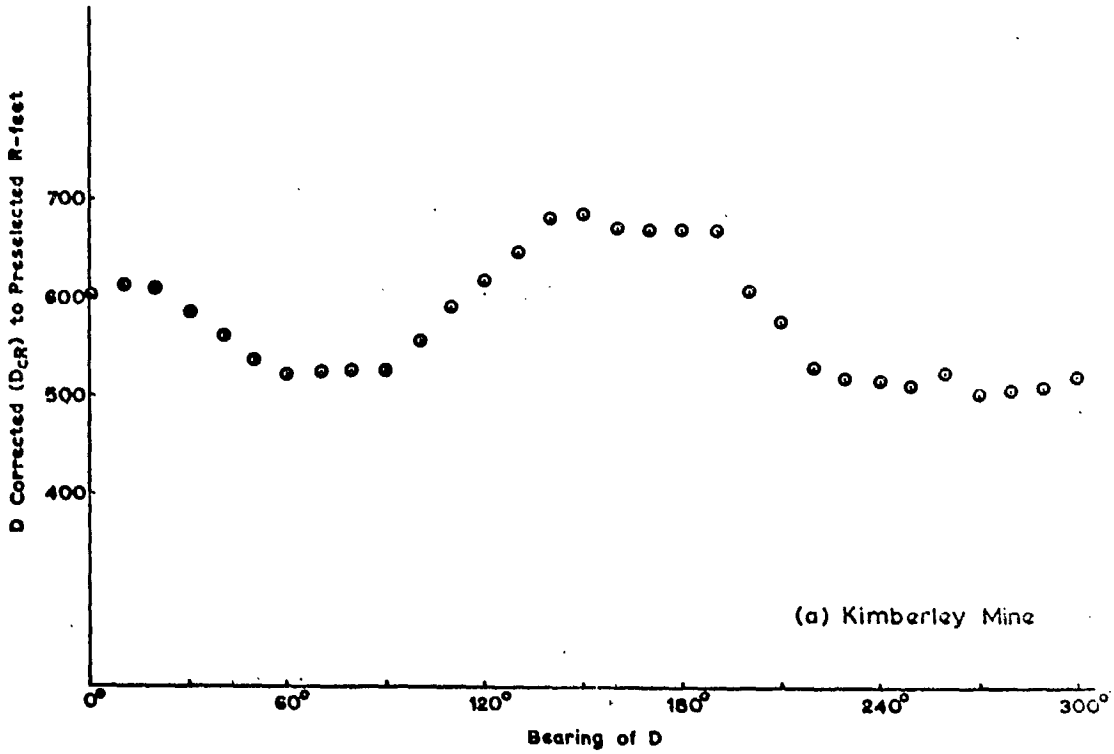

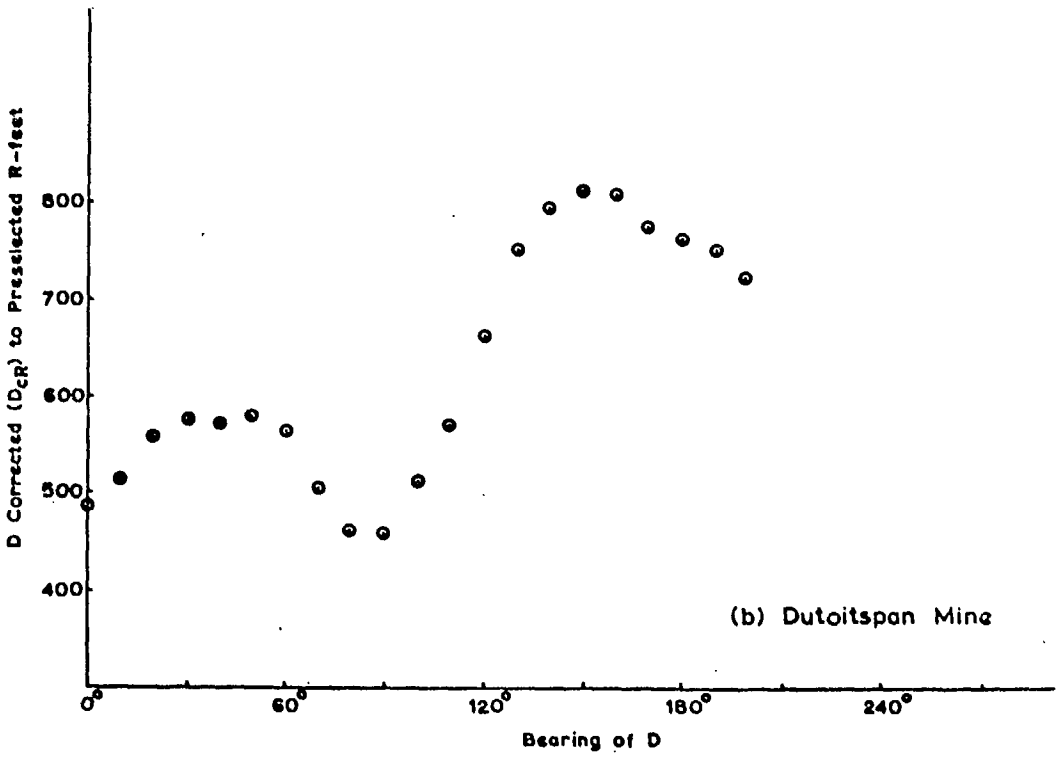

Fig. 10.5. Plot of D corrected (D_{cR}) to a preselected R against bearing for 665 ft radius case.

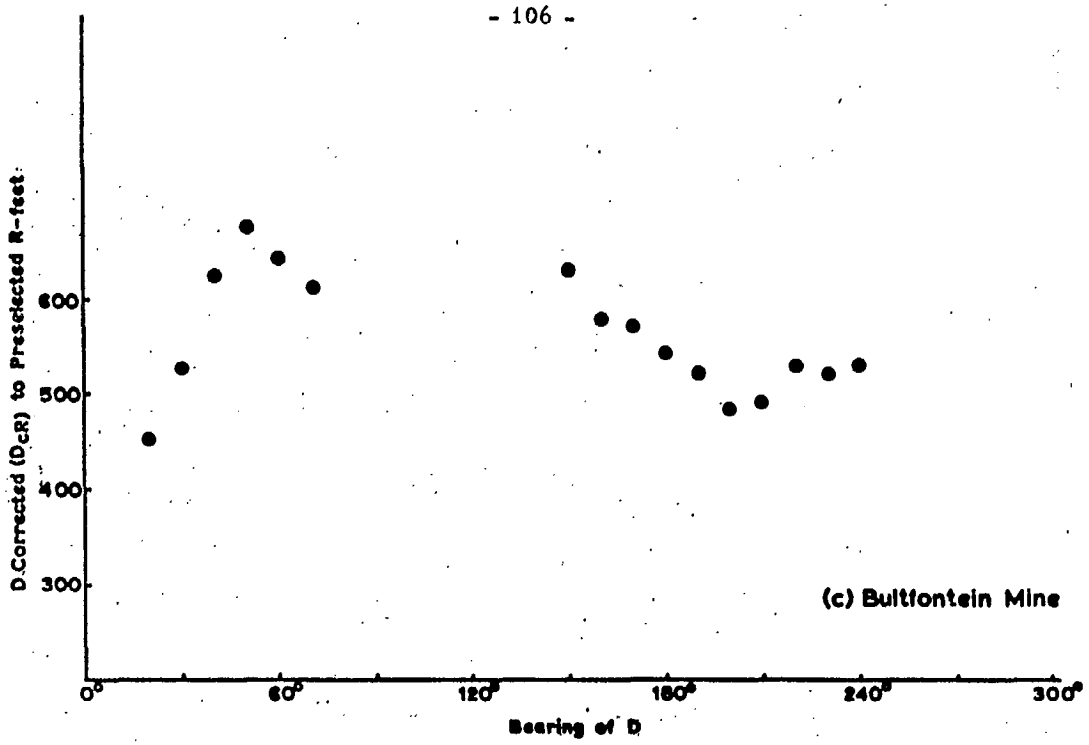

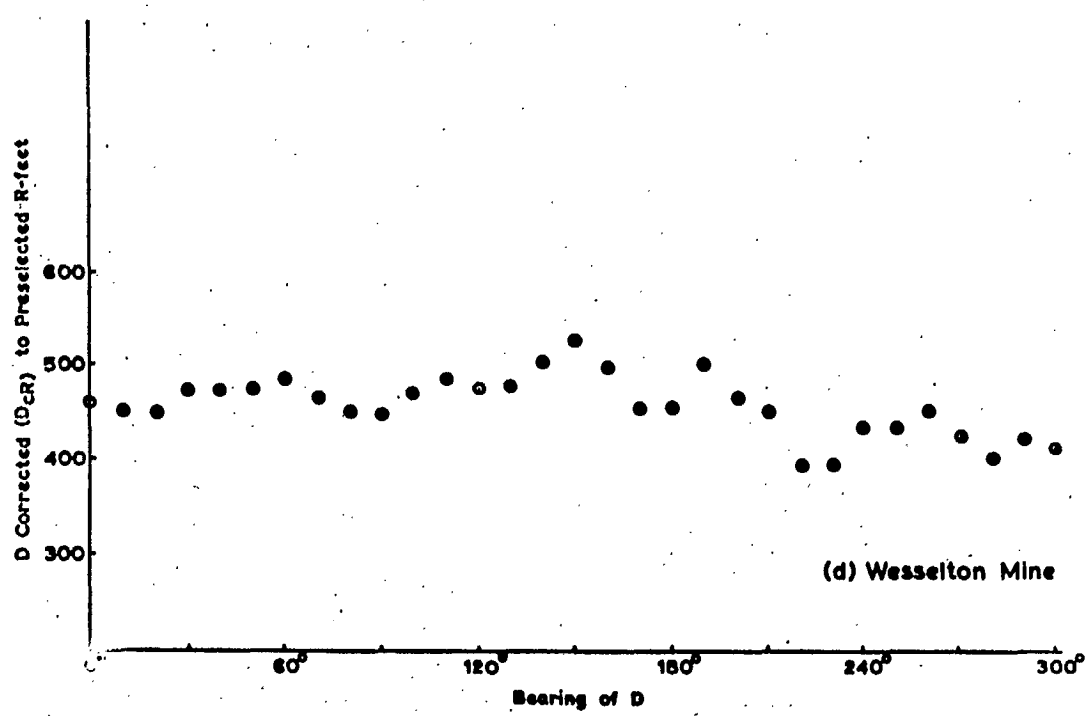

Fig. 10.5. Plot of D corrected (D_{cR}) to a preselected R against bearing for 665 ft radius case.

exists the crests and hollows would fall at approximately the same location in each plot. This situation is not seen, in fact, the opposite appears to be the case in some instances. Hence, it was concluded from inspection of these plots that definite trends or patterns could not be recognized which would suggest any directional effects.

10.2.2 Examination for Cyclic Effects for Variations of D Corrected and R for Different Compass Bearings Around the Big Holes

Another way of approaching the problem is to examine comparatively the variations of the D and R data originally given in Tables 5.11 (a to d), i.e. the D_{corr} and mean R, against compass bearing (θ) around the big hole. Plots of these quantities are given in Figs. 10.6 (a to d).

These curves clearly show cyclic effects as would be expected from the normal relationship of R vs D already firmly established. If regional stress is present, however, one would expect a cyclic effect to show some degree of interference from the extraneous influence.

10.2.3 Examination of Directional Affects on Breakback Rosettes of Azimuth Against D Corrected

A third approach to investigating for regional stress was to examine the variations of R and the values for D corrected (D_{corr}) to radii 540 ft and 665 ft by plotting D_{cR} values according to the bearing (θ) and side of the pipe where they were measured.

Once again the data from Bultfontein and Dutoitspan Mines were not sufficient for study. The results from Kimberley and Wesselton Mines were plotted on a "breakback" rosette, which presented an efficient way to examine directional effects diagrammatically. The rosette for both cases (i.e. D corrected to 540 ft and 665 ft) are given in Figs. 10.7 and 10.8 for Kimberley and Wesselton Mines, respectively.

These results show that the rosettes are slightly elongated and are symmetrical with the elongated ends being 180° apart. This effect, however, appears to be directly related to the pipe geometry and not to regional stress. It is reasoned that the direction of elongation of the rosette, however slight this elongation may be, is almost exactly at right angles to the direction of elongation of the pipe in both cases. That is, the position of the cyclic variation is different with respect to each mine. Hence, it can be stated that evidence of regional stresses from this analysis was not found.

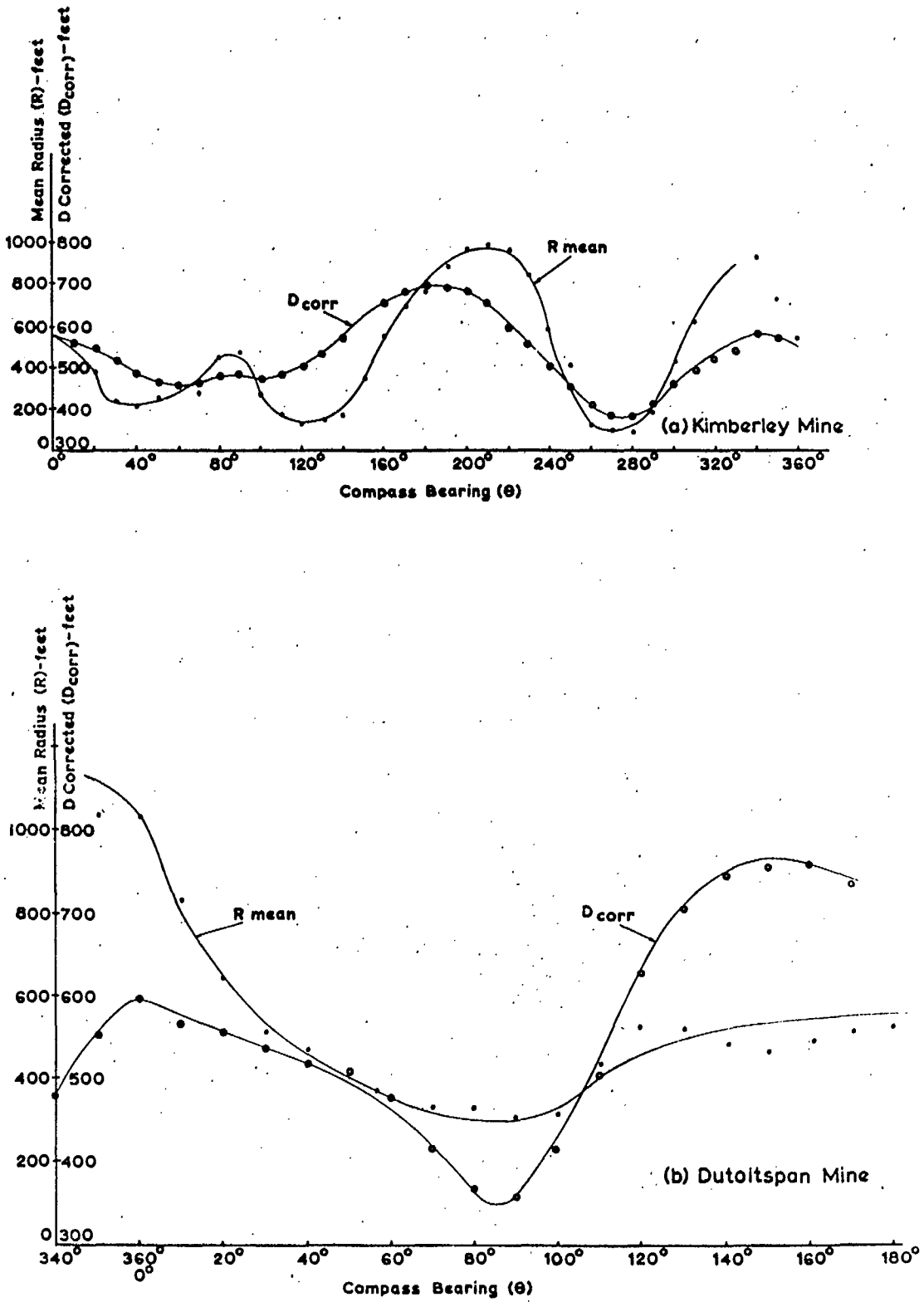

Fig. 10.6. Plots of mean radius (R) and corrected breakback (D_{corr}) against the compass bearing (θ) where the observations were taken.

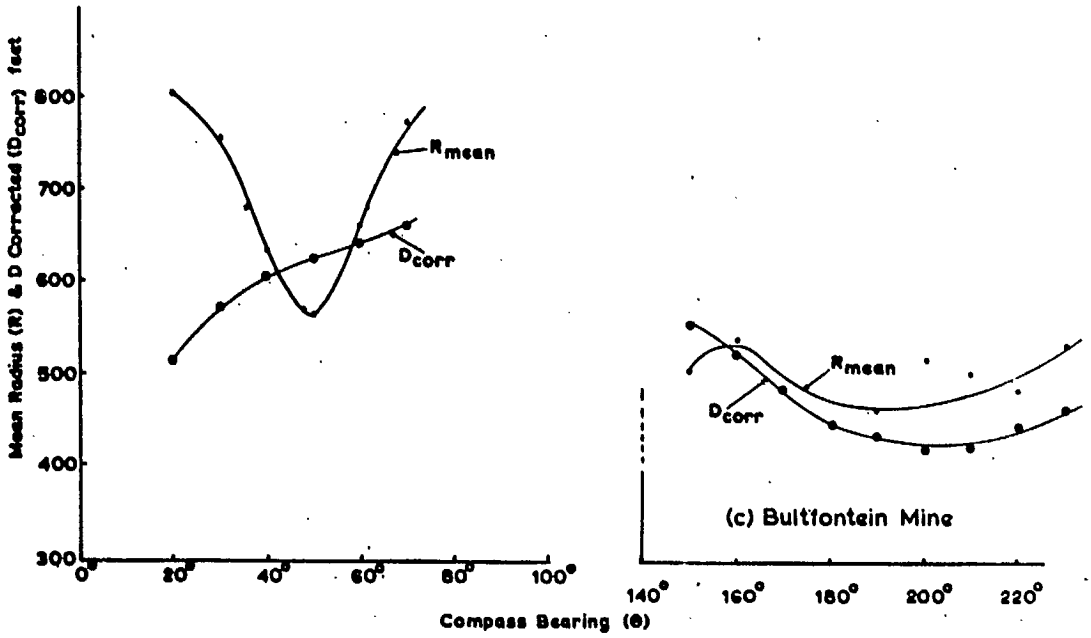

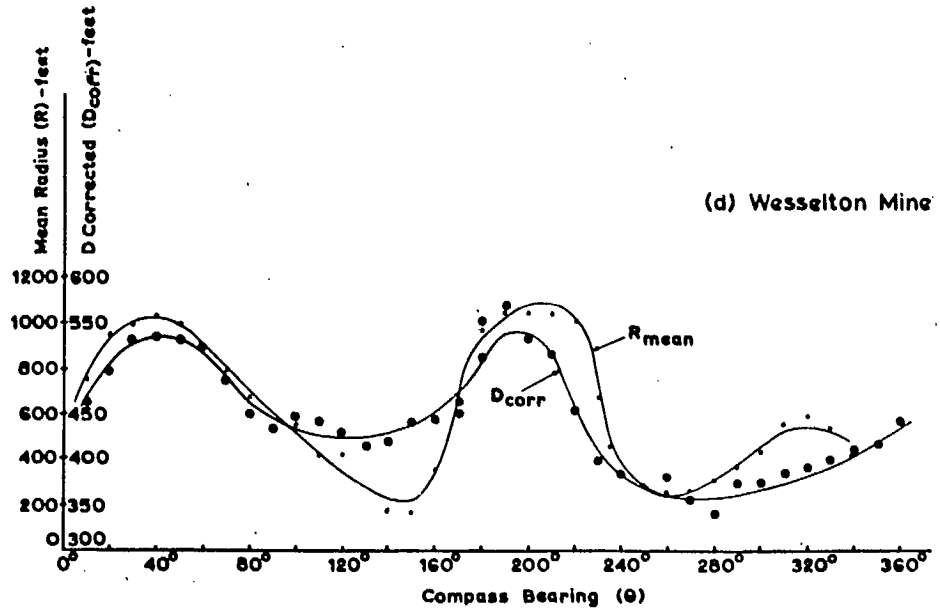

Fig. 10.6. Plots of mean radius (R) and corrected breakback (D_{corr}) against the compass bearing (θ) where the observations were taken.

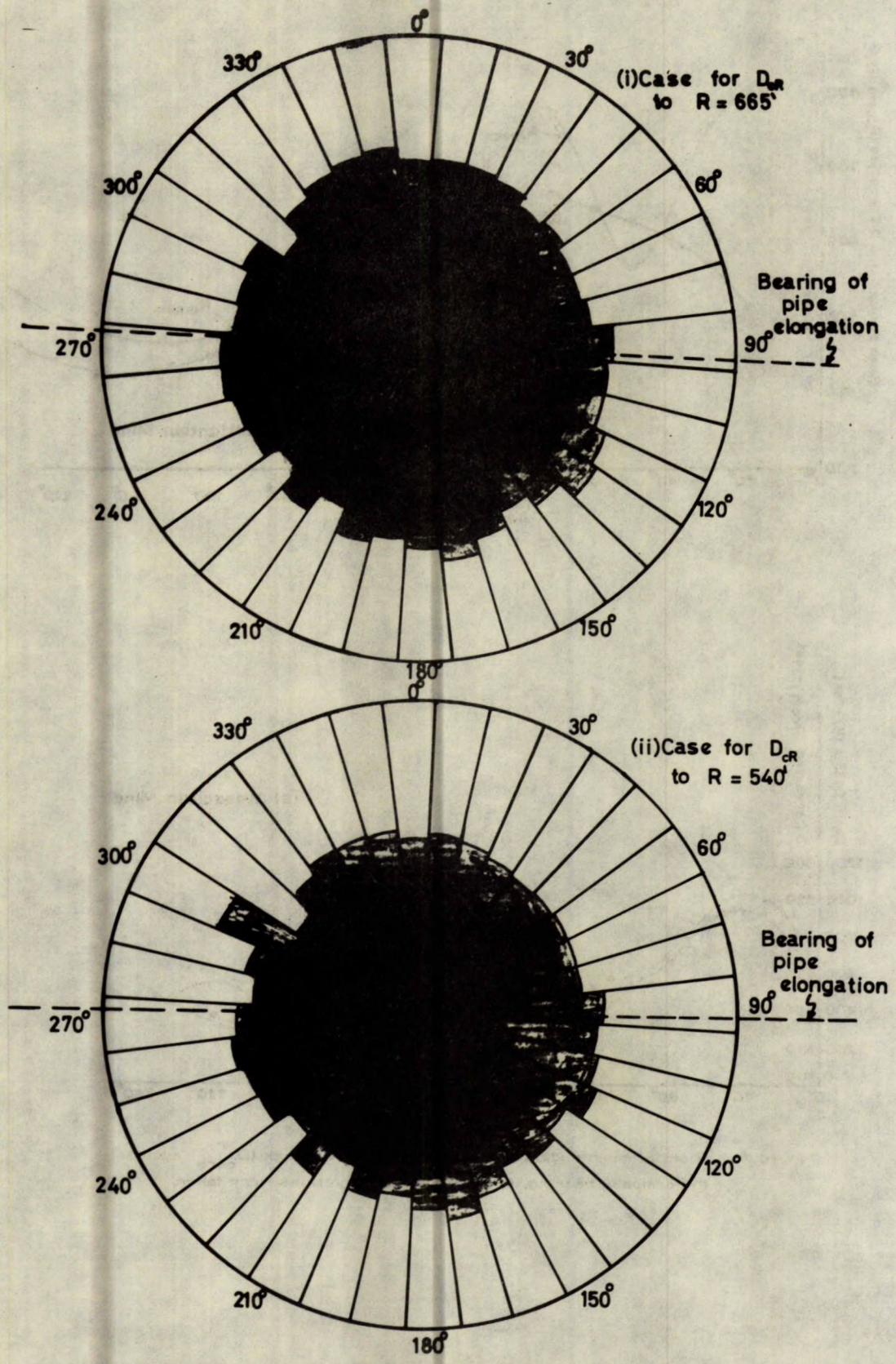

Fig. 10.7. Kimberley Mine: breakback rosette showing D corrected (D_{cR}) to preselected R plotted with respect to bearing and side of pipe where data was recorded.

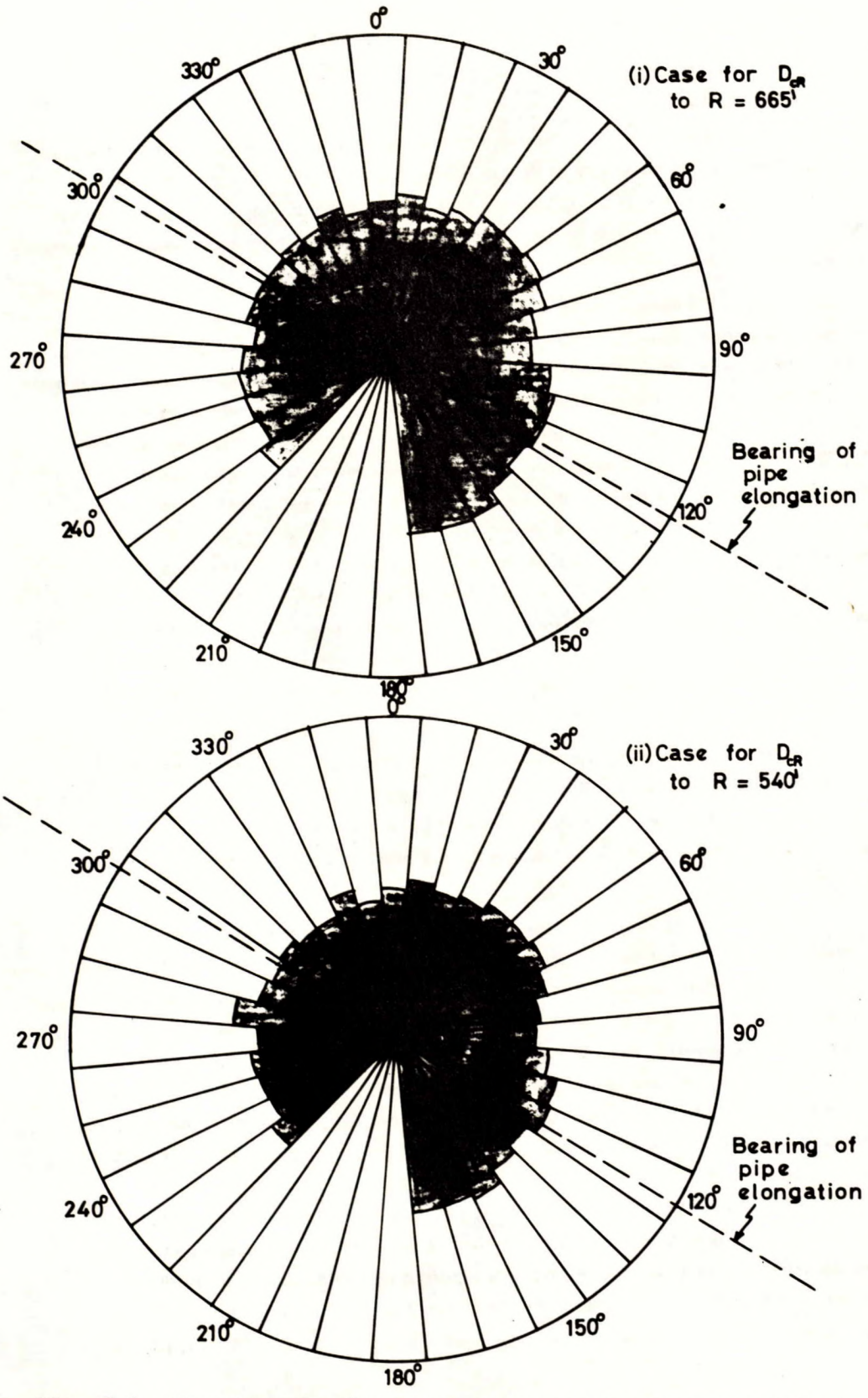

Fig. 10.8. Wesselton Mine: breakback rosette showing D corrected (D_{cR}) to preselected R plotted with respect to bearing and side of pipe where data was recorded.

10.3 DISCUSSION OF THE RESULTS

The most important results are those from Kimberley and Wesselton Mines where the data are nearly complete around the whole of the compass circle. The results from the other two mines are incomplete and hence can only be used by inference to examine the conclusions from the Kimberley and Wesselton Mines.

Both Wesselton and Kimberley pipes are elongated with obvious major and minor axes. If the cyclic effects coincided with the axes of these mines then their effects would be masked by the radius of curvature influence. It is fortunate, however, that the major axes of these two mines are not parallel, but bear 29° away from each other. The bearing of elongation for the Kimberley and Wesselton pipes are 93° and 122°, respectively. These two pipes are approximately five miles apart and there is absolutely no reason to think that effects which are known to occur on a wide scale such as regional stress will change orientation in this relatively small distance. Regional stress has been known to be both evident and consistently orientated some tens of miles from their origin. If this is accepted and if the interpretation is valid that there is no evidence of the effect of regional stress in both big holes simultaneously, it can be concluded that no such effects exist.

Reasoning along the same lines, in regard to the bearings of the major axes, the curves of R and D plotted against bearing (Figs. 10.6 (a to d)) should show phase displacement between the two curves for at least one of these two mines if some directional effects are present in the slopes.

The finding that regional stress does not affect the breakback of the big holes is not entirely unexpected. It should be noted that, of the rocks that form the slopes of the big holes, the principle lithologic unit that controls the angle and breakback of the slopes is the shale. Geologically speaking, shale is a reasonably soft rock and one would expect that with ancient tectonic activity, such as is considered to apply in the Highveld Plateau of South Africa, any regional stress in these rocks would have been relieved by plastic flow. Further, Jennings and Black (1963), Black (1964) and others point out that a slope in horizontally bedded material, as shown in Fig. 10.9, is analogous to a trapezoidal cut in a material resting on a frictionless base in that horizontal stresses are easily relieved, whereas in homogeneous material with no bedding planes, as previously explained in Chapter 3 (Vol. I), there will be high stress concentration around the bottom of the cut as shown in Fig. 10.10.

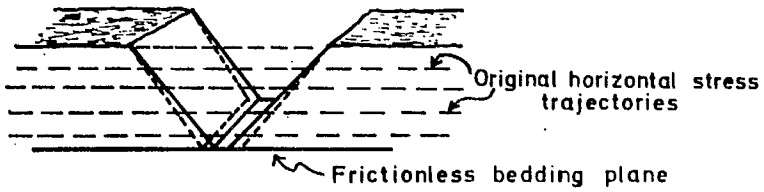

Fig. 10.9. Section of a long trapezoidal pit resting on a frictionless plane at the base (after Black, 1964).

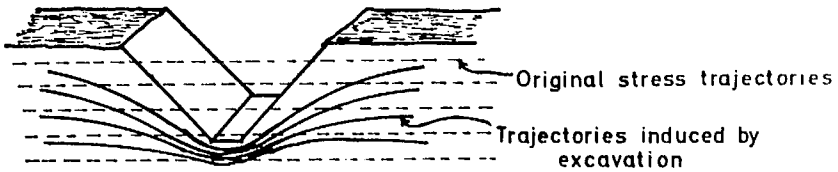

Fig. 10.10. Section of a long trapezoidal pit cut in elastic material - homogeneous with no bedding planes (after Black, 1964).

Also, the very nature of the dolerite, being completely traversed by columnar joints of a contractile origin, would suggest that any regional stress previously existing would long since have been mainly relieved.

CHAPTER II

CONCLUSIONS

Detailed investigations of natural slopes of big holes which have developed naturally around the four pipes of mines in the Kimberley area show that studies of natural conditions of slopes can be rewarding. In these studies it was possible to ascertain important natural and unnatural influences of the slopes which affect their stability. Most particularly, these studies have shown in an empirical way a relationship between slope angle and slope curvature and also that general plan geometry of the pipes in these big holes is of significance.

These slopes were measured and a clear relationship was found to exist between the plan radius of curvature of the toe of the slope and the angle of the slope which has formed naturally through the process of breaking-back. Small radii in plan give rise to steeper slopes (i. e. less breakback) indicating that plan radius of curvature of a slope has significant affects on the stability of the slope. Current theories of slope stability deal mainly with the slope as a two-dimensional situation whereby it is assumed that the plan radius of curvature of the slope is infinite. The resulting analysis, therefore, is carried out on a basis of plane strain for a slice of unit thickness cut from within an infinitely long slope. As is seen, this does not satisfy the condition encountered with curved slopes in practise, a situation particularly common in open pits, where curvature of the slope could have important affects on the slope angle.

It is observed that the outlines of the pipes and edge of the big holes have approximately elliptical shapes. Any one mine may be composed of four quadrants, each with different ellipse axes, but nevertheless the elliptical forms still seem to apply. The geometric properties of concentric ellipses were calculated choosing as variables the radius of curvature R at any point A (x, y) on the inner ellipse and the breakback D or distance AB between points (x, y) and (x_o, y_o) which represent the pipe margin and edge of the big hole, respectively. From the examination of values of R and D to seek a suitable form of plotting which would yield a straight line function, it was found that the direct plot R:D gave as reasonable a plot as any other. It was also found that the pipe shape (i. e. the ratio a/b) was an important factor, making the plot of R:D steeper as the pipe became more circular, i. e. for the case $a \longrightarrow b$. The actual plots of R:D for the various big holes also show that each of the four mines gives a different straight line typical of the hypothetical ellipses described above, the slope of the line being steeper the larger

the shape ratio (S.R.). This means that the shape of the pipe, as described by the ratio of its major and minor axes, must be taken into account for practical predictions of breakback of other big holes (De Beers Mine) in the area. These findings indicate in general that the major plan dimensions (plan shape) are important factors in determing the stability of surface openings in rock.

Based on the generalized plan shape and radii of curvature of the pipe margin, the final position that the slopes of the De Beers Mine would eventually assume, for the condition that the slopes would be allowed to break back naturally, was predicted. It was clear, after having established the predicted limits to where the slopes would eventually break back to under natural conditions, that if measures were not adopted to remedy the situation certain civil works located in close proximity to the pit would be jeopardized. Such a situation, therefore, had to be prevented with the result that remedial measures had to be applied to maintain the slopes at angles steeper than would have been the case had they been allowed to develop naturally.

Following the finding that the curvature of the slope significantly affects the stability in the area, a series of experiments using cohesionless material for tests of model slopes, with different radii of curvature and shape of orifices, led to an understanding of the general type of failure mechanism that is dominant in the big holes. It was found that for any given way of placing and for any constant density, the average slope angle remained constant for the different radii of curvature of the slopes. From these results it was concluded that, if a slope forms by a ravelling process, the radius of curvature of the slope in plan appears to have no significant affect on the slope angle which is formed. In view of the effects of slope curvature found to exist, it was further concluded that the most significant mechanism of failure in the Kimberley big holes was one of a deep-seated nature, and that ravelling does not appear to occur on a large scale.

Comparative analysis of profiles taken at the sides and ends of the pipe from the upper and lower parts of the shale slope indicates that the curvature of slope has the greatest relative effect with respect to the top and bottom of the slope where the radii are least.

Utilizing the data at hand concerning the slope curvature - slope breakback relationships already firmly established, additional analyses to investigate the possibility of the existence of significant regional stress in the Kimberley area showed that such stress, at least of

sufficient magnitude to affect the stability of the big hole slopes, does not exist. Assuming that these effects would be found to be included in the observations if significant regional stress existed, various forms of analyses of the R and D data showed that no clear cyclic variation in the pattern of breakback with an amplitude of 180° could be discerned. Effects of regional stress in the big holes in the Kimberley area were considered to be unimportant and therefore were ignored.

In concluding it should be noted that every attempt must be made to characterize the geological factors numerically, but, while quantitative description of these factors has many advantages, it can also be misleading if used without the benefits of sound judgment and experience with the full advantages of a background furnished by a thorough understanding of the geology.

Many of the geological factors significant to the stability of slopes in rock are difficult to assess in a quantitative manner and herein lies the challenge for the engineering geologist. In this respect the most encouraging of the possibilities would appear to involve empirical information - systematic back analysis and precise observations of case histories of stable as well as failed slopes. This will lead to a better appreciation of the problem, for the task lies not only in improving theoretical approaches to the problem, but in understanding the very basic problem itself.

ACKNOWLEDGEMENTS

These studies were carried out on behalf of De Beers Consolidated Mines Limited to whom the authors express their appreciation for permission to publish the results. The author wishes to express his appreciation to Messrs. A. MacG. Robertson who carried out the laboratory experiments described in Chapter 9, and I. Hutchinson and J. Hellings for assistance with the statistical and computer analyses.

REFERENCES

Black, R. A. L. (1964): Economic and engineering design problems in open-pit mining: technical and geological factors in slope stability, Mine and Quarry Engng. , Feb. pp 66-74.

Brink, A. B. A. and Williams, A. A. B. (1964): Soil engineering mapping for roads in South Africa, C. S. I. R. Research Report, Pretoria, No. 227, 30 p.

Eubanks, R. A. (1954): Stress concentrations due to a hemispherical pit at a free surface, Journ. App. Mech. , Vol. 76, pp 57-62.

Forster, W. (1966): The influence of curvature of open cuts on the stability of slopes in open work mining, Proc. First Intnl. Cong. Soc. Rock Mech. , Vol. II, pp 193-200.

Jenike, A. and Yen, B. (1963): Slope stability in axial symmetry, Proc. Fifth Symp. Rock Mech. Univ. Minn. Pergamon.

Jennings, J. E. and Black, R. A. L. (1963): Factors affecting the angle of slope in open cast mines, Trans. Soc. Min. Eng. , Mar.

Jennings, J. E. (1970): A Mathematical Theory for the Calculation of the Stability of Slopes in Open Cast Mines, in The Theoretical Background and Planning of Open Pit Mines with Special Reference to Slope Stability, a symposium: South Africa Inst. Mining and Metallurgy, Johannesburg.

Lacy, W. C. (1964): Quantitizing geological parameters for the prediction of stable slopes, Trans. AIME, Vol. 226, pp 272-276.

Leeman, E. R. (1964): The measurement of stress in rock, Jour. S. Afr. Inst. Min. Metall. , Vol. 65, No. 2. pp 48-114.

Liang, T and Belcher, D. J. (1957). Landslides and engineering practise, Highway Research Board Special Report 29, Nat. Res. Council, Chap. V, pub. 544, Washington, D. C.

Long, A. E. , Merrill, R. H. and Wisecarver, D. W. (1966): Stability of high road bank slopes in rock - some design concepts and tools, Highway Research Record, No. 135, pp 10-26.

Merrill, R. H. and Wisecarver, D. W. (1967): The stress in rock around surface openings, Failure and Breakage in Rock, Ed. C. Fairhurst, Amer. Inst. Min. Metall. Petr. Engrs. , New York, pp 337-350.

Metcalf, J. R. (1966): Angle of repose and internal friction, Intnl. J. Rock Mech. Min. Sci. , Vol. 3, pp 155-161.

Mollard, J. D. (1962): Photo analysis and interpretation in engineering - geology investigations: a review, Review in Engineering Geology, Geol. Soc. Am., Vol. 1, pp 105-127

Piteau, D. R. (1970a): Engineering Geology Contribution to the Study of Stability of Slopes in Rock with Particular Reference to De Beers Mine: University of Witwatersrand, Ph. D. Thesis.

Piteau, D. R. (1970b): Geological Factors Significant to the Stability of Slopes Cut in Rock, Symposium: The Theoretical Background and Planning of Open Pit Mines with Particular Reference to Slope Stability, South Africa Inst. Mining and Metallurgy, Johannesburg.

Robertson, A. MacG., (1970), The Interpretation of Geological Factors for Use in Slope Theory: Symposium: The Theoretical Background and Planning of Open Pit Mines with Particular Reference to Slope Stability, South Africa Inst. Mining and Metallurgy, Johannesburg.